INVESTIGATION OF CORROSION IN OIL PIPELINES THROUGH SURFACE NANO-TREATMENT

A DISSERTATION

by

MOHAMMED SALIH AHMED

Submitted to the
Graduate School of Sciences and Engineering
In Partial Fulfillment of the Requirements for

the Degree of
Doctor of Philosophy

in the
Department of Mechanical Engineering

Özyeğin University
2020

INVESTIGATION OF CORROSION IN OIL PIPELINES THROUGH SURFACE NANOTREATMENT

Approved by

Assist Prof. Dr. Özgür Ertunç Advisor,

Department of Mechanıcal Engineering

Özyeğin University

Assist Prof. Dr. Zeynep Başaran Bundur.

Civil Engineering Department

Özyeğin University

Assist. Prof. Dr. Ramazan Ünal

Department of Mechanıcal Engineering

Özyeğin University

Assist. Prof. Dr. Mete Budaklı

Department of Mechanical Engineering

Turkish-Germany University

Prof. Dr. Ayşegül Akdoğan Eker

Department of Mechanical Engineering

Yildiz Technic University

Date Approved: 2020

DEDICATION

To

My parents

My wife

My Childs Moath, Anas and Malek

All other family members

ABSTRACT

Corrosion is the unintentional and degradation of a material caused by the reaction of that material with its environment and a natural possible hazard correlated with gas and oil generation and transportation facilities. Steel with low percentage of carbon are utilized in gas and oil industries specially for the pipelines because its excellent mechanical properties and low cost. However, the pipelines are predisposing to failure with one or more types of corrosion when unprotected to acidic or salty environment.

The financial issues and the high cost of the equipment maintenances after corrosion, in oil and gas industries and several sectors have increased the need of improvement in corrosion control strategies. Thus, preventing corrosion is often an important part of an overall design philosophy. The main motivation behind a corrosion study always lies in the desire to optimize the life cycle cost and ensure technical integrity of facilities in an industry. The mitigation of corrosion can be achieved by employing various types of surface treatments. This study investigates the chemical mechanical polishing (CMP) as a novel surface treatment technique for corrosion inhibition of carbon steel used in petroleum industry. The behavior of corrosion phenomenon of carbon steel has been investigated in three phases.

In the first phase the samples were immersed in DIW having different pH values in order to study static corrosion behavior the steel. Moreover, the dynamic corrosion behavior was investigated, with the flow setup developed for this purpose. Atomic Force Micrography (AFM) was utilized to observe the morphology of surfaces after in steel pipelines. The effect of wall shear stress and time of immersion was evaluated under the dynamic corrosion test. Under the dynamic and static condition, the rate of corrosion of

the steel samples was calculated through the weight loss measurements. The scientists reported that rate of corrosion in steel samples under static condition is higher at lower pH values where the minimum and maximum corrosion rates were obtained at pH = 6 and pH = 4. Also the static corrosion tests suggest that the corrosion rate was high throughout the first 48 h and decreases with the increasing time of tests. The results suggest that increased wall shear stress results in increased the corrosion rate specially at pH=4.

In the next phase of the current work, CMP applied to the samples by polishing with polymeric pad using the oxidizer in silica based slurry and abrasive paper with only oxidizer. The surfaces obtained are tested under range of flow velocities at changed pH values for their corrosion behavior. The influence of the fluid flow on the surface roughness are evaluated in the developed experimental set up under turbulent conditions. Potentiodynamic analyses are also conducted to understand the electrochemical behavior of the produced surfaces. The outcomes suggest that the corrosion rate of steel samples polished with oxidizer in the silica based slurry is lower as compared to samples polished using abrasive paper in the presence of oxidizer only which can be attributed the formation of oxide film on the surface. This oxide layer formed act as a protective shield against corrosion. Furthermore, the influence of hydrogen peroxide in silica slurry on the wettability, surface roughness and hardness of steel has been investigated using contact angle measurement, profilometry, Scanning Electron Microscopy and Micro Hardness Tester.

In the final phase the surfaces prepared with MP and CMP were coated with a set of coating prepared using sol-gel method. These coated samples upon corrosion

investigation in an acidic medium offered advanced corrosion resistance characteristic comparing with uncoated samples.

The present study conclude the static corrosion rates measured after every 24 hours for seven days show an almost linear decrease with time after 48 hours. The dynamic corrosion rates obtained utilizing the developed setup show that for the same velocity the corrosion rate drops with time. Although the corrosion rates increase with increasing velocity until critical velocity after which the corrosion rate decreases. However, at pH=4 beyond critical velocity an increase in the corrosion rate was observed, which can be liked with more pronounced influence of the acidic environment on steel corrosion as compared to the momentum of the flowing fluid inside the pipe. All the other cases of dynamic corrosion show an inverse relation between corrosion and time. This relationship has also been observed in static corrosion presented above and also proven in other studies.

ÖZET

Korozyon çevresel etkiler sonucu oluşan, malzeme için yıkıcı, petrol ve gaz üretimi ve taşınması için potansiyel risk oluşturan bir etkendir. Uygun mekanik özellikleri ve fiyatı nedeniyle karbon çeliğinden yapılmış boru hatları petrol ve gaz taşınmasında yaygın olarak kullanılır. Ancak, bu tip borular asidik ve tuzlu ortamlarda kullanıldığında iç korozyona yatkındırlar.

Korozyon, pek çok alanda sebep olduğu yüksek maliyet sebebiyle önlenmesi konusunda yoğun çalışmalar yapılan ve ürün geliştirilmesinde önemi yüksek bir unsurdur. Korozyon üzerine yapılan çalışmalarda genellikle ürünün uygun teknik özelliklere ve maliyete sahip olması amaçlanmaktadır. Korozyon farklı yüzey iyiliştirme yöntemleri ile önlenebilir. Bu tez çalışmasının amacı kimyasal-mekanik parlatma yönteminin petrol sanayiinde kullanılan karbon jhuh çeliği üzerindeki korozyon dayanımı arttırıcı yönde etkisini araştırmaktır.Karbon çeliğinin korozif ortamlardaki davranışı üç bölümde incelenmiştir.

İlk bölümde örnekler, karbon çeliğinin statik korozyon davranışının incelenmesi amacıyla farklı pH değerlerine sahip deiyonize suya bekletilmiştir. Ayrıca, geliştirilen akış düzeniği ile malzemelerin dinamik korozyon davranışı da incelenmiştir. Çeliklerin yüzey morfolojileri Atomsal Kuvvet Mikroskobu vasıtasıyla incelenmiştir. Yüzey kayma gerilmesi ile deiyonize suda bekletilme süresi arasındaki ilişki dinamik korozyon testi vasıtasıyla incelenmişltir. Hem statik hem de dinamik testlerde ki korozyon hızı, örneklerin ağırlık kaybı hesaplanarak hesaplanmıştır. Statik testlerde düşük pH değerlerinde korozyon hızı daha fazla olmuştur (pH = 6 minimum; pH = 4 maksimum). Ayrıca, statik korozyon testi esnasında korozyon hızının ilk iki günde yüksek olduğu; artan gün sayısı ile azaldığı

gözlemlenmiştir. Artan yüzey kalma gerilmesi, özellikle de pH = 4 iken, korozyon hızını arttırmıştır.

İkinci bölümde, örneklerin bir kısmı oksitleyici içeren silika bazlı karışım ve polimerik ped ile bir kısmı ise, yalnızca oksitleyici ve aşındırıcı kâğıt vasıtasıyla kimyasal-mekanik parlatma işlemine tabi tutulmuştur. Parlatma işleminden elde edilen yüzeyler korozyon davranışlarının belirlenebilmesi için farklı akış hızları ve pH değerlerinde test edilmiştir. Akışın yüzey pürüzlülüğü üzerindeki etkisi, geliştirilen test düzeneği ile türbülanslı akış ortamında test edilmiştir. Ayrıca, potansiyodinamik analizler ile yüzeylerin elektrokimyasal davranışları da incelenmiştir. Sonuçlar, oksitleyici içeren silika bazlı karışım ile parlatılmış örneklerin korozyona karşı oksitleyici içeren aşındırıcı kağıt ile cilalanmış örneklerden daha dayanıklı olduğunu göstermiştir. Bu durum, malzeme yüzeyinde oluşan ve koruyucu bir tabaka görevi gören oksit katmanı ile açıklanabilir. Ayrıca, silika bazlı karışımda bulunan hidrojen peroksitin ıslanabilirlik, yüzey pürüzlülüğü ve sertliği üzerindeki etkileri temas açısı ölçümü, profilmetre, Taramalı Elektron Mikroskobu ve Mikro Sertlik Ölçüm Cihazı ile incelenmiştir.

Son bölümde, mekanik ve kimyasal mekanik parlatma işlemi ile hazırlanan ve sol-gel yöntemi ile kaplanan örneklerin korozyon davranışları incelenmiştir. Yapılan testlerde kaplanmış olan örneklerin, kaplanmamış olanlara kıyasla asidik ortamda korozyona karşı daha dayanıklı olduğu gözlemlendi.

Çalışmada statik korozyon testi sırasında yedi gün boyunca, 24 saatte bir yapılan ölçümler sonucunda korozyon hızı ilk 48 boyunca lineer olmultur. Kurulan test düzeneği ile gerçekleştirilen dinamik korozyon testi, aynı akış hızında gerçekleştirilen testlerde korozyon hızının zamanla azaldığı; ancak kritik bir hızın altında akış hızı ile korozyon hızı

arasında doğrusal bir korelasyon gözlemlenmiştir. Bununla birlikte, pH değeri 4 iken kritik akış hızının üstünde dahi korozyon hızı artmıştır. Bu durum, asidik ortamın çelik malzemenin korozyonu üzerinde akış hızından daha etkili olması ile açıklanabilir. Dinamik korozyon için bu vaka dışında ki bütün diğer vakalarda korozyon hızı ve zaman arasında ters bir ilişki gözlemlenmiştir. Aynı bağıntı statik korozyon için de gözlemlenmiş ve bu durum, yapılmış diğer bilimsel çalışmalar ile paralellik göstermektedir.

ACKNOWLEDGMENTS

I would like to express my deepest gratitude to my advisor, Asst. Prof. Dr. Özgür Ertunç, for his inspiration, guidance and encouragement. The door to Dr. Ertunç's office had always been open for me whenever I faced a problem or needed guidance and has consistently steered me in the right direction to accomplish this work. I would also like to acknowledge the other members of my dissertation committee for their valuable effort and contributions to this dissertation.

Also, I would like to thank Assistant Professor Dr. Hussein Çimenoğlu from Istanbul technical University for his help in roughness measurements. I also would like to thanks PhD candidate Ali Abdul Munim Alhattab and Mertcan Kaba from Istanbul Technical university for their help in roughness and XRD measurements. I am grateful to my colleagues PhD students Wazir Akbar and Ziba Nazarlou who have contributed to my Ph.D. lifespan by their wonderful friendship and for their help with CMP and AFM experiments and coating of samples. I would like to thank staff of ALAHDAB Iraqi oil company for preparing and providing the raw material and all the data for experimental work.

Finally, thanks are due to my wife and my children for being behind me at all time.

Sincerely,
Mohammed

TABLE OF CONTENTS

LIST OF TABLES

LIST OF FIGURES

CHAPTER I

INTRODUCTION

Corrosion of metals is a chemical or electrochemical process which involves the reaction of atoms of the metal surface with a substance in interaction with the bare surface. Generally liquid substances are the most influential corroding mediums, but gases and even solid materials may perform as corroding media. For example, the corroding media can be a liquid or a thin film in a system, in another system it can be droplets, or a material adsorbed on or absorbed in another solid.

All metal parts can be corroded in a specific environment (e.g., the atmosphere, soil, or waters). Bronze, brass, most stainless steels, aluminum, and also zinc corrode gradually with low rate in different applications which can guarantee their long life without any protective coatings. The huge losses that the United States is exposed to annually due to the corrosion are estimated at billions of dollars, which raised concern to find appropriate solutions to this type of problems [1].

1.1 Mechanism of Corrosion

Corrosion is an easily and naturally happening phenomena usually described as the weakening of a material or its properties due to the response with surrounding environment [2]. Oxidization of substances is unavoidable because of the essential requirement of lowering of Gibbs energy [3]. Low energy level is favor of the materials and corrosion is a way to reach to this goal. Although mentioned phenomenon is mutual among every material, the level of oxidation in metals are higher than the others then scientists focus on

decreasing the rate of corrosion and optimizing the environment of metals in their applications.

Since the main reason of the failures in pipelines in oil and gas industries is corrosion, engineers consider the majority of production time to enhance the corrosion resistance of their systems [4].

Electrochemistry and metallurgy are two main roots of advanced corrosion science. Whereas metallurgy contributes to the knowledge of corrosive materials and on the other hand, electrochemistry offers data, regarding the performance of alloys and compounds.

The sort of environment (such as water, soil, air, etc.) that corrosion is taking place there, is the main parameter which can determine the types of corrosion and it's attacking rate. The condition of the environment can be suitable for increasing the rate of corrosion while sometimes it can be inappropriate for that. Hence, the products or wastes of the industries can either act as a catalyst or inhibitor for corrosion. For example, corrosion rate in gas and oil pipelines can be directly affected by H_2S, CO_2, mass flow rate, temperature, formation water, pH, and some the other of flow with different contribution rate [5-8].

The presence of cathodic anodic sections on the surface of substrate refers to the variation of electrical potential on the metal surface. Corrosion is generating by the aforementioned potential difference. In the case that a gas or oil pipeline is located in a place filled by clay soil which has a low oxygen concentration to a zone of sand with a high oxygen level, the interface between the clay and pipeline becomes anodic and suffers damage.[3].

Most of the metals are formed as polycrystalline materials including the small grains. In the polycrystalline materials, grain boundaries as an example of planar defects

have a high potential to be the suitable places for chemical reactions. Also, with considering the weaknesses of boundaries, it can be concluded that stress corrosion cracks will be started from that zones.

Exposing a steel surface to an electrolyte normally increases the probability of corrosion on these areas [2, 3]. These sections produce corrosion cells. Figure 1.1a illustrates the anodic reaction includes the separation of metal to create both soluble ionic product and insoluble compound which is generally an oxide. On the other hand, for figure 1.1b represents the cathodic reaction which oxygen produced could be diminished or water is decreased to generate hydrogen. The electrochemical cell is the product of simultaneous anodic and cathodic reactions.

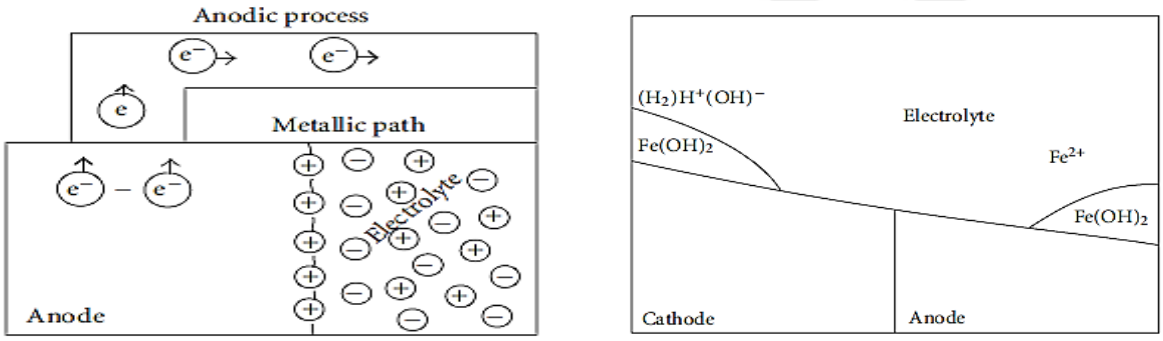

(a) (b)

Figure 1-1 Schematic of (a) Anodic and (b) Cathodic processes [3]

Both anodic and cathodic reactions which occurs in an alkaline and natural condition are displayed in Figure 1.2. On the other hand, for an anodic situation, the anodic and cathodic reactions are illustrated in Figure 1.3.

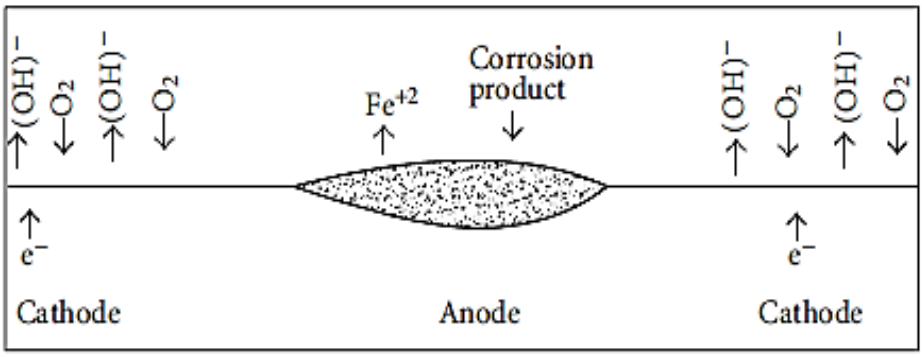

Figure 1-2 Schematic of alkaline and natural condition of *corrosion* [2]

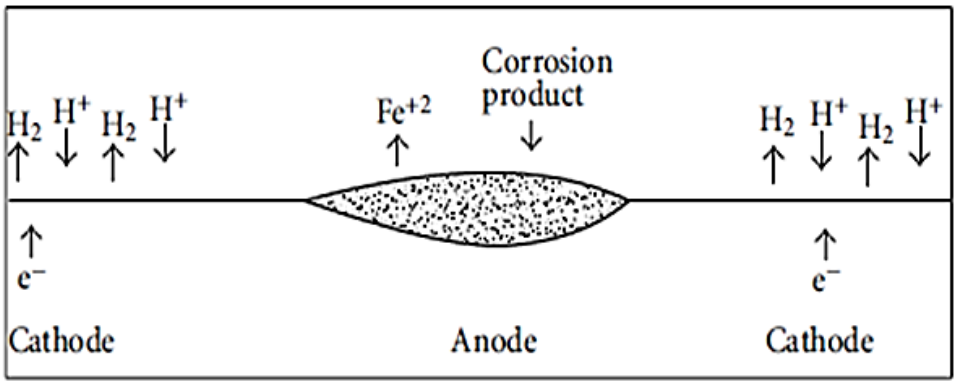

Figure 1-3 Schematic of acidic condition of corrosion [2]

Also, a summary of equations related with the different conditions of corrosion is listed in Table 1.1 with a brief description to explain about each chemical reactions throughout a corrosion process [9].

Table 1.1 The Chemical equations of the reactions in different condition of corrosion

Number	Description	Chemical equation
1	Cathodic reaction in oxygen free water	$2H^+ + 2e^- \rightarrow H_2(g)$
2	Cathodic reaction in the presence of oxygen	$2H^+ + \frac{1}{2}O_2 + 2e^- \rightarrow H_2O$
3	Presence of hydrogen ion in water	$2H_2O \rightarrow 2H^+ + 2(OH)^-$
4	Association of iron to form a ferrous ion	$Fe \rightarrow Fe^{+2} + 2e^-$
5	Reaction of ferrous ion with the hydroxide ion to form unsolvable ferrous hydroxide	$Fe^{+2} + 2(OH)^- \rightarrow Fe(OH)_2$
6	cathodic reaction in the presence of ferrous ion in the anodic reaction	$\frac{1}{2}O_2 + H_2O + 2e^- \rightarrow 2(OH)^-$
7	Corrosion reaction in deoxygenated solution	$Fe + 2H_2O \rightarrow Fe(OH)_2 + H_2(g)$
8	Corrosion reaction in oxygenated aqueous systems	$Fe + H_2O + \frac{1}{2}O_2 \rightarrow Fe(OH)_2$

9	Hydroxide readily decomposes into magnetite in deoxygenated water above 100◦C	$3Fe(OH)_2 \rightarrow Fe_3O_2 + H_2(g) + 2H_2O$
10	The net corrosion reaction with the magnetite	$3Fe + 4H_2O \rightarrow Fe_3O_4 + 4H_2(g)$
11	Formation of Insoluble iron hydroxide which is transformed to hematite	$Fe(OH)_2 + \frac{1}{2}H_2O + \frac{1}{4}O_2 \rightarrow Fe(OH)_3$
12	The ferric oxide (Fe^{+3}) is converted to magnetite	$2Fe(OH)_3 + Fe(OH)_2 \rightarrow Fe_3O_4 + 4H_2O$

Cathodic and anodic parts might be created because of changing the metallic microstructure alteration, environmental situations, and difference in environmental intensity of oxygen at various areas of a metal [3]. The mentioned ions at the anodic places, produces an electron movement among the non-corroding and corroding cathodes and anodes, respectively. The flow rate of mentioned electrons determines the rate of corrosion. The determination of corrosion rate is the most important factor however, discovering the tendency for corrosion is also necessary. This is because a special metal or alloy maybe has a tendency to corrosion in any environment but with a negligible rate.

1.2 Corrosion Management Techniques

Corrosion management includes the implementation, improvement, and even resources of corrosion policy. However, all the decisions related to the corrosion in an

industrial setting are based on the corrosion policy, this framework gives fundamental measures for risk measurement by the improvement of determined total risk control throughout the implementation, preparation, and control procedures. Corrosion management contributes to many advantages such as the reduction in leaks, safety enhancement, extending plant availability, diminishing unexpected maintenance in the system, and modification in delay expenses [9]. Figure 1.4 demonstrates a model of corrosion management includes the all stages of organization's policy.

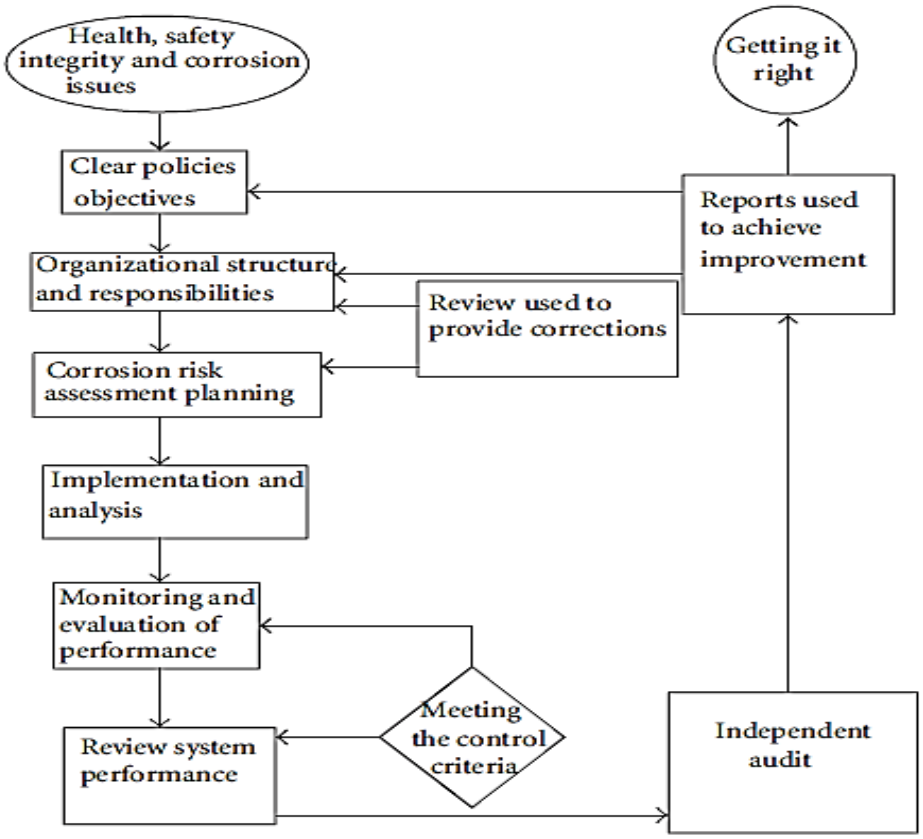

Figure 1-4 Corrosion management framework [9]

1.2.1 Corrosion Risk Assessment (CRA)

The first step in corrosion management is to classify the facilities that are highly prone to corrosion. therefore, evaluating corrosion risk is important. To this end, facilities should be classified based on their susceptibility to corrosion, removable facilities should

be listed, and the environmental condition may be improved in possible cases. To manage corrosion risks, an exact investigation method will be employed in each of the process stages of an organization. Failure probability estimation depends on suspected corrosion damage type and the failure consequences are assessed based on potential environmental hazards, safety considerations, and inadequate corrosion mitigation procedure risks.

1.2.2 Risk Based Inspection (RBI)

The RBI is a method used for generating a best possible strategy for the performance of the inspection activities to control corrosion of the pipelines. This technique generally utilizes the information arrested based on CRA or different risk analysis to prepare physical examination methods. Using these type of strategies can guarantee that the risk will decrease to the minimum. Also, it will improve the examination plan which concentrates to identification of suitable examination techniques [10].

1.2.3 Corrosion Monitoring Tools

Inspection of data gathered from corrosion investigation is the most important parameter to check that if pipeline integrity is maintained or not [11]. Various parameters for instance the temperature and pressure of the flow, temperature, corrosivity, fluid composition, equipment, and so on can influence on the choice of corrosion control measure in an establishment.

In order to measure and monitor the corrosion in surface and pipes, various monitoring tools were utilized in industry. The smart Pipeline Inspection Gauge (PIG), ultrasonic tools, internal Corrosion Sensor (ICS) Probes, optical inspection techniques, and galvanic sensing are different methods of corrosion monitoring tools.

The Pipeline Inspection Gauge (PIG) is the most conventional and highly utilized corrosion inspection tool. PIGs have many functions among such as structural health inspection which is the most important one of them. It is originally employed for cleaning the pipeline by moving it through the pipe by the flowing fluid from the pigging launch position. Figure 1.5 demonstrates that how corrosion and metal loss influence on the integrity of the magnetic flux, sensed using a Hall effect sensor.

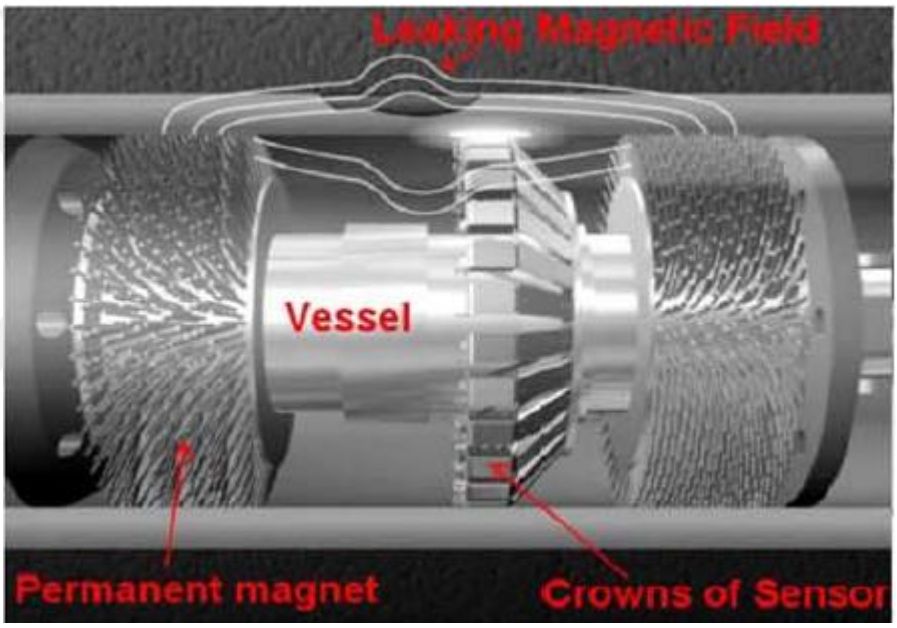

Figure 1-5 Magnetic flux leakage in the utilization of a smart PIG to measure the corrosion [12].

The ultrasonic tool (UT) is also a metal loss detection which provides the data to the magnetic flux leakage (MFL) with ultrasonic technology. It can transmit the ultrasonic pulses into the pipe surface and immediately measure its thickness. However, it is not as extensively employed as the MFL because of the specifically needed coupling medium among the substrate and the probe [13].

Another magnetic inspection tool alike to the smart PIG is the internal Corrosion Sensor (ICS) Probe with a different operating system. It employs the magnetic perturbation method instead of the established MFL method to measure the thickness of the metal surface at the probed neighborhood by quantifying its magnetic response [12].

Optical inspection working with Closed-Circuit TV (CCTV) camera is also employed to internally image and map the pipeline surface to recognize irregularities and defects. This method is not very popular because of the inadequate lighting situations inside of the pipeline.

1.2.4 Corrosion Mitigation Approaches

After CRA, gathering the data, and corrective operation, facility refinement based on the corrosion damages is necessarily required. The attitudes existing for modifying level of damages and corrosion involves surface coating to perform as a shield, limiting corrosion with adding chemical specie to the environment, modification of alloy elements to acquire more corrosion resistive alloy and finally using of alternative material [14]**.** Having a better understanding about the principle of corrosion process can help to restrict this procedure. As demonstrated in Pourbaix diagram in Figure 1.6, the basic corrosion control measurements are depending on electrochemical driving force.

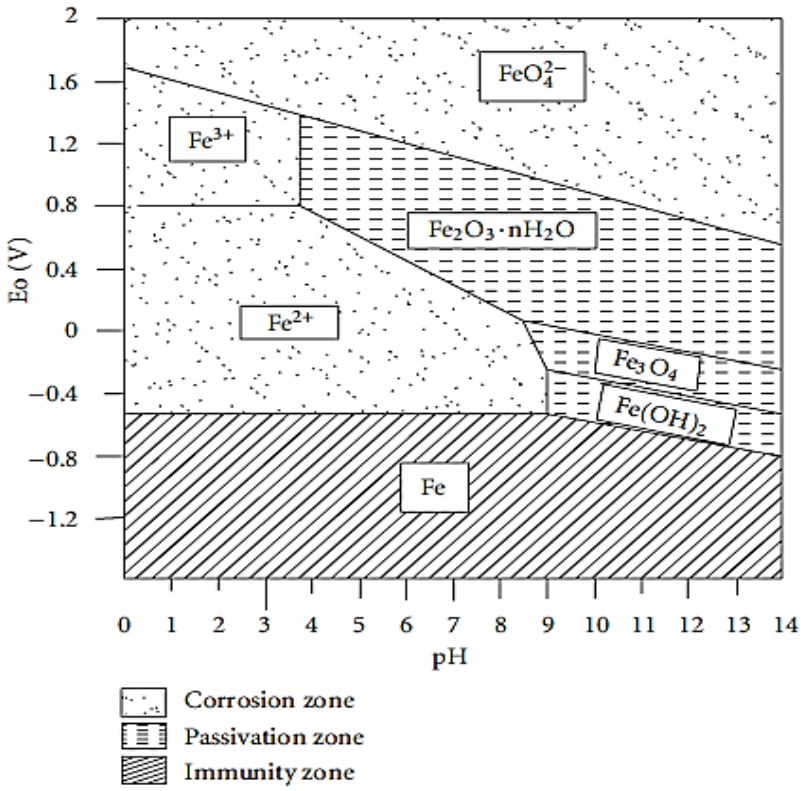

Figure 1-6 Pourbaix diagram for corrosion of iron, immunity and passivity [14].

1.3 Factors Effecting Corrosion Rate

1.3.1 Type of steel

Owing to high quality of mechanical properties, Different types of steel specially with high percentage of carbon has been employed in numerous engineering applications. Nevertheless, high level of corrosion rate still is a concerning shortcoming for industries. To this end, There have been many studies regarding corrosion protection methods.[15-17]

1.3.2 Effect of Time

Exposure time plays critical role on the life of pipeline carbon steel when exposed to the environment and can vary between locations [18, 19]. In a corrosive environment, the longer the steel material is exposed to the corrosive environment, the more destructive will be the carbon steel with time. Katayama et al. [20] investigated the atmospheric corrosion behavior of carbon steel, comparing the outdoor environment and in-chamber conditions. Temperatures of carbon steels and relative humidity of the chamber were control throughout the tests. The result showed similar corrosion performance of carbon steel in atmospheric and sheltered environmental conditions. However, the corrosion appears more severe on the carbon steel sample tested in the actual atmospheric condition as the exposure time was increased from 1 to 10days.

1.3.3 Effect of pH

However, pH on the other hand indirectly affects corrosion: changes in pH change conditions for formation of iron carbonates. Iron carbonate has solubility at higher pH: which increases the precipitation rate. The corrosion rate (CR) drops with increasing the level of pH in the corrosive environment, as in iron. At higher pH (i.e. greater than 10), corrosion retards attributed to the creation of a passive layer of hydroxide of metal. Acids (i.e. lower pH) are more aggressive for corrosion than alkaline medium. The amphoteric metals like Aluminum, Zinc and Lead, dissolve in alkaline solution in the form of complex ions. The (CR) of iron is much faster in oxygen-free water (i.e., pH<5). At pH<4, the corrosion of iron is stimulated by the oxidation of Fe^{+2} to Fe^{+3} by the dissolved oxygen and the subsequent reduction of Fe^{+3} to Fe^{+2} at the cathodic region. In less acidic solution, an

excess of OH- ions reacts with the metal ion (Fe^{+2}) to form unstable Fe(OH)2, which undergoes further oxidation to form rust.

Moiseeva and Rashevskaya studied the influence of pH level on corrosion resistance of steel in CO_2- containing aqueous media and they found that changing the temperature and the time of testing in a corrosive medium affects the variation of the pH of the medium and the rate of steel corrosion more strongly, than changing the partial pressure of CO_2 does. It is demonstrated that high total rates of corrosion of low-carbon steel, determined by the initial rate, are observed in a 3% solution of NaCl at $pCO_2 > 0.8$ MPa and T = 253 80 C^o [21]. In Rhee et al, found that decreasing pH values caused an increase in the (CR). Aforementioned increase in corrosion can be explained by high dissolution and instability of iron oxide at 150 C^o [22].

1.3.4 Selection of Materials

Variety of materials is used in making pipelines for oil and gas industries since they have to convey oil and gas from the source to the consumer. One of the basic requirements for a good and durable pipe is it should be resistant from acids thereby causing corrosion. The steels which are employed in well construction come in a broad spectrum from MS of grade N80 of API USA, J55, duplex and chromium steels etc. [23, 24]. One of the properties of metal corrosion resistance is the weld construction acid corrosion phenomena have to be well acquainted by a corrosion engineer. Steel metallurgy one of the greatest important principles for acidizing the CIs in laboratory testing [25, 26]. More corrosion resistant alloys for example austenitic or duplex stainless steels may find a place as good corrosion busters [27]. High-grade alloys are responsible for causing corrosion and also

hike the capital costs [24, 28] API N80 CS by American Petroleum Institute is utilized as the basic construction material for down hole tubular, flow lines, and transmission pipelines in the oil industry [28-30].

The degradation procedure during which the substrates quality reduces is called corrosion. therefore, the stream of liquid upon the substrate could affect the (CR) [31]. In some specific conditions, a liquid stream can increase corrosion resistance, for instance, a aqueus flow that prevents from accumulating of some solid substances on matal surface. However, in most cases, fluid flow decreases corrosion resistance for example, In mass transport control condition which takes place if the charge transfer rate(CTR) is extremely huge that the influence of abrasive solid volume at the metal surface is negligible [32]. By the way, fluid flow rate increment will raise the rate of the mass transport(MTR), therefore the corrosion rates, until the CTR becomes the decisive element; the additional increment in velocity won't affect the corrosion rates as presented in Figure 1.7 below [33].

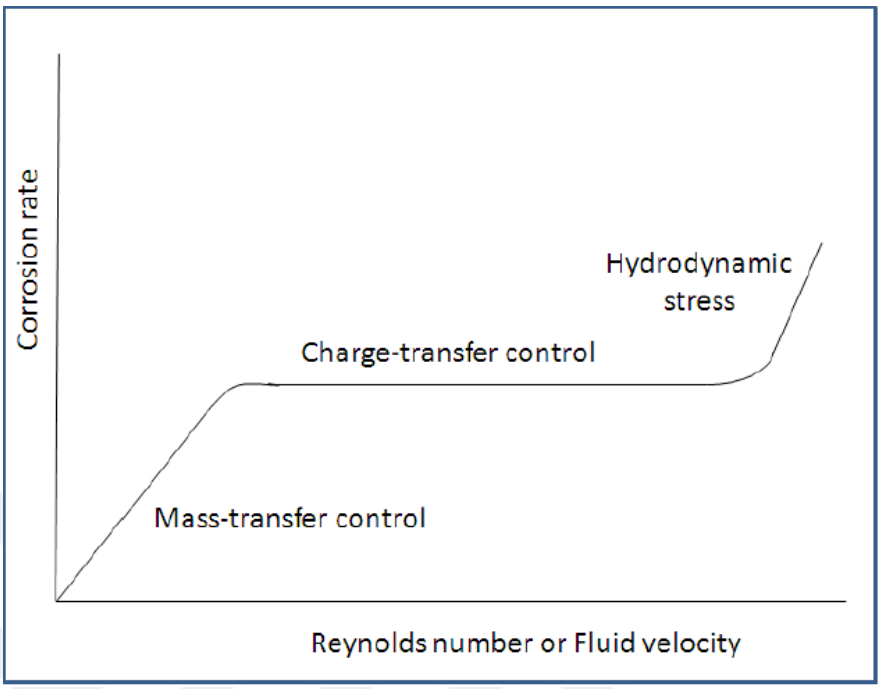

Figure 1-7 The effects of flow on corrosion rate [33].

The increase in corrosion rate with WSS is pronounced in a film-free condition. This is because there is no resistance to mass-transfer of the reactants to the metallic surface [34]. Fontana and others described the mechanism behind the relationship between that water flow and the changes or variations in corrosion. Rising the velocity of the flow has a negative effect on the (CR) even at critical velocity of the system. The passivation occurring on the surface of the steel, and the resulting low (CR), can be attributed to the formation of the oxide film on the surface. This oxide layer works as a protective film against corrosion and therefore, the corrosion rate decreases.[35]. Seheers studied the simultaneous effect of flow velocity and pH value on the (CR) of mild steel in a synthetic mine water. A rotating-cylinder electrode (RCE) was utilized to mimic the influence of flow velocity on the pipe corrosion. It was found that lower pH values result in higher corrosion rates [36].

Fredj and Burleigh investigated the effect of velocity and water with different purity on corrosion of carbon steel. A rapid decrease in the corrosion rate after a high increasing at the beginning of the test with a water of high purity containing oxygen. They also found increased corrosion rate as the velocity increased. Moreover, after 7 days of immersion the corrosion rate still increased with velocity but with a lower slope[37]. Ferry et al. studied the effect of the velocity of sea water on paint degradation and the corrosion rate of mild steel. Their findings also demonstrated higher corrosion rates as well as paint degradation with an increasing flow velocity. This mean that the sea water flow velocity is the main parameter that increased the paint damage and the rate of corrosion[38]. Rabald et al. studying the effect of flowing tap water and distilled water on the (CR) of steel and cast iron, found that in flowing tap water cast iron corroded faster than steel while in distilled water, it corroded about 300 times faster [39].

1.3.5 Effects on corrosion product layers

Depending on the environmental conditions like pressure, temperature, solution pH and dissolved anions in the fluid the iron compounds of corrosion product scales forming on carbon steel differs. The steel fabrication process that takes place under high temperatures, produces a film of a black oxide scale called mill scale which is a type of corrosion product scale. Mill scale is comprised of following oxide layers: outermost hematite (Fe_2O_3) layer; intermediate magnetite (Fe_3O_4) layer and the inner wüstite (FeO) layer. Scale composition mostly depends on temperature and accessible oxygen amount during the formation process[34]. Since scale growth reactions for anaerobic oil and gas generation pipelines is completely different, as it's a wet corrosion consisting an immediate

reaction with an aqueous solution, formation of corrosion product scales can be utterly distinguishing.

1.4 Corrosion in pipelines and protection mechanisms

Pipelines are the most effective and cost-efficient ways for wide scope fluid transportation comparing with tanker and other transportation methods in particular for raw oil and natural gas, since pipeline routes are so flexible. Due to the respectable mechanical properties of carbon steel and it's low cost and broader availability, and despite their comparatively low corrosion resistance, they are regularly used as a main material of pipelines.[40]. Generally, if the oil aging process takes place properly, oil production decrease while water and gas flow rises. Also, the corrosion rate of pipelines increases in the vicinity of highly dissolved corrosive agents like CO_2, H_2S, and chloride compounds[41, 42].

In pipelines, corrosion befalls mostly because of an electrochemical reaction. This reaction takes place due to the presence of an electrolyte in the fluid medium, such as soil water or potions of the carrying products. Both internal and external factors can affect the rate of corrosion. Working environment, soil chemistry, and in the case of buried pipelines soil moisture are examples of external parameters while oxygen content, the reactivity of the carried fluids, inhomogeneity of the materials which are used in pipelines, temperature, pressure, and flow rate constitute internal parameters[43].

The main parameter that affect wear resistance, corrosion resistance, and energy loss due to friction of all engineering parts is surface quality. [44-47]. A study declared, through the regular wear test with pin-on-disk method the usage of lubricant

decreases the friction coefficient of Steel (AISI 52100) due to the low roughness of steel disk [48], which shows that the surface roughness is highly sensitive to the amount of the lubricant used on particular components. Recently, a meticulous level of surface roughness is required for some engineering components. In some circumstances, the smoothness of parts in nanoscale is required for the appropriate working of the system and efficiency of the mechanical behavior of them [49, 50]. Since mechanical polishing is not an adequate method to achieve nanoscale smoothness of the surfaces, so to obtain the promising roughness smoothness for steels like AISI 52100, many different finishing methods of manufacturing and surface preparation are investigated [46, 49-55].

1.4.1 Chemical Mechanical Polishing

The (CMP) as a novel method was first suggested by Monsanto [56-58] in 1965. It is a vital step in semiconductor equipment production, a popular procedure conducted in wafer polishing for glass mechanical polishing and microprocessor utilization. The mentioned technique is a new process, which has been used widely in nanomaterial fabrication and maybe a crucial step for nanotechnology. CMP has found its place in nanomaterial fabrication in spite of enormous technical difficulties early on. Nowadays it is extensively employed in the semiconductor industry ([59] ,[60], [61], [62] to produce ultra-smooth surfaces with no measurable subsurface deficiency.

Glass polishing methods with suspensions of rare earth oxides and micro heterogeneous suspensions with particle dimensions of 0.1–0.5 μm diameter and new or tested rough ultra-disperse powders (UDP) combined with the new scientific studies in this area examined in electronics. Nowadays it's fairly common to use Chemical Mechanical

Planarization (CMP) for eliminating the overburden of metal layers during the production of integrated circuits. At first, It was used for polishing tungsten layers but soon its use has widened to copper and barrier (tantalum and tantalum nitride) materials, now this technique has proved to be effective for more advanced films like ruthenium and cobalt [63].

It is possible to optimize effective factors like apparatus and consumables. The slurry is the important consumables (typically including abrasives and chemicals acting simultaneously) which has a straight forward influence polishing and the quality of finished surface. Minor variations in slurry characteristics because of impurities, chemical degradation, grinding material volume or employed shear can decrease the polishing performance and effect on the final product. Correlation of slurry characteristic determination with an estimation of wafer polish rate, planarity, and imperfectness produces knowledge about the roots of degradation in polishing. Grinding solid particles suspended in a liquid chemical solution [64] containing one or numerous substances like oxidizers, pH stabilizers, ion complexants, and corrosion inhibitors comprise the standard slurry [65]. An abrasive in the slurry contributes both mechanically and chemically. The mechanical contribution is due to the action of abrasive nanoparticles and chemical contribution takes place due to the solution additives with a synergistic influence that causes material removal [66, 67]. The optimum abrasives' type, size, shape, and concentration are determined based on chemical and physical activities and the abrasive-liquid interplays[68]. The optimal slurry should grant fair removal rates, adequate polishing selectivity appropriate to the underlying layer, moderate surface defects after polishing and

reliable slurry suspense. In CMP the most important parameter in selecting slurry is the removal rates without causing defects.

Today, Chemical mechanical polishing is employed more often for planarization purposes [61, 69, 70]. Mechanical planarization couples with chemical surface reactions in chemical-mechanical polishing. This method for metals occurs in the following manner:

(i) Chemical decomposition of the film(s);

(ii) Exterior layer oxidation, accompanied by scraping of the porous (vulnerable to physical corrosion) exterior surface;

(iii) Generation of solvable exterior layer composites, which can be eliminated by the smallest physical corrosion.

A group pf researchers fabricated colloidal silica particles with various sizes in the nanoscale and investigated the efficiency of those in AISI 52100 steel chemical mechanical polishing. The outcomes revealed that the roughness of the resulting mirror-like surface was 8.4 nm. [49]. Yun and his colleagues [54] used CMP to produce mirror-like 304 and 430 types steel surfaces of elastic film transistors. The outcomes revealed that the employment of slurries with alumina as the main substance, the resulting roughness could reach about 2.5 nm. Other group applied the same slurry in the position of grinder and studied the impacts of acidity and oxidation agent on the surface finishing efficiency. The outcome that stated high pH accompanied by oxidation agent could result in great material removal rate (MRR). Nevertheless, 1-2 micrometer pits were detected on the surface of the components after the process[55] .

Many studies have been devoted to CMP since it is applicable to the large expensive aerospacial parts with complex shape as a final stage. CMP on steel surface using alumina slurry has been investigated. It's been found that CMP efficiency depends heavily on the oxidation agent types, contents, and grinder's volume. Substrates polished by alumina-based slurries with colloidal alumina particles in Nano size had a more moderate average roughness (Ra), fainter geometrical abnormalities and less corrosion. The MRR and the Ra were 124 and 7.61 nm when oxidation agent was H_2O_2, 2 weight percent, grinder's volume was only 1 weight percent, slurry flow rate was 10 ml/min, and polishing time was 5 min[53] .

De-Xing[71] examined alumina nanoparticles and Tuagachi approach to optimize the CMP parameters on roughness of the steel surface. Optimal results are employed in experimental tests executed to study the influence of grinders' contents, oxidation agent, slurry debi and duration of polishing in obtaining an ultra-smooth surface. Taguchi designed tests which are conducted to optimize the parameters of chemical mechanical polishing which took place on steel samples. The result was; the cracks of the surface, polishing fog and enduring elements were decreased; and the metal surface smoothness was assured.

The polishing pads, grinders, and chemical agents all together take part in removing material and polishing surfaces of components. Recently, CMP has been investigated profoundly to optimize the quality of the surfaces specially for the different types of steel [72]. The chemical process that takes place in the CMP is surface ingredients reacting with slurry elements producing a “soft” film. Besides, the mechanical part of CMP is the elimination of the soft film by grinders [73]. To reduce the creation of a surface defect

while maintaining the rates and removing the desired materials, chemical and mechanical reactions should be improved through the application [74].

Nowadays, silica is employed in the making of slurries for both dielectric and CMP for metal surface finishing. The application of commercial sols–gels of silicon acid [75] and of structures based on aerosol type UDP SiO_2 (Siemens,Degussa) and Al_2O_3 (Union Carbide Corp.) headed to the evolution of colloidal silica. Robert Walsh (Monsanto), patent and papers of other authors [60] up to the opening of the eighties provided the foundation for the growth of microelectronics with the progress of colloidal silica sol and silica gel.

1.4.2 Sol-Gel Technique and the Coatings

1.4.2.1 Sol-Gel Technique

The history of sol-gel chemistry started literally in 1842 when J.J. Ebelmen performed the synthesis of uranium oxide by heating the hydroxide form of uranium [76]. Consequent studies throughout a hundred years later illustrate the gradual evolution of sol-gel chemistry [77, 78] peaking in a pivotal stage in the annals of the sol-gel area in the ’80s, with a description for the organized hydrolysis and condensation of alkoxides [78]. These accomplishments helped the development of sol-gel chemistry into various disciplines of science, for instance ceramics, plastics as well as moderating corrosion, and surface manufacturing [78-80]. The sol-gel method is created on the synthesis of a gel from an organic-inorganic sol by means of gelation [78]. In the conventional sol-gel process different precursors can be alkoxides of the transition elements of the periodic table (e.g., zirconium, aluminum, cerium, titanium) or Silicon alkoxides (e.g., tetraethyl orthosilicate (TEOS), tetra methyl orthosilicate (TMOS)). Hydrolysis and Condensation reactions take

place in carefully chosen media with the addition of an appropriate catalyst. The solvent is the element that determines the final properties of sol-gel coatings such as the final structure, thickness, and density. At the same time, catalyst choice affects those properties but in most cases, catalysts' effects are not as significant as the solvent. [14]. In particular, the selection of an acidic catalyst elevates the formation of randomly branched or linear structures [81, 82], but the final product of cases in which a basic catalyst is used is simply branched structures.

In the sol-gel method, sols have to be synthesized through the blending stage. It's been reported, using ultrasonic treatment increases the homogeneity and stability of the sol, since the chemical and physical properties of sol together determine the properties of the final coating such as smoothness, roughness, and durability. It's been expected that during the aging stage, further condensation and molecule bridging occurs, which guarantees more compact but porous structure. Besides, the main property of sol-gel coatings can be the porosity, which heavily impacts all the properties of the final coating, particularly its corrosion resistance.[83, 84].

The next stage in achieving sol-gel layers is that of the deposition of the sol-gel layer upon the underlying layer. Thermal stabilization is the last state that the process will go through. In this stage, the temperature will be the determining parameter. Final sol-gel coating's properties heavily depend on the heating schedule. Proper heating and cooling times and temperatures will guarantee the quality of the coating film. [85, 86].

The sol-gel method has been studied vastly in material engineering due to its controlled surface features and porous structure which can create coating layers between 1 nm and 500 nm.[87-90]. The films achieved by the sol-gel method are appropriate for

efficient shielding of metallic surfaces from oxidation and corrosion in more general saying [91, 92]. They are capable of increasing the long-term durability of metals considerably[92-94]. Ceramic oxides like SiO_2, CeO_2, ZrO_2, TiO_2, Al_2O_3 do possess excellent chemical and thermal endurance which makes them suitable for obtaining exceptional corrosion resistance [91].

Sol-gel films are excellent substitutes for toxic methods for corrosion protection of metallic heritage objects. Sol-gel films mainly protect the metallic surface by creating a physical barrier between them and destructive environments [95]. At first Investigations were concentrated mostly on the creation of pure inorganic sol-gel layers [86, 96]. The main problem of sol-gel coatings was the micro cracks, it was not possible to avoid them due to heat treatments in high temperatures and their number raised as the thickness increased. Recently results of some experimental investigations demonstrated that it's possible to get rid of those cracks by the use of organic compounds. Furthermore, heat treatment temperature can be reduced when the sol deposition and layers are more plastic. Therefore, the sol-gel method evolved to be the hybrid sol-gel [79].

Erika Kiele et al.[97] studied and employed the sol-gel process to protect different kinds of steel. Nano silica coatings were made utilizing tetra ethyl ortho silicate (TEOS) as a starting material. They prepared nano-silica coatings using tetra ethyl ortho silicate (TEOS) as basic material and applied it on steel surfaces. Their evaluations of the photochemical influence showed the drop of hydrophobicity and corrosion factors in all coatings. Nevertheless, the most promising coating was the one treated with HMDS. They concluded that HMDS (hexamethyldisilozane) treated silica coatings applied on steel substrate could shield steel at ambient conditions.

1.4.2.2 Coatings

Nowadays owing to the developments of technology and the enormous research, there are numerous corrosion-resistant coatings available both for metallic and nonmetallic surfaces. Amongst the most well-known non-metallic coatings are inorganic coatings, like adaptable, anodized or ceramic coatings [98]. Among these coatings again, those who are organized by the sol-gel technique are used more extensively [78-80, 85, 99].

The sol-gel method is very flexible and it can be utilized for different types of material. The ability to control the morphology of the resulting thin-film is one of its attractive features. Other than that, This method is an appropriate technique for various kinds of coatings, for instance, hybrid films, inorganic thin layers or coatings doped with several active substances, like corrosion-resistant agents [78, 85].

In recent decades, the sol-gel process as a coating technique has attracted more and more attention..[100, 101]. SiO_2 coatings are widely employed as an oxidation-resistant coating given their extremely low oxygen diffusivity [102]. Tetra ethyl ortho silicate(TEOS) coatings have also been confirmed to increase the protection of different metals and their alloys [103]. Nevertheless, as a result of the ubiquity of micro-cracks or remaining porosity, TEOS coatings show limited resistance toward electrochemical corrosion, because of their high diffusivity for electrochemical.[100, 104]. On the other hand, alkylalk oxide precursors dramatically increase the resistance of these coatings to both oxidation and electrochemical corrosion. Also, ‘hybrid’ SiO_2 sol-gel layers have been shown a similar effect. [96]. Besides, adding other oxides such as Al_2O_3, TiO_2, ZrO_2 has expanded the corrosion protection to alkaline and neutral media.[105] Sol-gel coatings doped with eco-friendly inhibitors is another possible method to obtain high corrosion

resistance, which enhances ‘barrier’ characteristics with active corrosion restrain when the film is degraded.

In a recent study, the group has prepared sol-gel thin coatings of ZrO_2, SiO_2, $70SiO_2$-$30TiO_2$ and $88SiO_2$-$12Al_2O_3$ compositions (mole%) from sonocatalyzed sols and applied it on 316L stainless steel foils by dip-coating method [106]. They have studied the impact of the films on the chemical corrosion of the material. they measured the impact using potentiodynamic polarization curves in aqueous 15% H_2SO_4 solution in the range of room temperature up to 50° C. they have concluded that the coatings appear as a physical barrier against exposure to corrosion media and enhanced the durability of substrate up to 8.5 times, this conclusion was more apparent at 50 °C.

1.4.2.3 Sol gel coating advantages

Today, it is widely accepted that the sol-gel method is an appropriate and powerful technique to enhance the corrosion resistance of some substrates such as, which include aluminum alloy[107-111], steel [112-114] and other metal [115].

The sol–gel method has many advantages hence, only the most important characteristics are listed below [93, 94]:

1. Mostly, the Sol-gel method takes place in low temperatures, most of the time it's just about the ambient temperature. Consequently, evaporation and degradation of dissolved compounds, like organic inhibitors, are decreased.

2. Due to the employment of liquid precursors, it is probable to apply coatings on components with complex shapes and to fabricate controlled thin layers and there is no need for the machining process.

3. The sol-gel method is a “green” coating technology, during which no waste is produced. This is because it utilizes mixtures that do not include impurities, so no waste is produced and there is no need for washing stage.

4. Last but not least, the Sol-gel method is cheap and needs no high-tech equipment, so it's possible to use the sol-gel method in almost any scale of industrial applications.

1.5 Open questions

In spite of the availability of a great deal of literature, there is ample gap in understanding the corrosion in pipe flow in terms of wall shear stress, pH and exposure time. For an in depth understanding of corrosion in petroleum pipes a combination of parameters such as the generated wall shear stress, range of pH values and various exposure time needs to be studied. This work takes into account all the above parameters and their effect on corrosion rate of carbon steel in DI water.

There are several commonly used techniques to alter the corrosion prevention of steel including surface treatments such as shot peening[116], use of the inhibitors [117, 118] and used surfactants with inhibitors [119, 120]. CMP is surface polishing technique which is commonly used in semiconductor manufacturing [121]. However, CMP as alternative surface treatment for corrosion prevention of metals has not been studied. CMP is known to result in smoother surface, change the surface wettability behavior, roughness

and forms a protective layer on the surface. These exceptional modifications to surfaces properties are expected to significantly affect the corrosion resistance behavior of metals. This study provides in depth information on how CMP modifies the metal surface properties and in turn how these surfaces react to different media both in static and dynamic conditions to understand their corrosion behavior. Furthermore, there is a lack of information about the combination between CMP treatments and different types of coatings, which is covered in the current study.

1.6 Thesis objectives

1.6.1 Main objectives

The current study investigates the influence of CMP treatment on surface properties of steel to validate the process as surface treatment of metals for increasing dynamic corrosion resistance especially for oil field. In this study CMP treated samples with polymeric pad and H_2O_2 in silica based slurry, and samples polished with abrasive paper both in the absence and presence of H_2O_2 are compared for their corrosion resistance behavior.

1.6.2 Specific objectives

The study objectives also include the investigation of static and dynamic corrosion. The static corrosion rates are determined in beakers filled with DIW. A setup is designed and manufactured in the lab to investigate the effect of flow velocities of DIW on steel surface. The study also investigates the effect of pH, oxidizer (H_2O_2) in MP and CMP on the surface properties of steel before and after static and dynamic corrosion experiments.

Moreover, three different types of coatings prepared using sol-gel method are applied on treated samples' surfaces and investigated for their corrosion resistance. Finally, an optimized combination of input parameters for steel surface treatment via CMP is proposed to achieve maximum corrosion resistance. The study provides an insight in to the relationship between steel's surface properties and its corrosion resistance. Also, different conditions of coating have been studied to have a better understanding about the effect of surface coating on the corrosion behavior of CMP treated steel samples in a harsh medium.

1.7 Methodology

Corrosion of metals often referred to as rust is the degradation of metals that has serious consequences. The total annual costs in the U.S. are expected to above $1 trillion in 2013. The cost of Corrosion also includes waste of valuable resources, plant shutdowns, costly maintenance, loss or contamination of product(s) etc. Therefore, there is a stringent need to seek new ways to improve the corrosion resistance of metals which is the main objective of this study. This study has been divided into the following three parts.

In the first phase the samples obtained from Iraqi Oil Fields were cleaned with abrasive paper in DIW. The produced surfaces were then characterized in terms of their wettability, roughness and finally corrosion resistance. The wettability was evaluated KSV Attention Theta Optical Light Goniometer using sessile drop method. The surface roughness was measured with a 2D contact type profile meter (Veeco Dektak 6M stylus, while the corrosion rates were measured by weight difference.

In the second phase of the study the samples were mechanically polished and treated via CMP under different input conditions such as absence and presence of oxidizer,

solid loading in slurry etc. The prepared samples were characterized as in the first phase. In this phase the main objective was to compare the samples for their corrosion rates. The dynamic corrosion rates were determined as function of pH, wall shear stress and exposure time in the setup developed in the lab. It was found that the samples treated with CMP, in the presence of H_2O_2 in silica based slurry, offer higher corrosion resistance as compared to mechanically polished samples.

Additionally, for the final phase of the current study, in order to investigate the effect of coating on the corrosion resistance of the samples, immersion tests in an acidic medium have been done for both surfaces prepared with MP and CMP coated with sol-gel method.

1.8 Thesis organization

This thesis has six chapters: Chapter One demonstrates an overview of the corrosion and corrosion mechanism. A historical perspective on corrosion and its mechanism and its mitigation strategy is shown. Chemical Mechanical Polishing(CMP) process and its basic properties are explained. Sol gel concepts and characterization are explained. The chemical mechanical polishing and sol gel coating as corrosion prevention methods are explained in this chapter as well. Chapter one also provides a brief summary of literature on corrosion in oil pipes and corrosion prevention methods, which covers the following topics: corrosion of pipes at different media, chemical mechanical polishing as alternative method to protect pipes against corrosion and the sol gel method with silica Nano particle as a new method used to coat the steel surfaces. Chapter two shows the research methodology which is divided into three parts; introduction, materials and equipment and the experimental procedure. In the materials and equipment section, the

materials which are used in the research are explained. Also, the experimental procedure is shown.

Chapter four demonstrates the evaluation of static and electrochemical corrosion of steel pipes at different pH values. The influence of immersion time on the corrosion rate of steel samples mechanically polished and CMP treated samples with different abrasive papers and polymeric pad were examined. DIW with different pH values are applied to test potentiodynamic and potentiostatic of steel samples mechanically polished and CMP treated. Surface characterization measurements tests are explained. The related results and discussion are also included in this chapter. Chapter five includes the dynamic corrosion at different conditions, the effects of the pH values, flow velocity and time test are explained. Also, the wall shear stress and its effects are explained for steel samples mechanically polished. Dynamic corrosion of CMP treated samples are examined as well. Roughness measurements after dynamic corrosion are examined. The related results and discussion are also included in this chapter. Chapter five contains the chemical mechanical polishing and sol gel methods. Potentiodynamic and potentiostatic tests with CMP treated are explained. Material removal rate and wettability the and the related parameters on the CMP treated samples are examined as well. Different types of coating are used with potentiodynamic and potentiostatic tests are explained. Static corrosion at pH=2 are explained as well. The related results and discussion are also included in this chapter. Chapter Six shows the concluding remarks and future studies, and the summary and future studies are explained.

CHAPTER II

RESEARCH METHODOLOGY

2.1 Introduction

Despite a plethora of available literature, several questions still need to be resolved regarding the influence of wall shear stress and pH values on carbon steel corrosion and the prevention methods of this kind of corrosion. Therefore, an experimental study has been conducted where corrosion of carbon steel was examined as a function of WSS, different pH values and different time tests. Also, electrochemical behavior of carbon steel has been investigated in DIW having different pH values. The second and the third parts chemical mechanical polishing and sol gel coating methods were investigated as alternative methods of corrosion prevention.

2.2 Experimental set up

2.2.1 Equipment

Several types of setups depending on the experimental tests were utilized to study the corrosion behavior of carbon steel.

2.2.1.1 Electrochemical corrosion software

A special three –electrode setup was used (Gamry 1000) as shown in figure (2.1) which contains, a counter electrode (CE) made of platinum. a saturated silver-silver chloride (Ag/AgCl) reference electrode and rectangular steel sample with a dimensions 10*10*2 mm^3 was used as a working electrode.

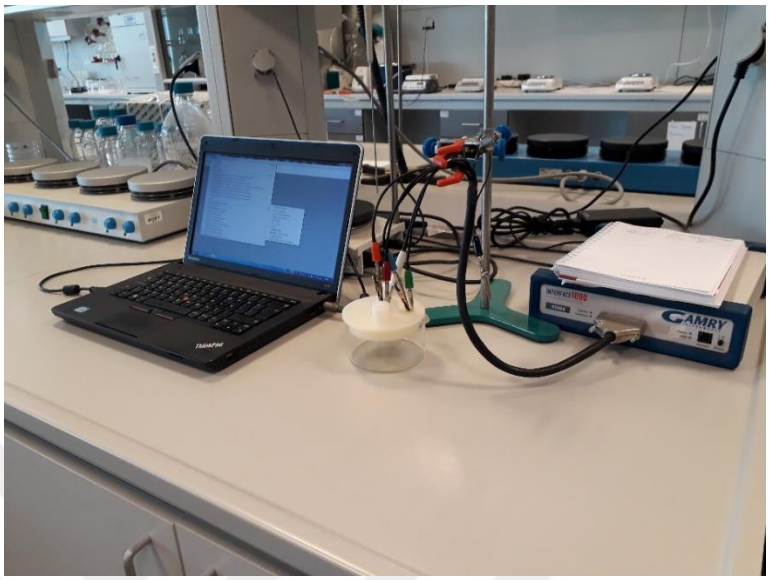

Figure 2-1 Experimental set up for electrochemical corrosion testing

2.2.1.2 Static Corrosion setup

A static corrosion tests setup contains group of glass bottles filled with deionized water (DIW) adjusted at different pH values, on magnetic stirrer. The samples were immersed in DIW with a glass rod to hold the samples still. The tests were conducted for seven days and weight loss was measured every 24 hours. The setup is shown in figure (2.2).

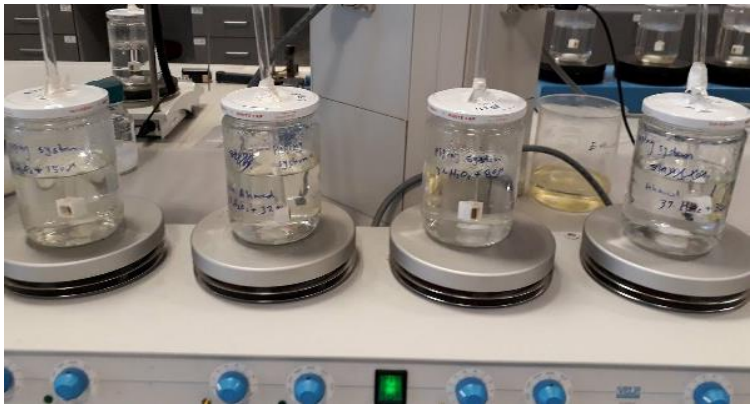

Figure 2-2 Experimental set up for static corrosion testing

2.2.1.3 Dynamic Corrosion Setup

An experimental developed setup was used to measure the dynamic corrosion in fluid flow under turbulent conditions. This setup is shown in figure (3.3) and consists of tank (1), an electric pump (2), a digital flowmeter (3), steel samples (4) and a regulator (5). The flow meter was employed to measure the flow rate and also the flow energy was provided by an electrical pump, see Figure 2.3. The experiments were conducted at three flow rates and 4 pH values.

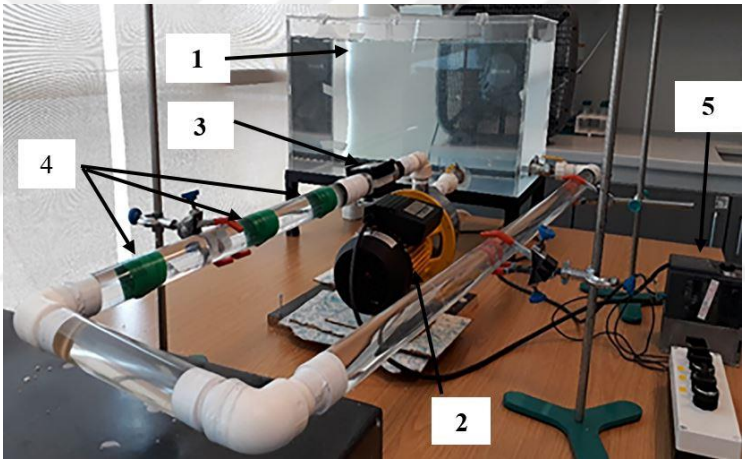

Figure 2-3 Experimental set up for dynamic corrosion testing

2.2.1.4 CMP Setup

The CMP tool, employed in the current study is demonstrated in Figure 2.4 where the material to be polished is held upside down against a rotating polymeric pad or sand paper. At the same time, a polishing slurry flows in between the substrate and the polishing pad. Therefore, planarization of the surface layer and material removal are the dual action of the CMP technique. Moreover, the CMP process can be utilized for polishing various metallic materials, insulators, polysilicon, ceramic materials and also packaging elements.

The quality of CMP depends on the components of the process, surface to be polished, polishing slurry and the polishing pad material, downforce, and rotational speed.

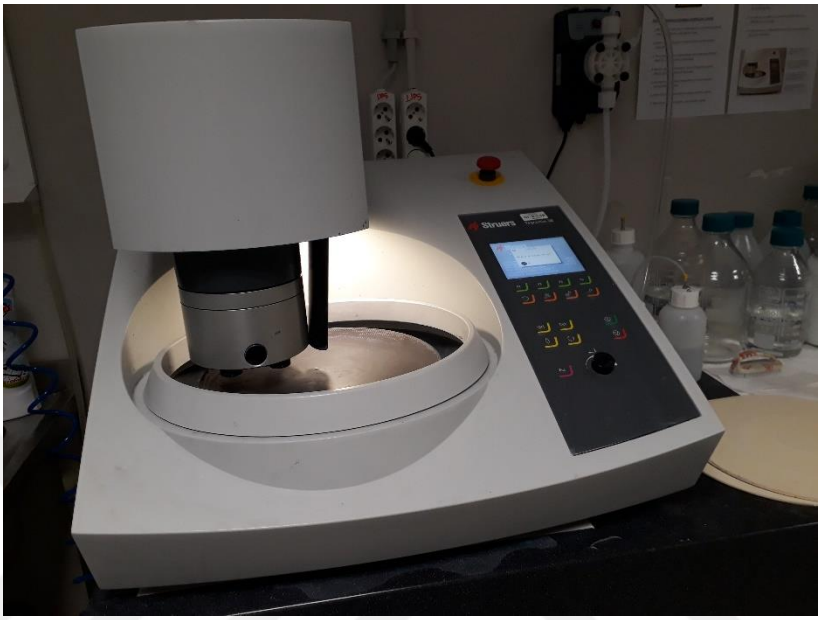

Figure 2-4 Chemical mechanical polishing tool

2.2.1.5 Wettability analyses Setup

The steel samples were characterized for wettability after Mechanical polishing and CMP treatments through contact angle measurements with DIW. The contact angles were measured via sessile drop method by means of a KSV ATTENSION Theta Lite Optical Goniometer. The size of the drop was maintained at ~180 μm. Three tests were performed for each sample at ambient temperature.

2.2.1.6 Roughness measurements setup

The steel samples were scanned by a 2D contact type profile meter (Veeco Dektak 6M stylus, USA) which measures the roughness values in μm scale in X-Y dimensions.

3×3mm^2 length were scanned on the steel samples and the average values were taken after three measurements of each sample.

2.3 Materials

The carbon steel alloy utilized in the current study to study the corrosion was obtained from Al AHDAB Iraqi Oil Field Company in the form of pipe and its composition is shown in Table 2.1. The specimens were cut into squares of 10*10 mm^2 with 2mm thickness. The surface was grinded with 180-grit SiC paper and then polished with 320, 400, 600, 1000 µm grit size silicon carbide paper until a coarse scratch were removed.

Table 2.1 Chemical composition (wt%) of steel sample

elements	C	Si	Mn	P	Cr	Mo	Fe
%	0.0946	0.0204	0.903	0.00054	0.0353	0.0222	Balance

2.3.1 Methods

The pH of DIW was adjusted (ranging from pH4 to pH7) by adding drops of HCl or NaOH. Prior to the immersion test and electrochemical measurements, the samples were rinsed with alcohol and dried with air.

Potentiodynamic and potentiostatic scans were obtained to understand the electrochemical behavior of carbon steel corrosion. Potentiostatic scans (current versus time) were obtained for 1800 s. The density and the average area in the experimental setting were taken 7.85 g/cm^3 and 1 cm^2 respectively. The tests were conducted in 250mL DIW

having different pH values and concentrations of H_2O_2. After the potentiostatic scans the samples were washed with DIW and dried with nitrogen.

Potentiodynamic polarization were implemented on the steel plate samples in four different pH values and H_2O_2 solutions in 200 ml solutions which were already prepared prior to the scan. The voltage of open circuit delay was measured before starting the polarization scans. Potentiodynamic scan output signal (current Im) was collected with the parameters listed in Table 2.2.

Table 2.2. Potentiodynamic scan parameters.

total scan period (min)	input potential (V)	scan rate (mV/s)	Scanning step (mV)
45	-0.5 to 1.6	50	1

The V-logI curves were plotted and Tafel data were evaluated for all scan, which were utilized to determine the I_{corr}, E_{corr} and corrosion rate.

The samples were prepared, with a mechanical polishing, CMP treated samples with (10% SiO_2+ 3% H_2O_2+pad) and CMP treated samples with (3% H_2O_2+ abrasive paper 80μm) were tested for dynamic corrosion in pH adjusted DIW. The flow velocity was calculated using the digital flow meter. The steel samples were placed at the bottom of the pipe at the same level with the tube surface.

A tabletop Tegrapol-31 polisher was used for CMP process and Figure 3.2.a demonstrates the 2-D standard CMP machine. A commercial silica based slurry (SiO_2) 10 wt.% obtained from BASF, SE company in Germany was utilized in experiments. The pH

values were adjusted according to the selected nanoparticle's isoelectric point (IEP) which is equal to 4 to ensure the stability during the polishing process. The downforce was set 80 N on holder having four samples in it. The rotational speed was 120rpm and the time of test was adjusted to 3.00 minutes. Also, three sizes of sand papers (silicon carbide, 80µm, 150µm, 320µm) were utilized in CMP process with hydrogen peroxide to investigate the effect of the oxidizer with these sand papers on the performance of CMP.

CHAPTER III

EVALUATION OF STATIC AND ELECTROCHEMICAL CORROSION IN PETROLEUM PIPELINES

3.1 Introduction

Water with higher conductivity is considered to be more corrosive than water with lower conductivity, as corrosion is an electrochemical reaction. It is evident from the higher corrosion in seawater as compared to fresh water. However, steam condensate and distilled water are also considered as highly corrosive [122].

In this chapter, static corrosion of steel samples was evaluated after mechanical polishing with different abrasive papers and CMP with and without of hydrogen peroxide using polymeric pad with silica slurry. The corrosion tests were conducted by immersion of the samples in DIW with different pH values for seven days and the corrosion rate was determined through weight loss measurements after every 24 hours. Since the corrosion behavior of metals is attributed to the electrochemical reactions, it is vital to study the electrochemical characteristics of metals during corrosion tests to understand the mechanism and rate of the corrosion process [123]. Experimental

3.1.1 Static corrosion

Static corrosion tests were conducted by dipping samples for 7 days in a DIW with different pH values as shown in Figure 2.2. The corrosion rate was measured by the weight loss every 24 hours. The samples utilized had exposed surface area of 10*10 mm^2. Before

measuring weight loss, the samples were rinsed with DIW and dried with pressurized air. Corrosion rates were calculated by expression:

$$V_a = C \times \frac{Wo - W}{\rho A t} \qquad 3.1$$

where, V_a is the corrosion rate (mm/y), C is the conversion factor (8.76×10^4), W_o is weight of sample before test(g), W is weight of sample after test(g), ρ is the density of the sample 7.85 $g.cm^{-3}$), A is working area of the specimen (cm^2), t is testing time (24 hours in our case).

3.1.2 Electrochemical measurements

In a testing system, an electrochemical (polarization) cell is setup as shown in Figure 3.1 which consists of an electrolyte solution, a reference electrode, a counter electrode, and the metal substrate of interest connected to the working electrode. The electrodes are connected to an electronic instrument Gamry potentiostat. All the electrodes are immersed in the electrolytic solution, which is usually a solution that very closely resembles the materials actual application environment[124].

3.1.2.1 Potentiostatic measurements

A potentiostatic scan allows controlled polarization on metal surfaces where constant potential is applied between the sample (working electrode) and the reference electrode. The reference electrode is utilized to monitor and maintain potential at the electrode surface. The potentiostat monitors ionic current passing through the electrolyte solution among the counter electrode and the working electrode, and electron current passing through the counter electrode and the working electrode. The resultant current

measured on the sample's surface is plotted versus time. Depending on the surface characteristics and the applied potential in reference to critical (pitting) potential, the response can indicate film growth (passivation), pitting or breakdown as demonstrated in Figure 3.1.

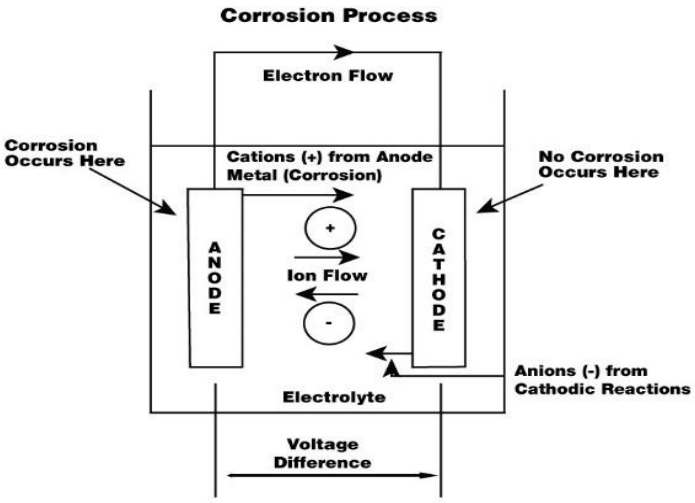

Figure 3-1 Electrochemical measurement schematic [125].

3.1.2.2 Potentiodynamic polarization

Potentiodynamic polarization method provides a scientific insight to charge transfer reaction in an electrochemical corrosion reaction. An electrical current is passed through an electrochemical cell, which causes deviation of the potential of the working electrode from the equilibrium potential and is termed as the polarization. To study the corrosion behaviors, its parameters are computed by Tafel extrapolation. The potential difference between the polarized (working) electrode and un-polarized (equilibrium) electrodes is known as over potential (ŋ). Figure 3.2 shows Stern diagram for electrochemical polarization curve showing Tafel extrapolation, which relates to the reaction kinetic parameters. This graphical representation is helpful to understand the

electrochemical behavior of polarized working electrode in an electrolyte containing hydrogen (H^+) ions. Corrosion parameters are calculated via extrapolation of the linear portion of the anodic and cathodic lines in Tafel polarization curves. Cathodic Tafel slope (βc) and anodic Tafel slope (βa) are measured from smaller linear parts of the cathodic and anodic curves respectively. The points of intersection of both the curves are termed as corrosion current density (I_{corr}) and corrosion potential (E_{corr}), which is steady state potential [126].

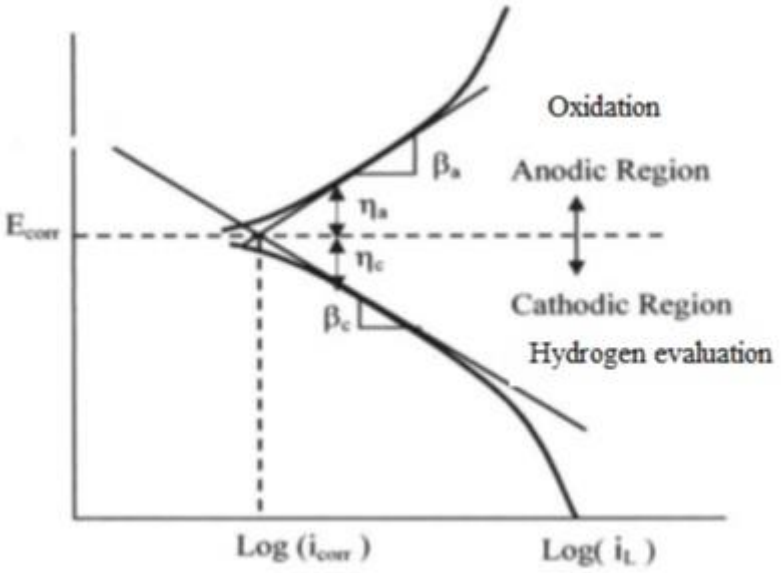

Figure 3-2 Stern diagrams for electrochemical Tafel extrapolation [126].

This potentiodynamic non-linear Tafel curve is divided into two parts,

(i) If $E > E_{corr}$, the upper curve represents the anodic polarization behavior due to the oxidation of the metal.

(ii) If E < E_{corr}, the lower curve represents the cathodic polarization due to the hydrogen evolution.

Due to the corrosion process, the anodic and cathodic reactions are combined on the metal electrode surface at a current density known as corrosion current density (I_{corr}). The potential changes from steady state corrosion potential (E_{corr}) for the anodic and cathodic current densities are expressed as,

$$I_a = I_{corr} exp\left[\frac{2.303(E - E_{corr})}{\beta_a}\right] \quad 3.2$$

$$I_c = I_{corr} exp\left[\frac{-2.303(E - E_{corr})}{\beta_c}\right] \quad 3.3$$

let we assume that the current density applied is,

$$I = I_a - I_c \quad 3.4$$

Substitute the expressions of I_a and I_c to yield ***Buttler-Volmer equation***, which explains the kinetics of the electrochemical corrosion.

$$I_a = I_{corr}\left\{exp\left[\frac{2.303(E - E_{corr})}{\beta_a}\right] - exp\left[\frac{-2.303(E - E_{corr})}{\beta_c}\right]\right\} \quad 3.5$$

The corrosion current is related to the corrosion rate (CR in mpy), through the following equation,

$$CR = \frac{0.13\, I(E.W)}{d} \quad 3.6$$

Where E.W.= equivalent weight of the corroding species in grams.

d = density of the corroding species, g/cm^3.

I = corrosion current density, $\mu A/cm^2$

3.1.3 Surface characterization

3.1.3.1 Surface roughness characterization

The surface roughness was determined using DEKTAK 6M stylus profile which measures the roughness values of the steel plates in μm scale in X-Y dimensions. $3\times3mm^2$ length were scanned on the steel samples and the average values were evaluated after three measurements of each sample.

3.1.3.2 Hardness measurements

The hardness of steel samples after MP and CMP treatments were evaluated using Vickers hardness test protocol with ARS9000 Full Automatic Micro hardness testing system (Future Teach, FM-300e, Kanagawa, Japan) with applied load of 1000 g. Three values were taken on each sample to calculate the average hardness value.

3.1.3.3 Wettability analysis

The steel substrate was considered for wettability after CMP treatments over contact angle measurements with DIW. KSV ATTENSION Theta Lite Optical Goniometer was used to measure the contact angles via sessile drop technique. The size of the drop was maintained at ~1.6 mm. Three tests were performed for each sample at ambient temperature to calculate the average value.

3.1.3.4 Surface energy and Work of adhesion

Surface free energy of the solid material is equal to surface tension of the liquid which is in contact with the solid surface. Surface wettability properties were determined through the contact angle of the liquid which depends on the type of the liquid utilized. In order to determine the surface energy of the steel samples, contact angle measurement was used. For this purpose, the contact angles of DIW was on the steel surface were determined. The average of three test performed for each sample at a room temperature are reported. Furthermore, work of adhesion was also evaluated as another useful measure to calculate the adhesion propensity of the surface.

Based on the utilized liquid the contact angle between the surface and liquid is changing and surface wettability properties were identified through the contact angle. Contact angles were measured to find the energy of the surface for treated titanium materials, including Lewis acid-base theory [127]. Moreover, the work of adhesion was counted as an extra helpful measure to determine the adhesion ability of the surface. Mathematically work of adhesion is manifested as:

$$\gamma_{sl} = \gamma_s + \gamma_l - W_a \qquad 3.7$$

Where the γ and W_a are the interfacial tension between the phases (surface free energy) and the work of adhesion, respectively. Also, subscripts *s* and *l* are referring for the phases for solid and liquid respectively. To determine the *Wa* for a substrate, three interfacial tension values are needed. Mentioned interfacial tensions can be evaluated based on the theory suggested by Van Oss et. al. [128]. This theory contains the Lifshitzs-van der Waals (LW) and polar acid-base (AB) interactions, written in equation 3.8;

$$\gamma_s^{tot} = \gamma_s^{LW} + \gamma_s^{AB} \qquad 3.8$$

The calculation of all aforementioned parameters is well explained by Massaro et al. [129] and Braceras et al. [130].

3.2 Results and discussion

3.2.1 Static corrosion evaluation of steel mechanically polished at different pH values

Figure 3.3 illustrate the relationship between the corrosion rate and the time of immersion. It can be observed that the corrosion rate is high after the first 24 hours for all the samples and it decrease with the increasing immersion time because of the passive layer formation on the surface of the metal which prevents it from further chemical attack. High CR values at the beginning in the region of active corrosion was caused by high interaction between the metal surface and the medium. Moreover, in the range pH 4-7 the behavior of the corrosion rate of samples at the beginning was found to nearly similar.

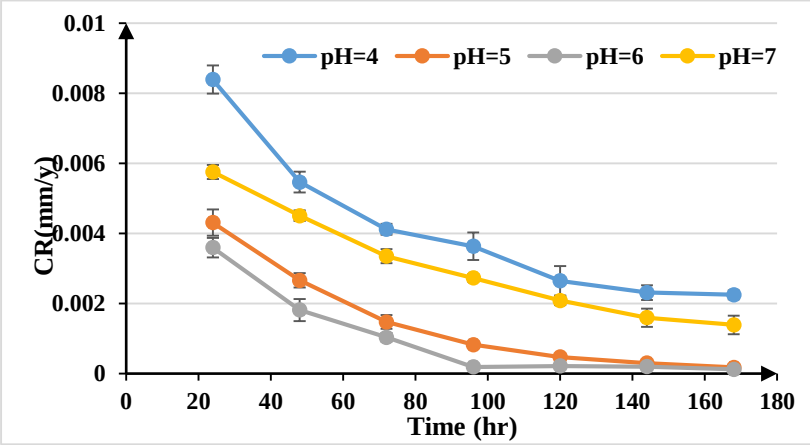

Figure 3-3 Corrosion rate as a function of time of steel samples mechanically polished

3.2.1.1 Static corrosion evaluation of steel chemical mechanical polishing

Figure 3.4 illustrate the relationship between the corrosion rate and the time of immersion. It can be seen that the corrosion rate is high after the first 24 hours for all the samples and it decrease with the increasing immersion time because of the passive layer formation on the surface of the metal which prevents it from further chemical attack [131]. High values of CR at the beginning in the region of active corrosion were caused by high interaction between the metal surface and the medium. Moreover, in the range pH 4-7 the behavior of the corrosion rate of samples at the beginning was found to nearly similar. After two days of immersion a decrease in corrosion has been observed which is a result of an increase in the formation of corrosion products over time. Since the corrosion tests of this part under study are conducted in static conditions, so this layer grows thicker over time and thus the corrosion rate decreases [132]

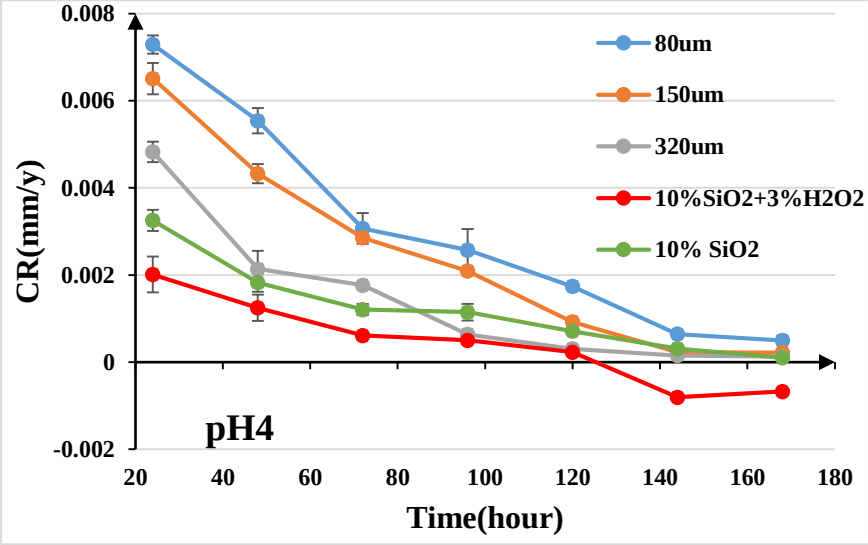

Figure 3-4 Static corrosion rate as function of time at pH4 at different abrasive papers CMP treated

Figure 3.5 demonstrates corrosion rate as function of immersion time, at pH=5 for CMP treated samples using abrasive papers (80,150,320µm) in the presence of 3% H_2O_2 and polymeric pad with the presence of silica slurry It can be detected that the corrosion rate of the steel samples was high during first two days and then decreases with time. It can also be observed that the corrosion of the steel samples with 80um abrasive paper still has the highest value while lowest corrosion has been detected at 10% wt. silica slurry with the presence of 3% H_2O_2. The values of the corrosion rate in this case is less than the previous one because of the less acidic nature of the medium.

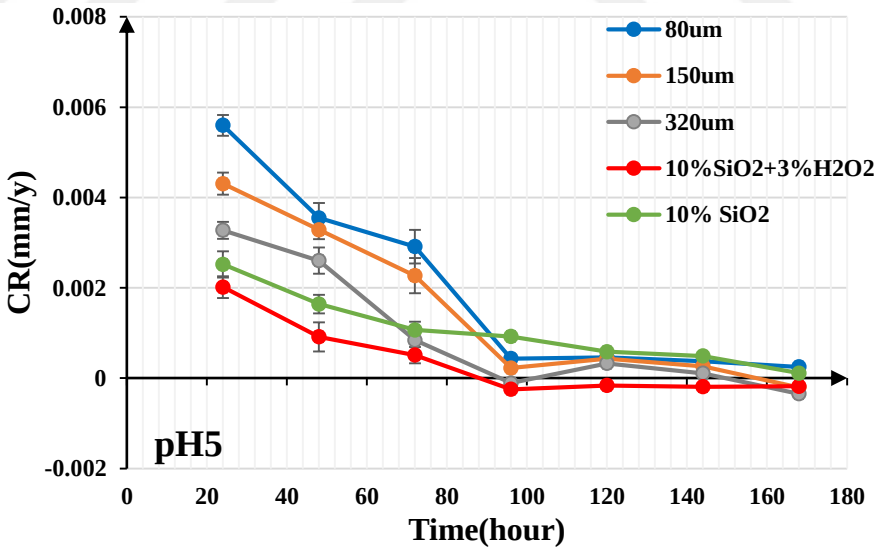

Figure 3-5 Static corrosion rate as a function of time at pH5 at different abrasive papers CMP treated

Figure 3.6 shows the corrosion rate as function of immersion time, at pH=6 for CMP treated samples using abrasive papers(80,150,320µm) in the presence of 3% H_2O_2 and polymeric pad with the presence of silica slurry It can be observed that the corrosion

rate of the steel samples was high during first two days and then decreases with time. It has been detected that the corrosion of the steel samples with 80um abrasive paper still has the highest value while lowest corrosion has been observed at 10% wt. silica slurry with the presence of 3% H_2O_2. The corrosion rate of the steel samples at pH=6 has the lowest value among the other medium because it is the natural pH. Moreover, the protective layer grows faster after two days in case of CMP treated samples with silica slurry in the presence of oxidizer which means that this combination increases the corrosion resistance.

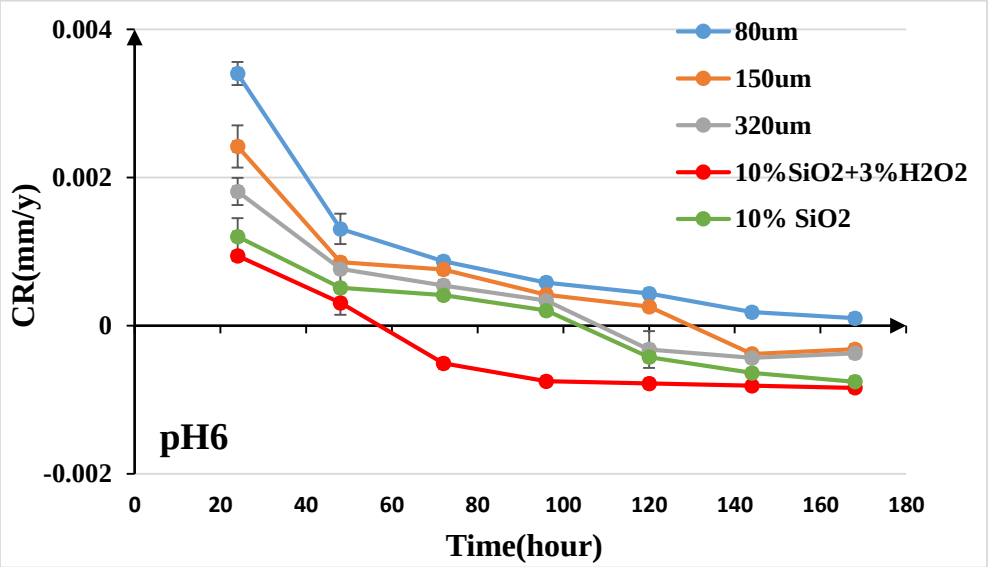

Figure 3-6 Static corrosion rate as a function of time at pH6 at different abrasive papers CMP treated

Figure 3.7 demonstrates corrosion rate as function of immersion time, at pH=7 for CMP treated samples using abrasive papers(80,150,320um) in the presence of 3% H_2O_2

and polymeric pad with the presence of silica slurry It can be noticed that the corrosion rate of the steel surface was high during first two days and then decreases with time. It has been observed that the corrosion of the steel substrate with 80um abrasive paper has the highest value while lowest corrosion has been observed at 10% wt. silica slurry with the presence of 3% H_2O_2. Moreover, the steel samples after 72 hours go to a stable and lower value of corrosion.

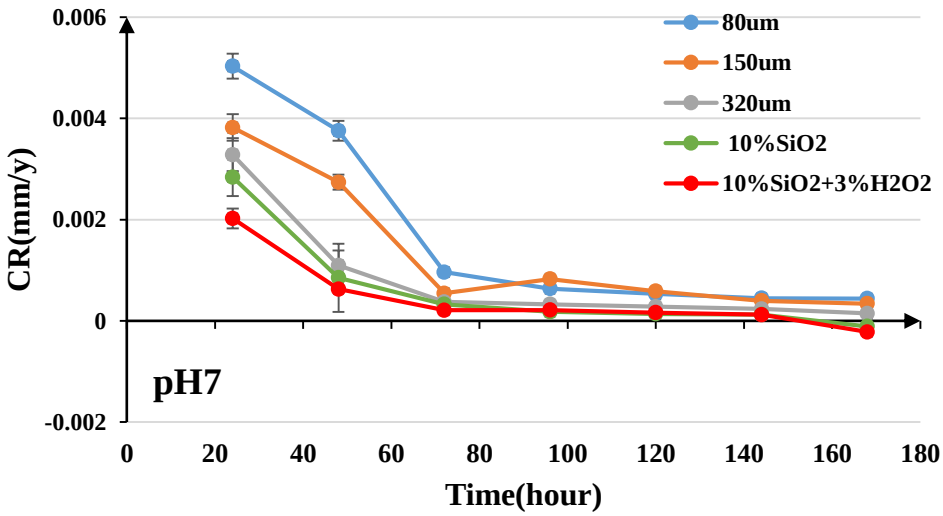

Figure 3-7 Static corrosion rate as a function of time at pH7 at different abrasive papers CMP treated

3.2.2 Evaluation of electrochemical corrosion mechanically polished at different pH values

Potentiostatic scans and potentiodynamic polarization techniques were utilized to understand the electrochemical behavior of the corrosion of carbon steel. DI water at different pH values was used as electrolyte. The pH values of the electrolyte were adjusted to the desired values using 0.01 M HCl and/or 0.01M NaOH. A three electrodes

cell with a Gamry 1000 Interface potentiostat which contents saturated calomel electrode (SCE) was used as reference, a helical platinum wire as counter electrode and steel sample was used as working electrode.

3.2.2.1 Potentiostatic measurements

The period of scan was set to 1800 seconds with an input potential of 0V vs. E_{ref}. The total volume of electrolyte used was 200ml in every test for every pH value. Figure 3.8 illustrates the potentiostatic scans of the samples in DIW at different pH values. Generally, carbon steel shows a passive behavior, that is, it becomes covered by an oxide layer that protects it from corrosion. However, in the acidic medium, that passive layer formation is not promoted and the surface is prone to corrosion and with the increasing time of exposure higher current is observed. Also, it has been noticed that a sharp increase of current with increasing time at pH=4 which indicate that the corrosion rate still increases with time, while at pH=7 there is a slight increase of the current with time at the beginning, then fluctuating increment in pH=7 and finally goes to a near steady state with time. Moreover, there is an increase of the current during the test with time at pH=5 but with a lower slope than pH=4. On the other hand, the low and constant slope of the curve which is corrosion rate of the pH=6 case, indicates the creation of protective layer on the surface of the steel. These results show a high degree of congruence with the results obtained through the potentiodynamic polarization as shown in figure 3.10 below.

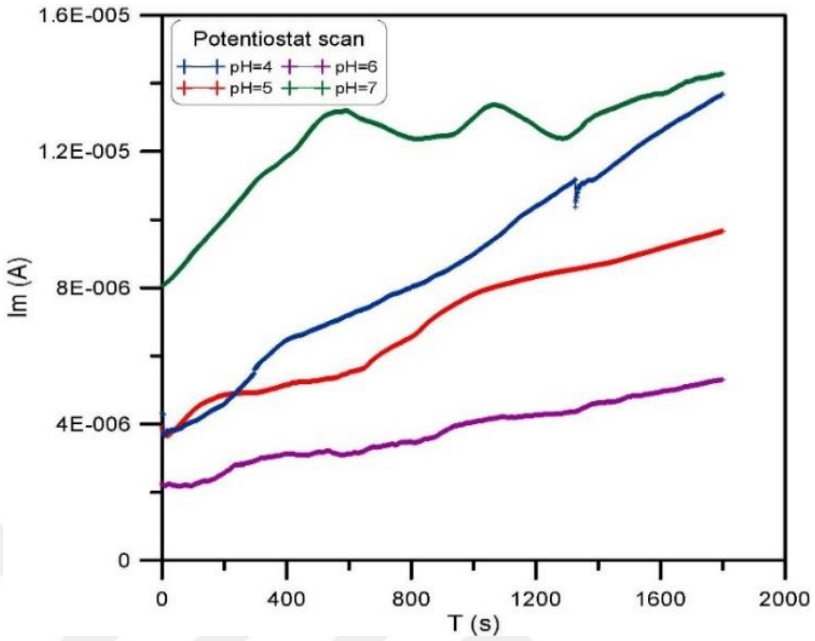

Figure 3-8 Potentiostatic (Im vs time) of steel sample at different pH

3.2.2.2 Atomic Force Microscopy

The surface morphology of the steel samples was evaluated via Atomic Force Microscopy (AFM) after potentiostatic tests with a scan area of 10*10μm and the scan speed was 5μm to evaluate the average surface roughness of three measurements for each sample. Figure 3.9. (a) and 3.9. (b) illustrate the surface roughness and the 3D AFM images after potentiostatic scans at different pH values. It has been observed that the mean roughness decrease with the increase in pH values. According to the fact that one of the key factors of corrosion is acidic medium of the environment, subsequently the surface roughness of steel is affecting by variation of pH value. Inspection of the results demonstrates that reduction of roughness can be attributed to the creation of less oxide layer on the surface as the environment changes from the acidic to the basic one [36].

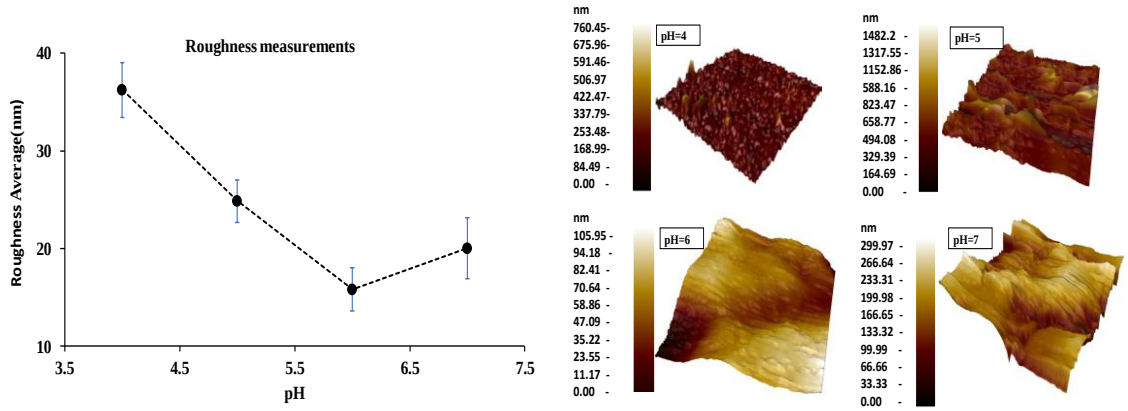

(a) (b)

Figure 3-9 (a) Root mean square (RMS) surface roughness measurements of the steel samples treated by static corrosion at PH 4, 5,6 and 7. (b) AFM surface micrographs of the samples treated at pH 4, 5, 6 and 7.

3.2.2.3 Potentiodynamic polarization

Figure 3.10. illustrate potentiodynamic polarization curves of steel samples immersed in DIW at pH 4, pH5, pH 6 and pH 7. The electrochemical factors like corrosion potential (E_{corr}), corrosion current density (I_{corr}) and corrosion rate in (mm/year) are presented in table 3.1. A significant increase in the rate of corrosion with decreasing of pH has been observed. Lowest corrosion has been observed at pH=6 where an oxide layer growth on the surface prohibits the chemical attack and make the corrosion minimum.

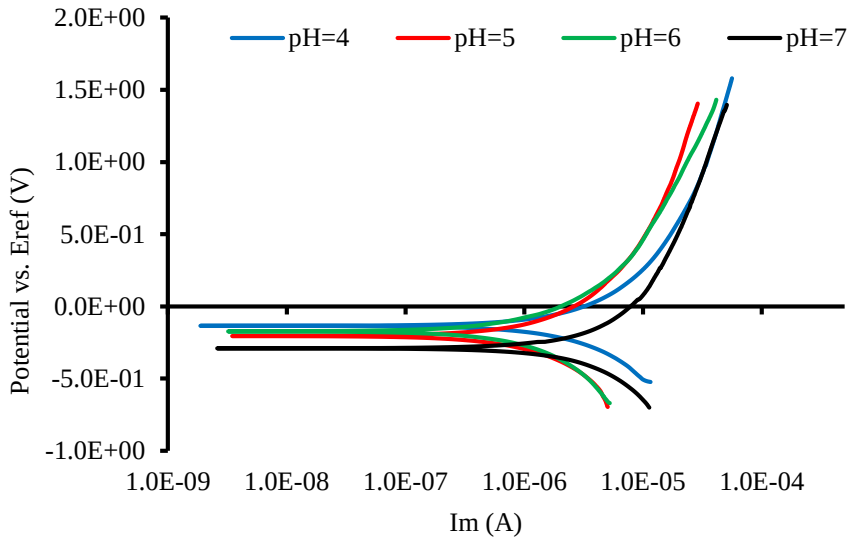

3-10 Potentiodynamic polarization curves of steel samples at different pH values.

Table 3.1 Tafel plots of steel sample based on potentiodynamic data analyses.

Tafel plot variables	**pH=4**	**pH=5**	**pH=6**	**pH=7**
I_{corr}(µA)	32.20	22.20	8.710	16.680
E_{corr}(mV)	-207.0	-143.0	-172.0	-290.0
CR(mpy)	15.053	9.84	4..07	7.83

3.2.3 Evaluation of electrochemical corrosion chemical mechanical polishing at different pH values.

3.2.3.1 Potentiodynamic polarization

Figures (3.11-3.14) demonstrate potentiodynamic polarization for carbon steel CMP treated with different abrasive papers (80, 150, 320) with the presence of 3wt.% H_2O_2 and 10%wt. silica slurry with the polymeric pad and 10%wt. silica slurry+3%wt.H_2O_2+polymeric pad. The potentiodynamic polarization of CMP treated samples at pH=4 are presented in Figure 3.11. The corresponding E_{corr}, $I_{corr,}$ and CR are listed in Table 3.2. Aforementioned values were calculated by the extrapolation method on the Tafel plot. At pH=4, it can be noticed that with change of the abrasive paper size from 80µm to 320µm with 3% H_2O_2 and then using the polymeric pad with H_2O_2 and silica slurry I_{corr} decreased from 44.8µA/cm^2 to 11.3µA/cm^2, Ecorr raised from -310V to -306V and the corrosion rate decreased from 20.9 mpy to 5.286 mpy.

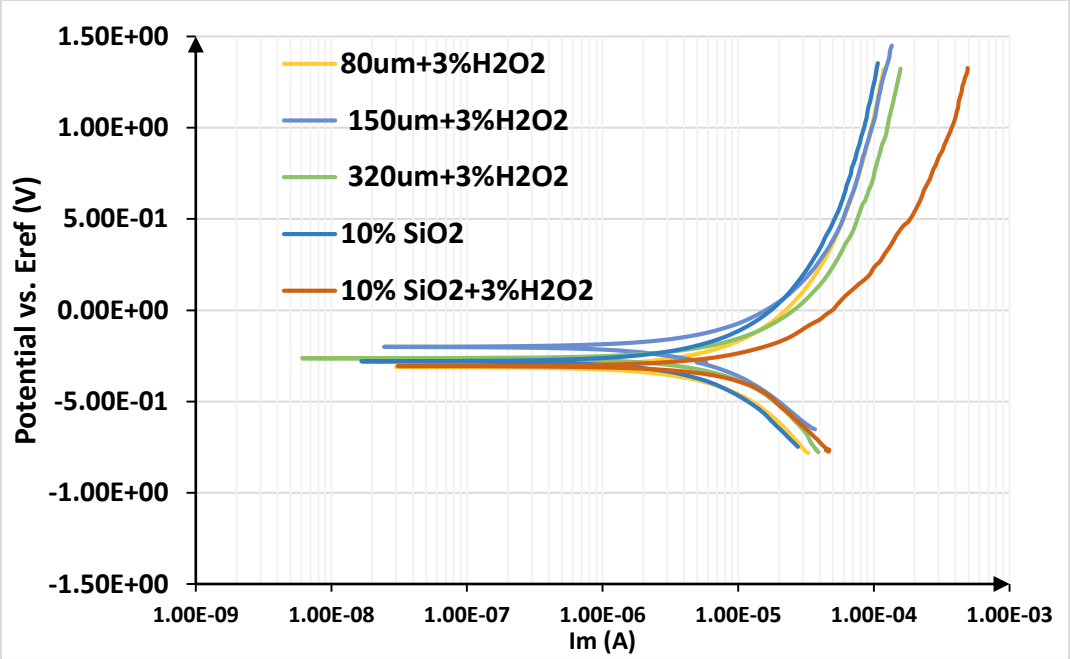

Figure 3-11 Potentiodynamic polarization of CMP treatment at pH=4.

Table 3.2 Tafel plot data of different CMP treatment at pH=4.

Tafel plot variables	3%H_2O_2+ 80μm	3%H_2O_2+ 150μm	3%H_2O_2+ 320μm	10% SiO_2	10% SiO_2+3%H_2O_2
I_{corr}(μA)	44.80	33.50	31.60	25.60	11.30
E_{corr}($_m$V)	-310.0	-200.0	-263.0	-279.0	-306.0
CR(mpy)	20.92	15.6	14.9	11.74	5.286

The potentiodynamic polarization of CMP treated samples at pH=5 are shown in Figure 3.12. The Tafel plot data are listed in Table 3.3. Aforementioned values were calculated by the extrapolation method on the Tafel plot. When the pH value increased to pH=5, with the decreasing of abrasive size and with the silica slurry, it can be seen that Icorr decreased from 7.1μA/cm^2 to 2.74μA/cm^2, E_{corr} raised from -280V to -249V and the corrosion rate decreased from 3.32mpy to 1.282mpy.

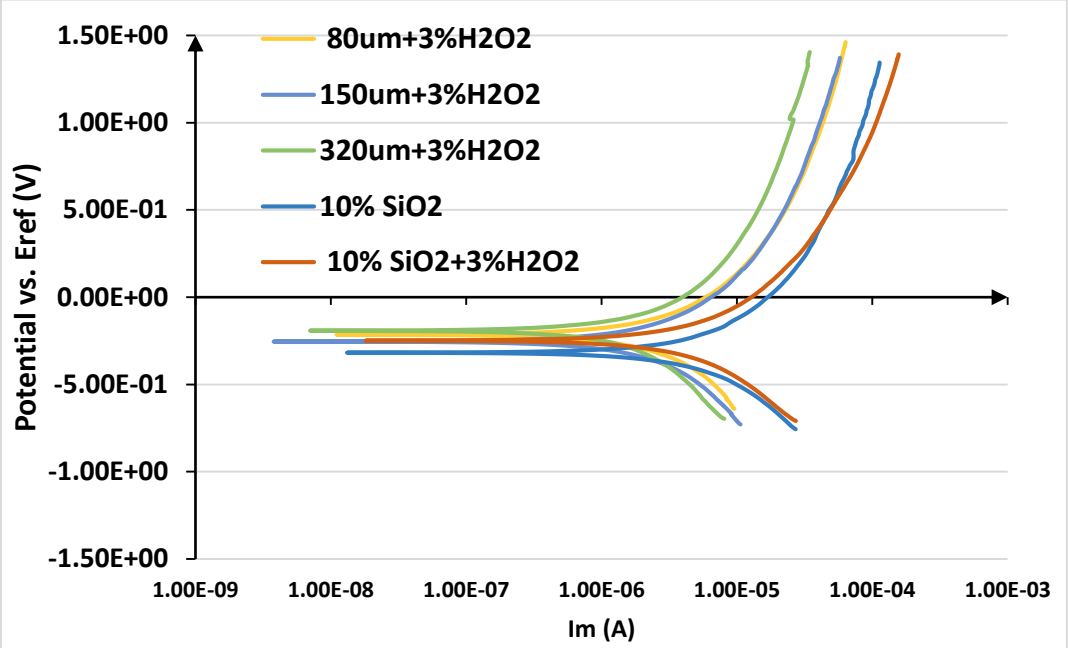

Figure 3-12 Potentiodynamic polarization of CMP treatment at pH=5.

Table 3.3 Tafel plot data of different CMP treatment at pH=5.

Tafel plot variables	3%H_2O_2+ 80µm	3%H_2O_2+ 150µm	3%H_2O_2+ 320µm	10% SiO_2	10% SiO_2+3%H_2O_2
I_{corr}(µA)	7.200	4.770	4.720	3.370	2.740
E_{corr}($_m$V)	-280.0	-254.0	-192.0	-318.0	-249.0
CR(mpy)	3.3214	2.231	2.206	1.574	1.284

According to the results listed in Table 3.3, it can be realized that with the change of the abrasive paper the corrosion current density decreases. While this occurs, the corrosion potential increases, which can be described by the decreasing in the level of anodic current density and as a result decreasing the corrosion rate.

The impact of different abrasive paper with the presence of hydrogen peroxide and the polymeric pad with or without the hydrogen peroxide in the silica slurry on the

electrochemical properties of the steel samples at pH=6 are shown in Figure 3.13. The data of corrosion potential (Ecorr), corrosion current density (Icorr) and the corrosion rate were obtained from tafel plot in the software which were listed in Table 3.4. It has been detected that with change of the abrasive paper size from 80µm to 320µm with 3% H_2O_2 and then using the polymeric pad with H_2O_2 and silica slurry Icorr decreased from 2.020 µA/cm^2 to 0.9320 µA/cm^2, E_{corr} raised from -252V to -201V and the corrosion rate decreased from 9.3mpy to 0.43mpy

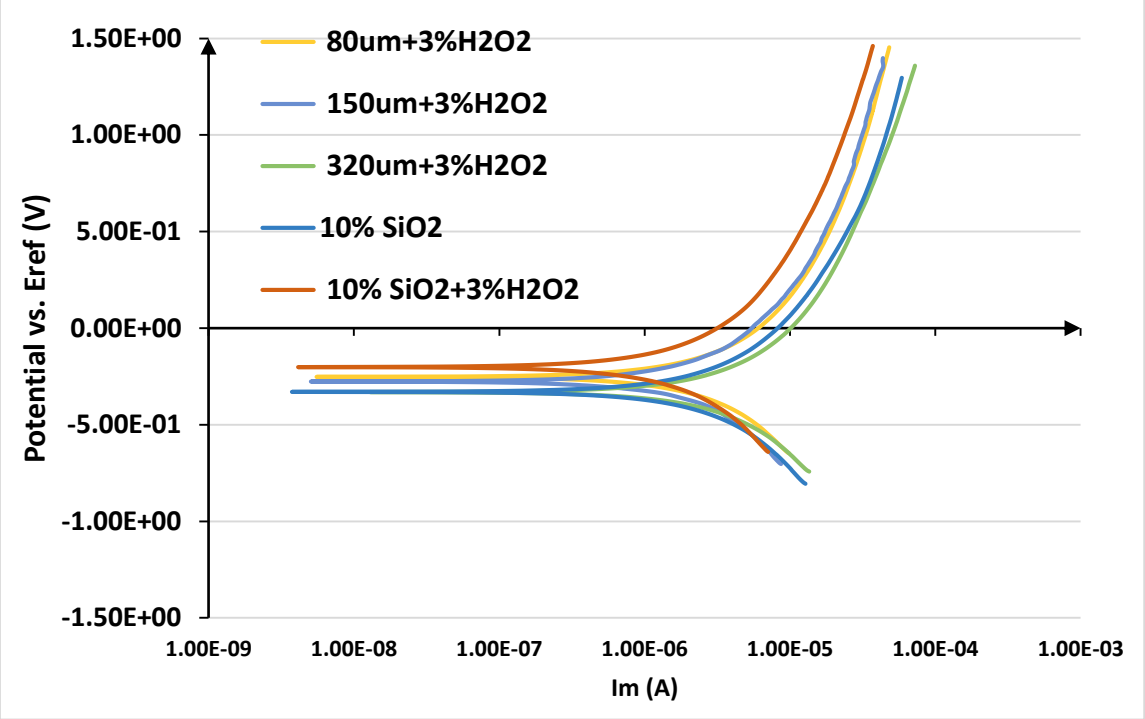

Figure 3-13 Potentiodynamic polarization of different CMP treatment at pH=6.

Table 3.4 Tafel plot data of dıfferent CMP treatment at pH=6.

Tafel plot variables	3%H_2O_2+ 80µm	3%H_2O_2+ 150µm	3%H_2O_2+ 320µm	10% SiO_2	10% SiO_2+3%H_2O_2
I_{corr}(µA)	2.020	1.760	1.520	1.370	0.9310
E_{corr}($_m$V)	-252.0	-276.0	-331.0	-330.0	-201.0
CR(mpy)	0.9470	0.8040	0.6954	0.6289	0.4355

The potentiodynamic polarization of CMP treated samples at pH=7 are displayed in Figure 3.14. The corresponding Tafel plot data are shown in Table 3.5. Aforementioned values were determined by the extrapolation method on the Tafel plot. It can be seen that with change of the abrasive paper size from 80µm to 320µm with 3% H_2O_2 and then using the polymeric pad with H_2O_2 and silica slurry Icorr decreased from 5.350µA/cm^2 to 2.090µA/cm^2 , E_{corr} raised from -215V to -362V and the corrosion rate decreased from 2.52mpy to 0.956mpy

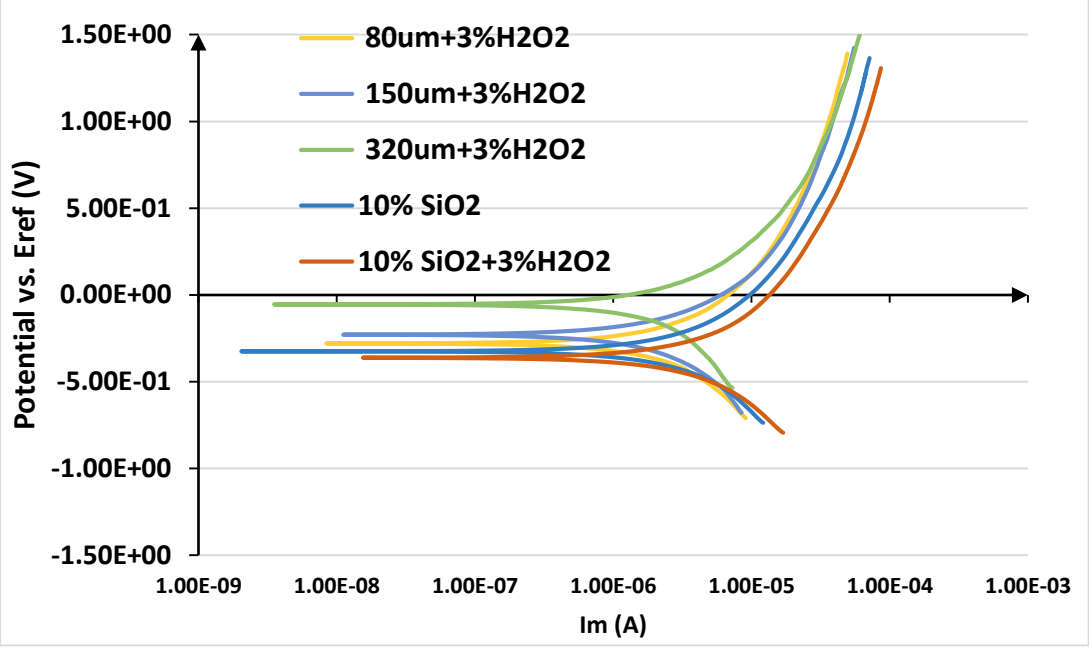

Figure 3-14 Potentiodynamic polarization of different CMP treatment at pH=7.

Table 3.5 Tafel plot data of dıfferent CMP treatment at pH=7.

Tafel plot variables	3%H_2O_2+ 80µm	3%H_2O_2+ 150µm	3%H_2O_2+ 320µm	10% SiO_2	10% SiO_2+3%H_2O_2
I_{corr}(µA)	5.350	4.370	2.460	2.090	2.090
E_{corr}($_m$V)	-215.0	-229.0	-54.80	-325.0	-362.0
CR(mpy)	2.52	2.0400	1.152	0.986	0.97564

3.2.4 Surface characterization

3.2.4.1 Surface roughness characterization

The mean surface roughness as an important function of the various surface treatment methods is shown in figure 3.15. The surface roughness in the case of the mechanically polished sample, which is the baseline, is the highest among the other cases since it was polished with sand-paper (800 µm SiC) with flowing DIW. In the case of samples treated with CMP with 3 wt.% H_2O_2 as an oxidizer in the silica slurry, the smoothest surface among these cases was obtained.

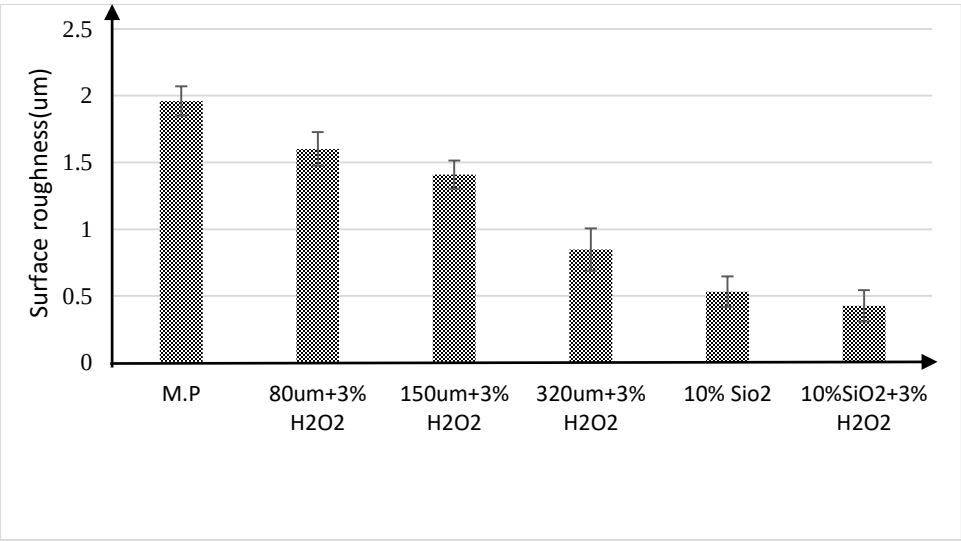

3-15 The average surface roughness of steel samples with different surface treatments.

3.2.4.2 Hardness measurements

The micro hardness testing results for the steel samples are shown in Figure 3.16. The CMP process improved the hardness value compared to that of the MP-process. Samples treated with CMP with an oxidizer in the slurry have the highest hardness values among the treated surfaces, which can be attributed to an oxide film growth on the steel surface. The film formed on the steel surface in the presence of H_2O_2 is composed of two layers. The outer layer is much stronger than the inner layer, which makes these samples harder than those obtained with MP.

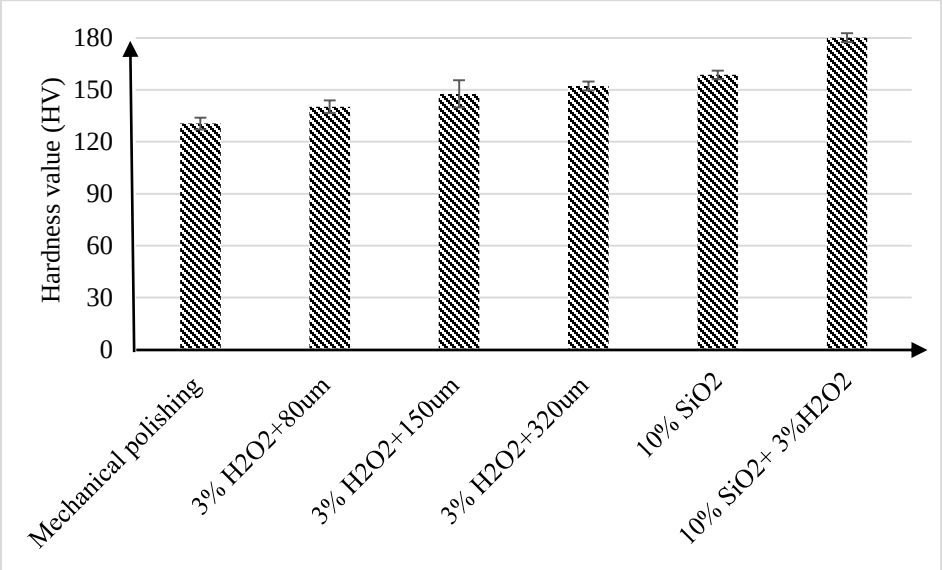

Figure 3-16 Hardness measurements of steel samples with different surface treatments.

3.2.4.3 Wettability analysis

Figure 3.17 demonstrates the wettability behavior of steel samples after different surface treatments. The contact angle value decreases when the surface becomes smoother; thus, the samples chemically mechanically polished with 10% slurry + 3% H_2O_2 show a

higher wettability compared to that of the other cases. Thus, the presence of the oxidizer in the silica slurry increases the contact area between the steel surface and the droplet, which results in a small contact angle.

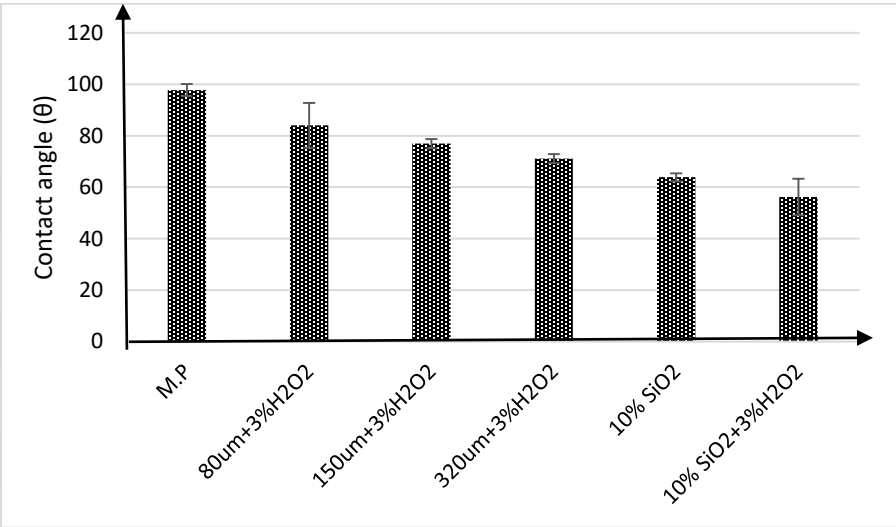

3-17 The wettability analysis of steel samples with different surface treatments.

3.2.4.4 Surface energy and Work of adhesion

Figure 3.18 demonstrates the surface free energy of steel samples with a mechanical polishing and different CMP treatment. It has been detected that the mechanical polishing has the lowest surface energy among the other surface treatment. The presence of H_2O_2 as an oxidizer in CMP treatments with different abrasive paper enhance the surface energy compared to mechanical polishing.

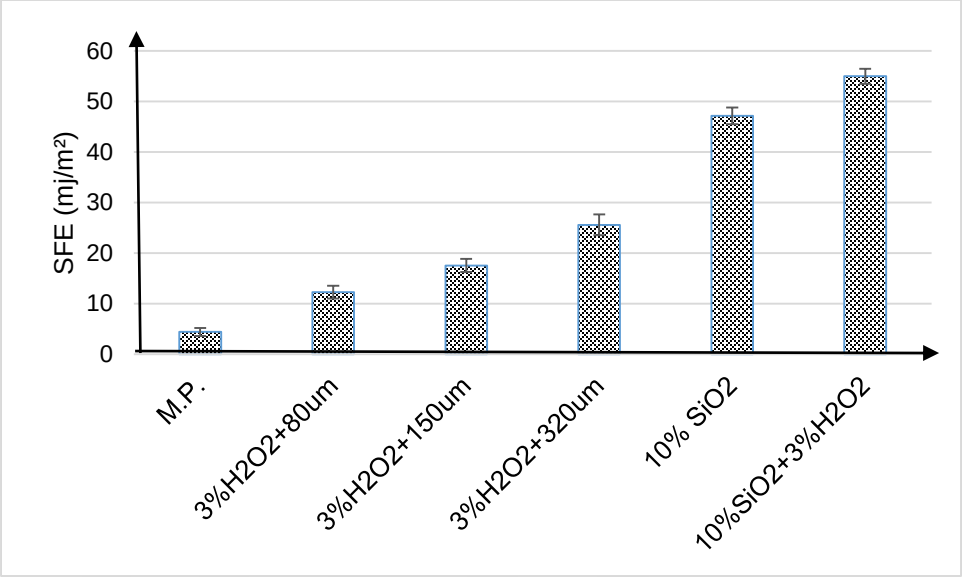

Figure 3-18 Surface energy of steel samples with different surface treatments.

The work of adhesion of steel samples with a mechanical polishing and different CMP treatment is shown in figure 3.19. It has been observed that the mechanical polishing has the lowest work of adhesion among the treated samples. The presence of H_2O_2 as an oxidizer in CMP treatment with different abrasive paper enhance the work of adhesion comparing with the mechanical polishing.

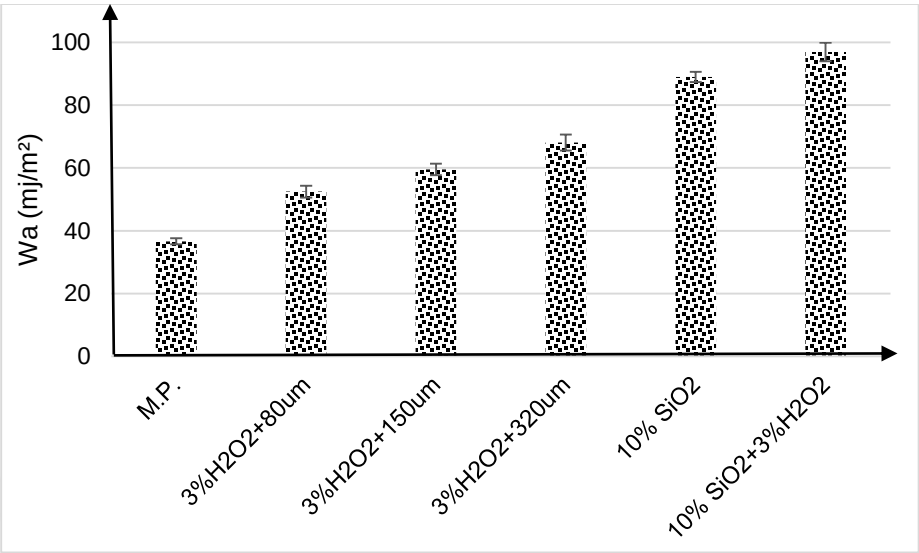

3-19 Work of adhesion of steel samples with different surface treatments.

3.3 Conclusions

In this chapter static and electrochemical corrosion were studied through an experimental set up with different pH values from acid to basic on the corrosion behavior of steel samples. In static tests, it is found that the corrosion rate decreases with increasing time and it was high in the first two days of the test then it decreases after that, but the acidic medium still has the high corrosion rate as compared to basic corrosion rate in basic medium. Moreover, in the active corrosion region the corrosion rate was high for all samples in the static tests. The potentiodynamic polarization measurements suggest that the corrosion rate decreases with increasing pH values going to towards acidic region. AFM measurement shows that the average roughness decrease with the increasing of pH values and vice versa because of the type of corrosion products formed on the sample's surface. On the hand, static corrosion of steel samples CMP treated were tested in the same medium and it has shown an enhanced corrosion resistance of the steel samples compared to mechanically polished samples specially for CMP treated in the presence of H_2O_2 in the

silica slurry. Surface characterization were investigated of steel samples in both cases mechanically polished and CMP treated. The results obtained in surface characterization indicate that the hardness values increase with the CMP and the roughness decreases when the combination of silica slurry and hydrogen peroxide are applied. It has been found that when the surface roughness decreases the corrosion resistance increases. Furthermore, the wettability analysis shows an increase with CMP process comparing with mechanically polished samples.

CHAPTER IV

EVALUATION OF DYNAMIC CORROSION IN PETROLEUM PIPELINES.

4.1 Introduction

The flow rate inside of the pipelines is one of the most important issues which can extensively affect the corrosion rate of the inner surface. If the anodic region is to the wall of the nearby pipe, a galvanic corrosion cell will be created. The inner surfaces of pipes can restrict the smooth flow of fluid, resulting in a localized fluid disturbance. This may lead to rise corrosion rates[133, 134].

4.2 Experimental

4.2.1 Dynamic corrosion

The dynamic corrosion was experimentally measured with the flow loop setup developed in the lab, shown figure 2.4. A flow meter was utilized to measure the flow rate and a pump for providing flow energy to the fluid. The experiments were conducted at three flow rates and 4 different pH values. Each test was repeated three times and the average results are reported. The corrosion rate was calculated by weight loss measurement.

The flow velocity was calculated from the equation of flow rate as follows

$$V = \mathrm{Q}/A \qquad (4.1)$$

where, Q is the flow rate ($m^3.s^{-1}$), A is the cross sectional area of the pipe (m^2), and V is the flow velocity ($m.s^{-1}$). An another important factor influencing the rate of flow induced corrosion is (WSS), which expresses the force per unit area exerted by the fluid on the solid boundary[135-137] . The correlation between the flow rate and the WSS for a single phase flow is well known and is best expressed in terms of non-dimensional parameters i.e. Reynolds number (Re) and the Fanning friction factor (C_f), as given in equation 4.2 below [138].

$$C_f = 0.079Re^{-0.25} \quad 4.2$$

WSS from the friction factor is calculated as:

$$\tau = \frac{\rho C_f V^2}{2} \quad 4.3$$

where ρ is fluid density ($kg.m^{-3}$); V is mean flow velocity ($m.\ s^{-1}$) and $\boldsymbol{\tau}$ is wall shear stress ($N.mm^{-2}$)

The Reynolds numbers, the Fanning friction factor and WSS for each case were calculated as shown in table 4.1. Table 4.1 provides as comparison of the calculated wall shear stress in our developed setup with WSS calculated in Iraqi oil field.

Table 4.1 Wall Shear Stress Calculation

Flow velocity (m.s-1)	Reynolds number(Re)	Friction factor(C_f)	WSS(experimental set up(N/mm^2))	WSS (Iraqi oil field(N/mm^2))
0.55	$1.854*10^4$	$6.77*10^{-3}$	1.012	0.5692
0.74	$2.494*10^4$	$6.2286*10^{-3}$	1.716	1.154
0.96	$3.236*10^4$	$5.893*10^{-3}$	2.707	1.914

It can be observed in Table 4.1 that the evaluated WSS from the experimental setup was in the same range as the WSS in the Iraqi oil field from which the steel samples are obtained. The results obtained for fluid used in our case mimics the real pipe flow corrosion behaviors in real applications.

4.2.2 Roughness measurements

The steel specimens were prepared polishing with 3%wt. H_2O_2 + 80μm grit abrasive and 10%wt. SiO_2 + 3%H_2O_2 with polymeric pad, washed in DIW, ultra-sonicated in DI water for 5 min to eliminate residual SiC particles, degreased with acetone, and dried. The surface roughness was measured using DEKTAK 6M stylus profilometer (for 3×3mm^2 area of the sample) in 2D dimensions. length was scanned on the steel samples and the average values were evaluated after three measurements of each sample.

4.3 Results and Discussion

4.3.1 Dynamic corrosion of steel mechanically polished

Turbulent flow usually affects the surface water chemistry by changing the mass transfer rate of species moving from the bulk to the steel surface and/or vice versa. Figure 4.1, 4.2 and 4.3 show the dynamic corrosion results for steel samples in a range of flow velocities of DIW at different pH values. It has been observed that the rate of corrosion increases with increasing flow velocity. In other words, increasing the wall shear stress along the wall increase the rate of corrosion as shown in Figure 4.1. This variation by th[139].

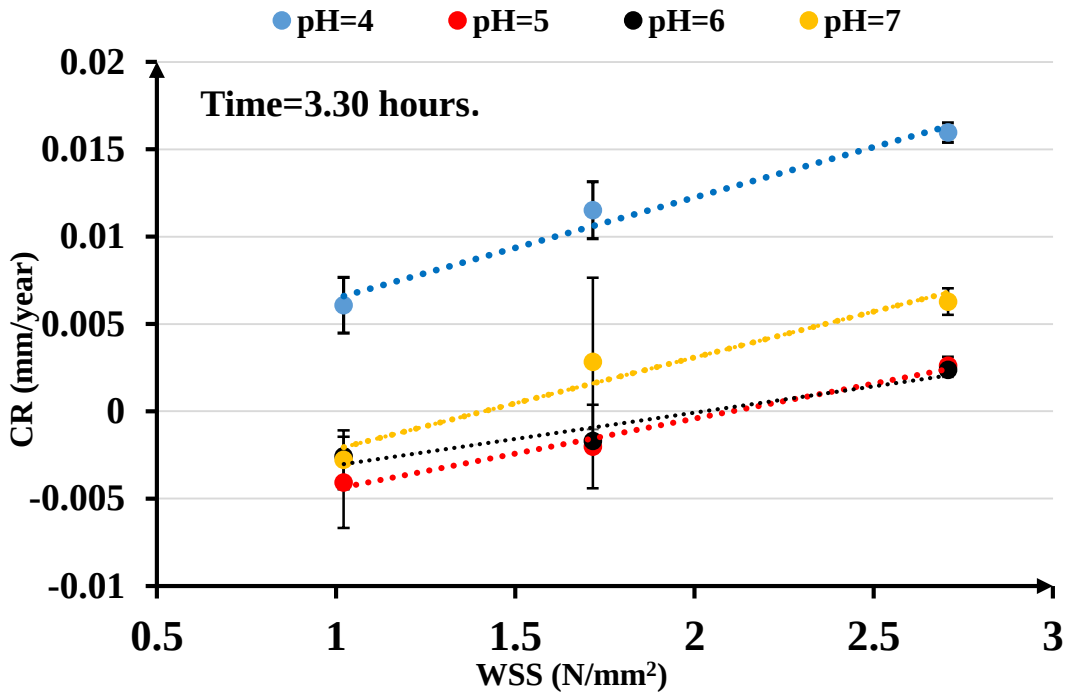

Figure 4-1 The relation between corrosion rate and wall shear stress with different pH values after 3.30 hours. (trend lines are linear)

Higher corrosion rates were observed when the testing time was increased. It has been detected that the corrosion rate at WSS (1N/mm^2) reached 0.005 mm/year after 3.30 hours while it reached 0.015 after 10.30 hours at the same WSS as shown in figure 4.1 and figure 4.3, this gives indication that increasing time test leads to an increase in the corrosion rate specially in the acidic medium. Moreover, it can be seen that in case of dynamic corrosion tests a decrease in the value of pH leads to an increase in the corrosion rate and this is evident with the value of pH=4. These results have a good covenant with those of Rhee [22] The corrosion behavior of the steel samples at pH=7 is similar to the behavior at pH=4 in all times and velocities except that corrosion rate at pH=4 is higher than in pH 7 as shown in figure 4.1, 4.2 and 4.3. However, at pH=6 corrosion is lowest as shown in Figure 4.3. This gives an indication that there is an access amount of corrosion products

growing on the steel surface and these products are denser and work as a protective layer against corrosion.

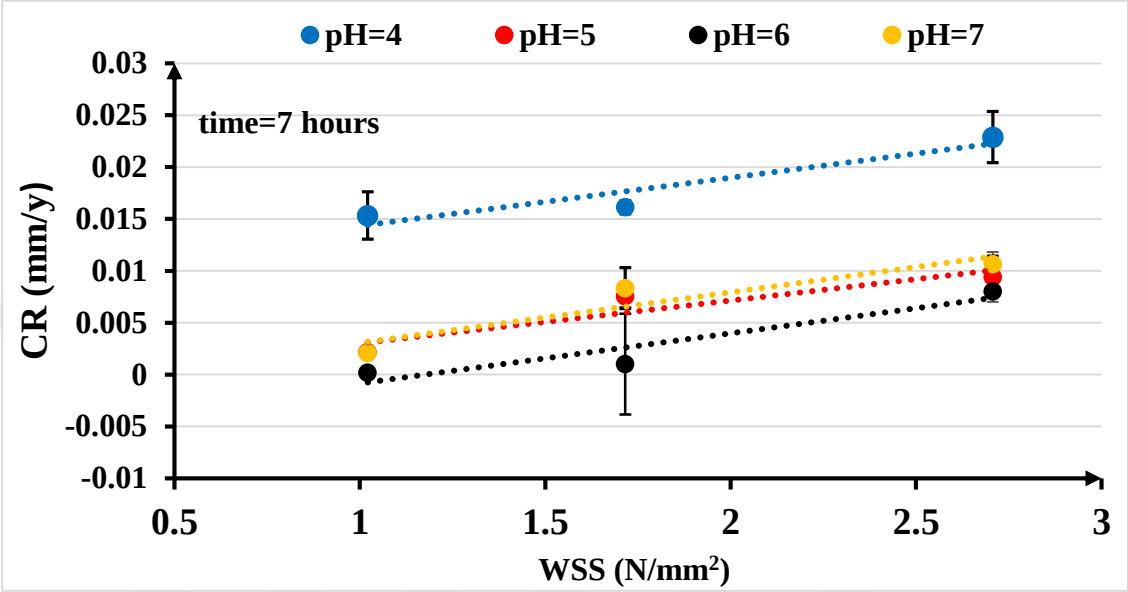

Figure 4-2 The relation between corrosion rate and wall shear stress with different pH values after 7 hours. (trend lines are linear)

The highest corrosion rate was observed at pH=4 and is further accelerated by the increasing velocity as a result of higher interactions between the WSS and the steel surface. The results showed that the corrosion at high velocity but short time give corrosion value less than the value when the time is long as we can see in all the figures. The value reached 0.015 mm/year at time 3.30 hours with WSS (2.75N/mm^2) while it reached 0.025 mm/year at time 10.30 hours at the same WSS which can be attributed to the combined effect of the WSS over longer periods of time as shown in figure 4.1 and 4.3. Similar behavior has been observed by Scheers [36], Fredj and Burleigh [37], Zhen Li and Young [140]

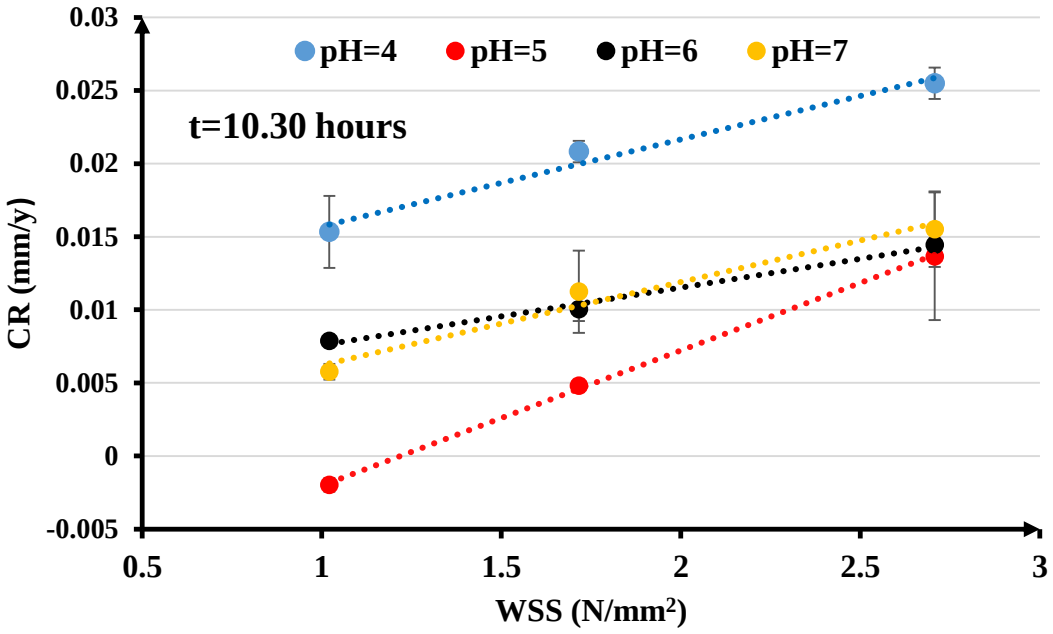

Figure 4-3 The relation between corrosion rate and flow velocity with different pH values after 10.30 hours. (trend lines are linear).

From mechanic's point of view increasing the flow rate increases the friction force and has a significant impact on the surface of the sample installed on the surface of the tube, in the developed setup this means increasing turbulence and finally the mass transfer of the corrosive species from the bulk to the pipe wall which may result in an increase in the rate of corrosion. Moreover, the increased turbulence in the bulk as a result of a high flow rate will bring the faster moving fluid closer to the wall (making the boundary layer thinner), results in a higher velocity gradient and higher WSS [136].The interaction between the surface of the metal and the acid media led to the formation of a visible thin layer on the surface but the increase in WSS as a result of increasing flow velocity leads to the breakage of this layer and which increases the rate of corrosion, this phenomenon was observed for 3.50 hours' tests. However, at pH=5 for lower velocity the corrosion products accumulate on the surface the metal which leads to an increase in the weight of the sample.

4.3.2 Dynamic corrosion for chemical mechanical polishing treated samples

4.3.2.1 Dynamic corrosion for chemical mechanical polishing treated samples with 3%H_2O_2+abrasive paper 80µm

The rate of corrosion was measured as a function of time after utilizing different WSS over the selected pH values and presented in Figure 4.4-4.7. It can be seen that the corrosion rate increases as the WSS increases until certain value (which in this case is 1.75 N/mm2) for all the exposure time and pH values. After the critical WSS the corrosion rate decreases.

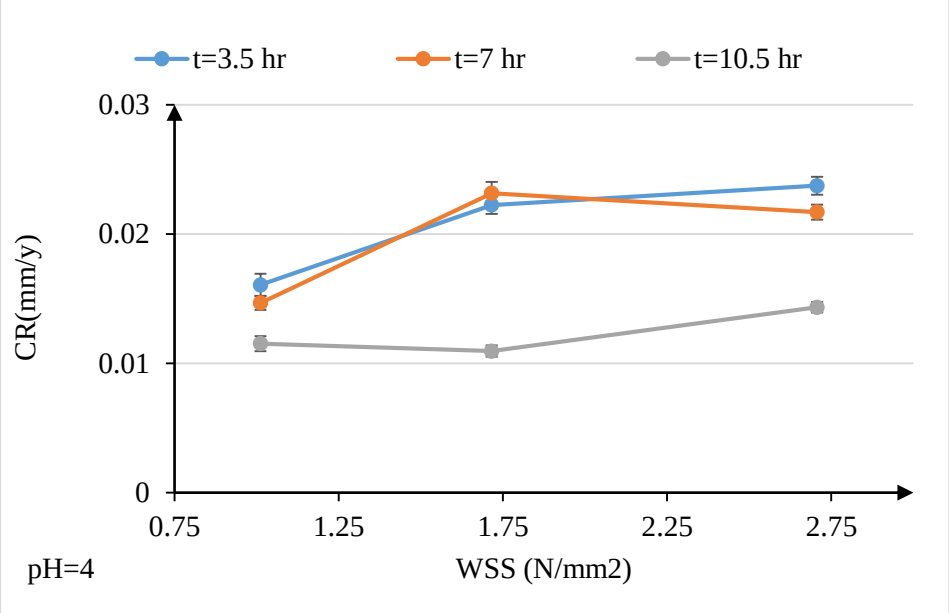

Figure 4-4 Corrosion rate values as function of WSS for CMP treated samples with 80um grit abrasive and 3%H_2O_2 at different test time at pH=4

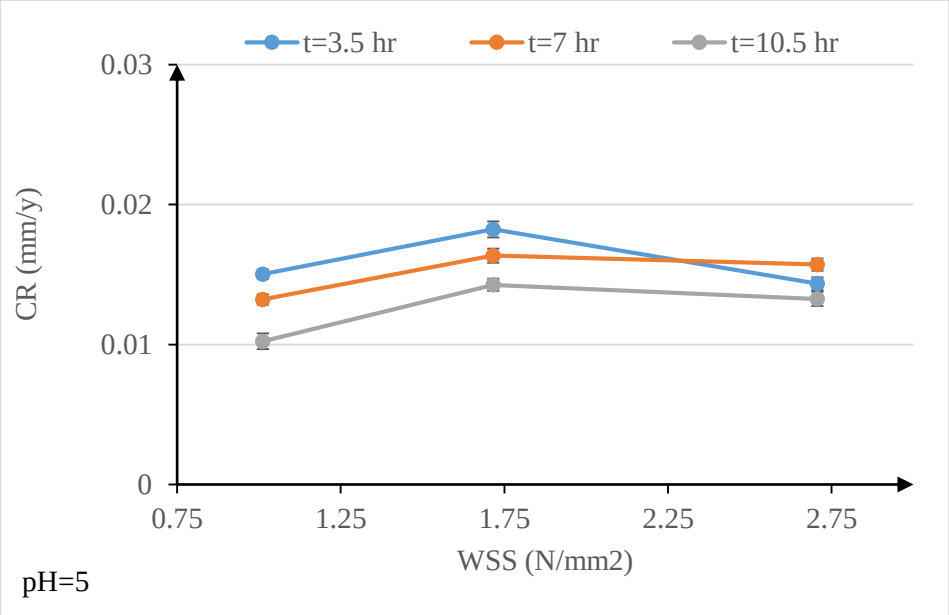

Figure 4-5 Corrosion rate values as function of WSS for CMP treated samples with 80um grit abrasive and 3%H_2O_2 at different test time at pH=5

It is generally considered that the valleys and roughness peaks disturb the viscous layer and the turbulence generated reduces the resistance to mass transfer across the concentration boundary layer[141]. The turbulent eddies, penetrate into cavities on the wall which non-uniformly reduces their momentum due to viscous friction with the wall surface. The non-uniformity within eddies causes the formation turbulence fluctuations in areas and may have relatively high kinetic energies [142]. Fogg and Morse [143] found out that with increase in internal surface roughness of the pipe the maximum flow rate decreases. Increased roughness affects the velocity sensitive corrosion and the corrosion is then mainly affected by environment (chemistry). It has been found that for all cases, the roughness value for steel has increased after corrosion which is due to the formation of corrosion products on the surface. Therefore, the corrosion mechanism here is dominated by pH of the fluid flowing within the pipe i.e. corrosion rate is higher at lower pH for the

same WSS and time duration. Figure 4-6 shows the corrosion rate increases with increase in WSS.

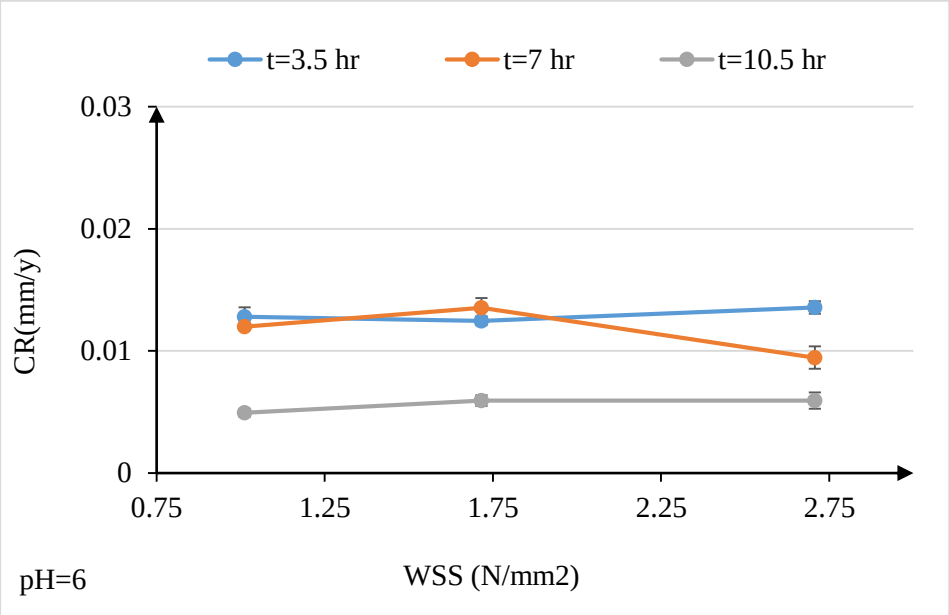

Figure 4-6 Corrosion rate values as function of WSS for CMP treated samples with 80um grit abrasive and 3%H_2O_2 at different test time at pH=6

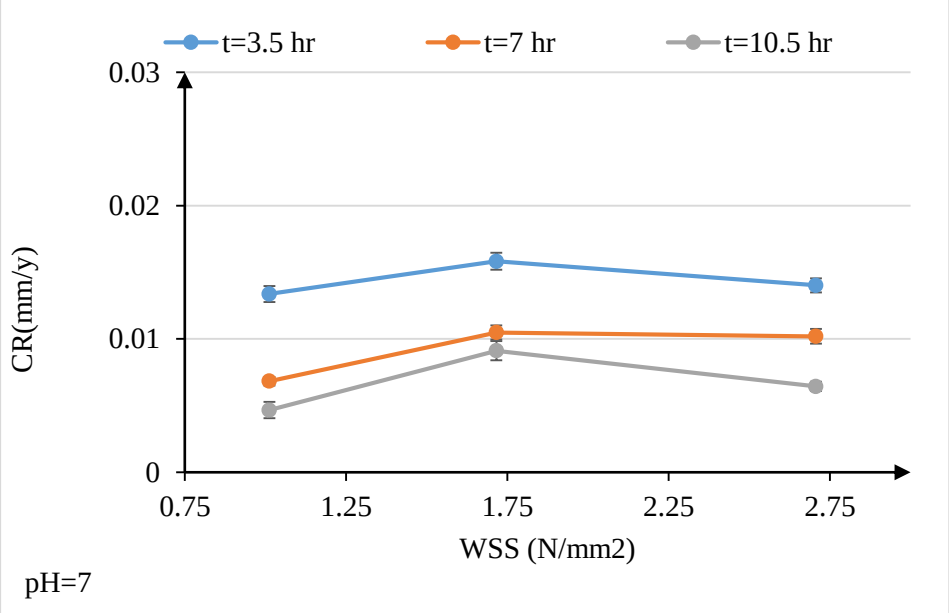

Figure 4-7 Corrosion rate values as function of WSS for CMP treated samples with 80um grit abrasive and 3%H_2O_2 at different test time at pH=7

4.3.2.2 Dynamic corrosion for chemical mechanical polishing treated samples with 10% silica slurry+3%H_2O_2+polymeric pad

Similar trend has been observed for corrosion of samples treated via chemical mechanical polishing and CMP with polymeric pad utilizing 10% silica slurry+3%H_2O_2 as can be seen in figure 4.8-4.11. However, the corrosion rate of samples treated via chemical mechanical polishing with polymeric pad utilizing 10% silica slurry+3%H_2O_2 is much lower than the corrosion rate in case of samples, chemically mechanically polished with 80um abrasive paper in the presence of 3% wt. H_2O_2.

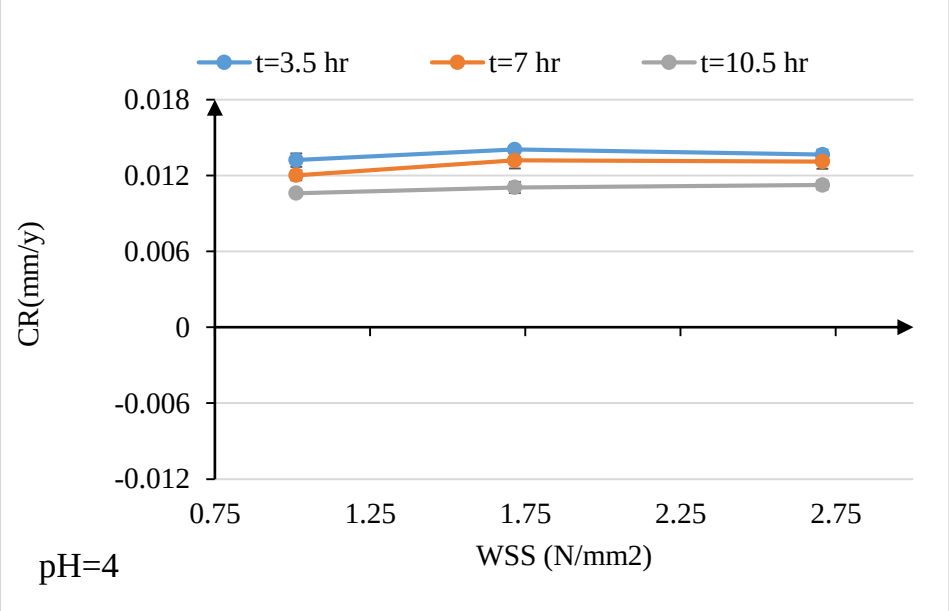

Figure 4-8 Corrosion rate values as function of WSS for CMP treated samples with 10% silica slurry+3%H_2O_2 with polymeric pad at different test time at pH=4

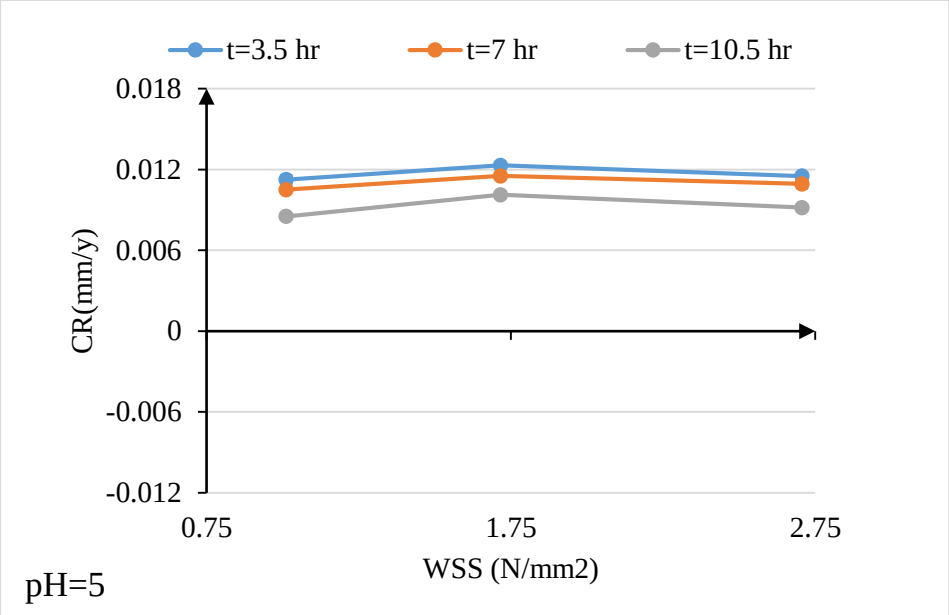

Figure 4-9 Corrosion rate values as function of WSS for CMP treated samples with 10% silica slurry+3%H_2O_2 with polymeric pad at different test time at pH=5

At pH 7 in figure 4.11 with lower WSS the corrosion products accumulate on the surface. However, WSS has a direct relationship with corrosion rate. It is also noticed from figure 10&11 that the increase in corrosion rate at the duration time of 10.5 hours is less than the corrosion rate at the duration time of 7.00 and 3.5 hours. This behavior is consistent with the static corrosion observed in Chapter III, which proved that corrosion decreases as the duration time increase.

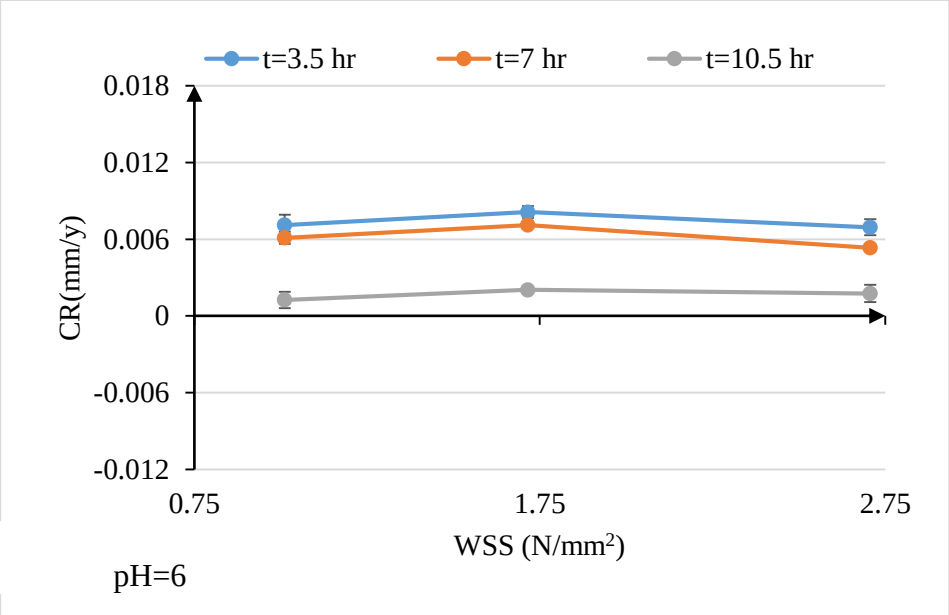

Figure 4-10 Corrosion rate values as function of WSS for CMP treated samples with 10% silica slurry+3%H_2O_2 with polymeric pad at different test time at pH=6

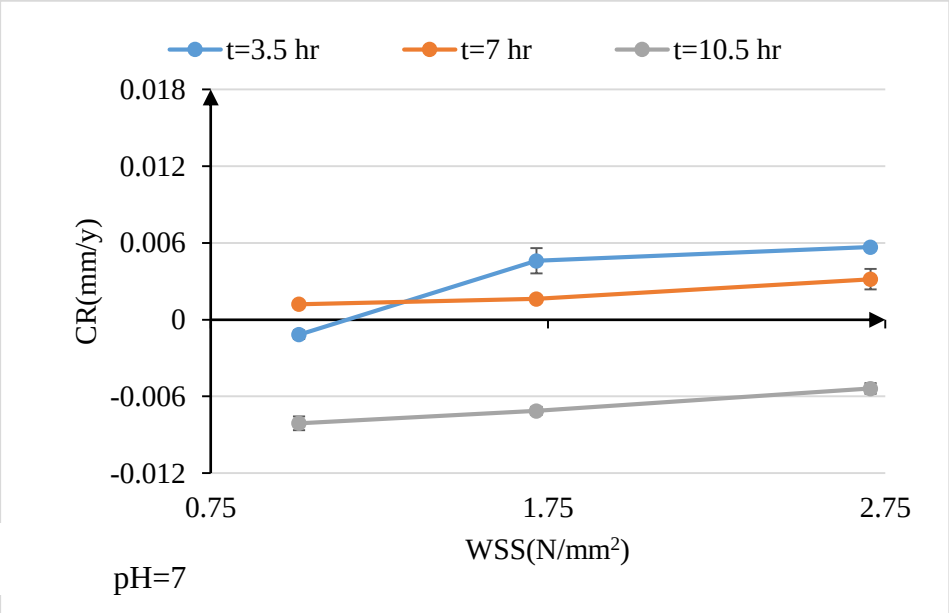

Figure 4-11 Corrosion rate values as function of WSS for CMP treated samples with 10% silica slurry+3%H_2O_2 with polymeric pad at different test time at pH=7

4.3.3 Roughness measurements after dynamic corrosion tests

The lowest and highest cases of the static corrosion test were chosen for investigating the dynamic corrosion tests in order to see the effect of flow on the surface roughness.

4.3.3.1 Roughness measurements for chemical mechanical polishing treated samples with 3%H_2O_2+abrasive paper 80µm

Since the corrosion can be associated to surface roughness, the impact of flow conditions on surface roughness was investigated to understand the relationship between corrosion and surface roughness. Figure 4.12-15 show the average surface roughness (R_a) at pH=4, pH=5, pH=6 and pH=7 respectively as a function of WSS and different time test. All the cases studied have a similar trend i.e. increasing surface roughness as the WSS increases however, as we go towards to the neutral pH of the fluid flowing in the pipe lesser surface roughness values are obtained. This decrease in the surface roughness can be attributed to chemical action of the shift from an acidic environment to neutral environment. Moreover, in the plots it can be seen that the surface roughness increases as function of time especially at pH=4 which is higher than the others, this increment can be attributed to the behavior of the acidic medium. This increasing surface roughness is related to the corrosion as explained in the previous section.

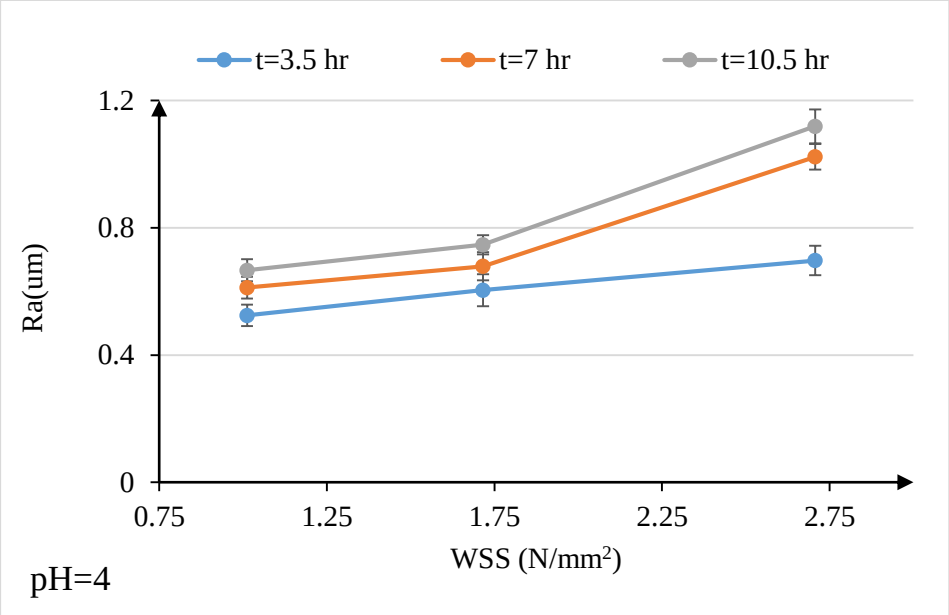

Figure 4-12 Roughness values as function of WSS for CMP treated sample with 80µm grit abrasive and 3%H_2O_2 at different test time at pH=4

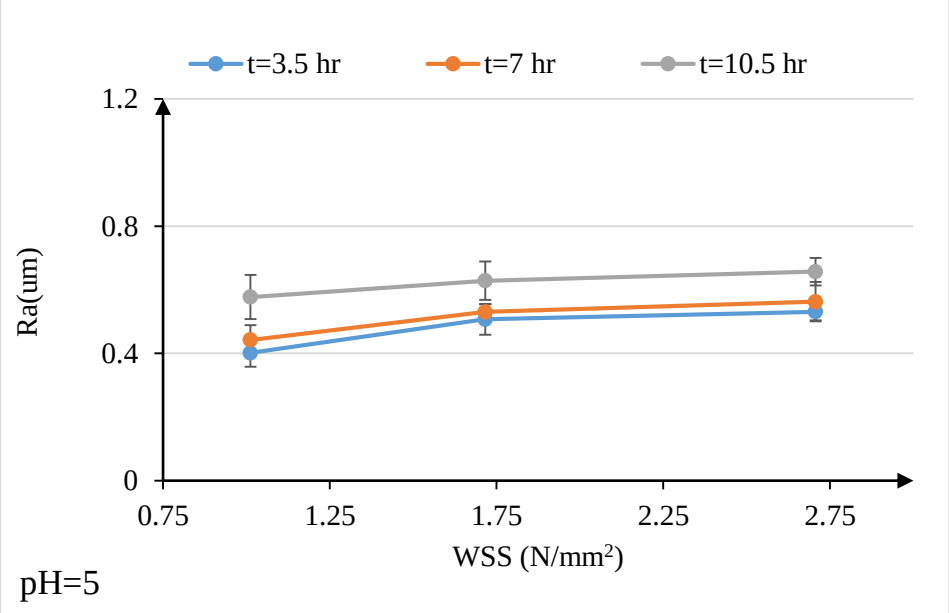

Figure 4-13 Roughness values as function of WSS for CMP treated sample with 80µm grit abrasive and 3%H_2O_2 at different test time at pH=5

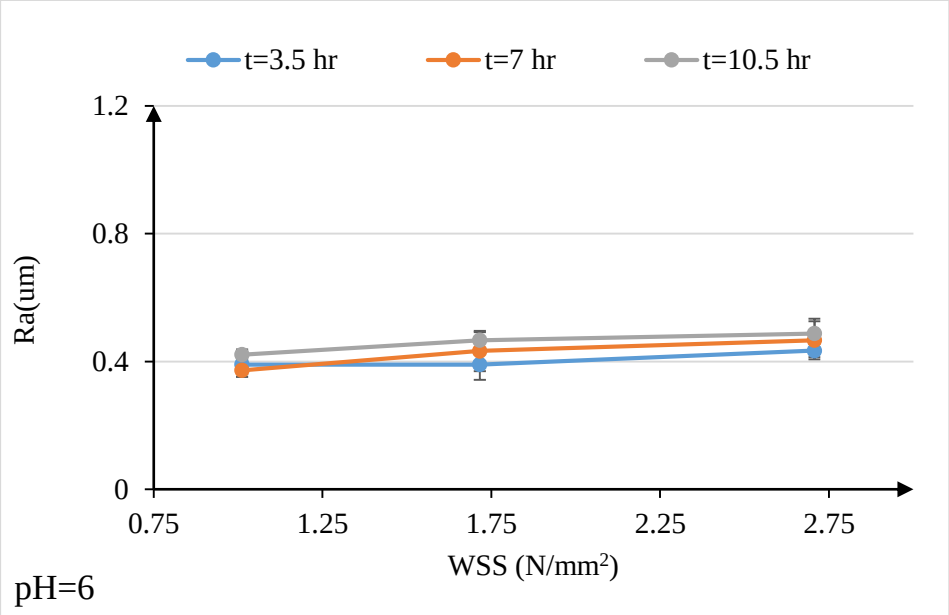

Figure 4-14 Roughness values as function of WSS for CMP treated sample with 80µm grit abrasive and 3%H_2O_2 at different test time at pH=6

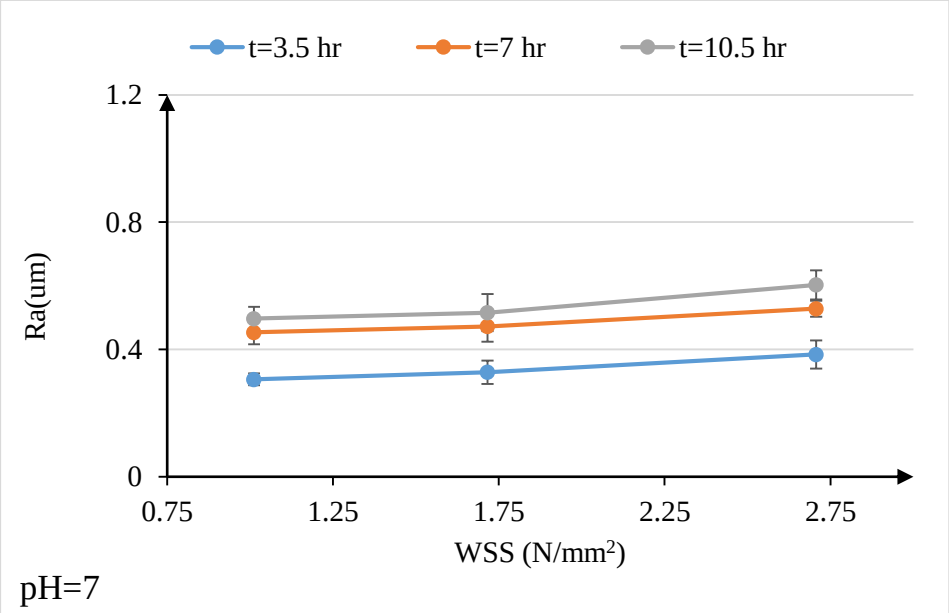

Figure 4-15 Roughness values as function of WSS for CMP treated sample with 80µm grit abrasive and 3%H_2O_2 at different test time at pH=7

4.3.3.2 Roughness measurements for chemical mechanical polishing treated samples with 10% silica slurry+3%H_2O_2+polymeric pad

Figure 4.15-18 demonstrate the average roughness of samples treated via CMP with polymeric pad utilizing 10% silica slurry+3%H_2O_2+polymeric pad as function of WSS at different test time. It has been observed that the average roughness increased as time and WSS increased. It can be noticed that the increasing in the roughness values is less than the increasing in the case of 3% H_2O_2+80um grit abrasive even at pH=4.

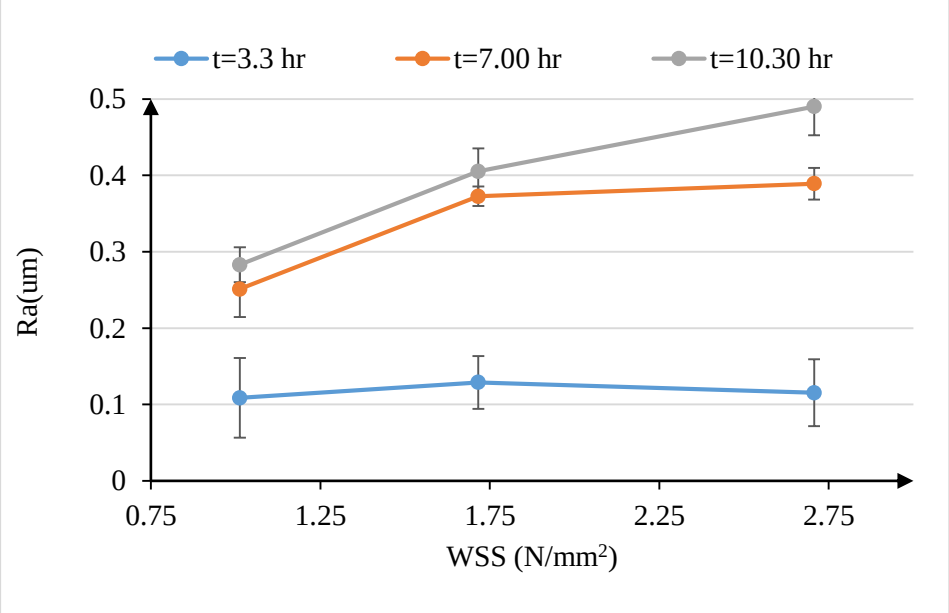

Figure 4-16 Roughness values as function of WSS for CMP treated samples with 10% silica slurry+3%H_2O_2 with polymeric pad at different test time at pH=4

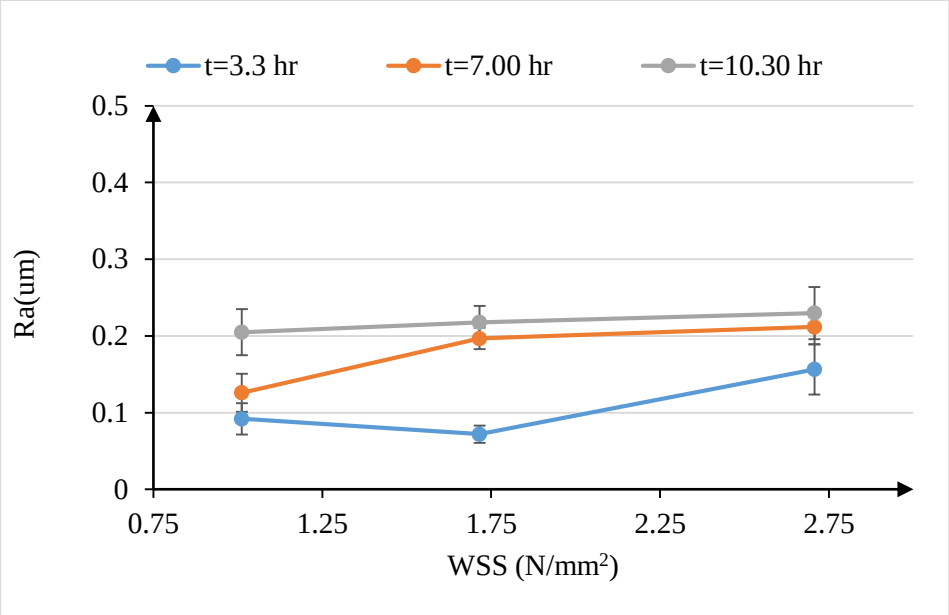

Figure 4-17 Roughness values as function of WSS for CMP treated samples with 10% silica slurry+3%H_2O_2 with polymeric pad at different test time at pH=5.

The roughness values at pH=6 and pH=7 has less roughness values comparing with those of 3% H_2O_2+80um grit abrasive. This behavior can be referred to the smoothness of the surface and the passive layer formation due to the combination between the silica slurry and hydrogen peroxide.

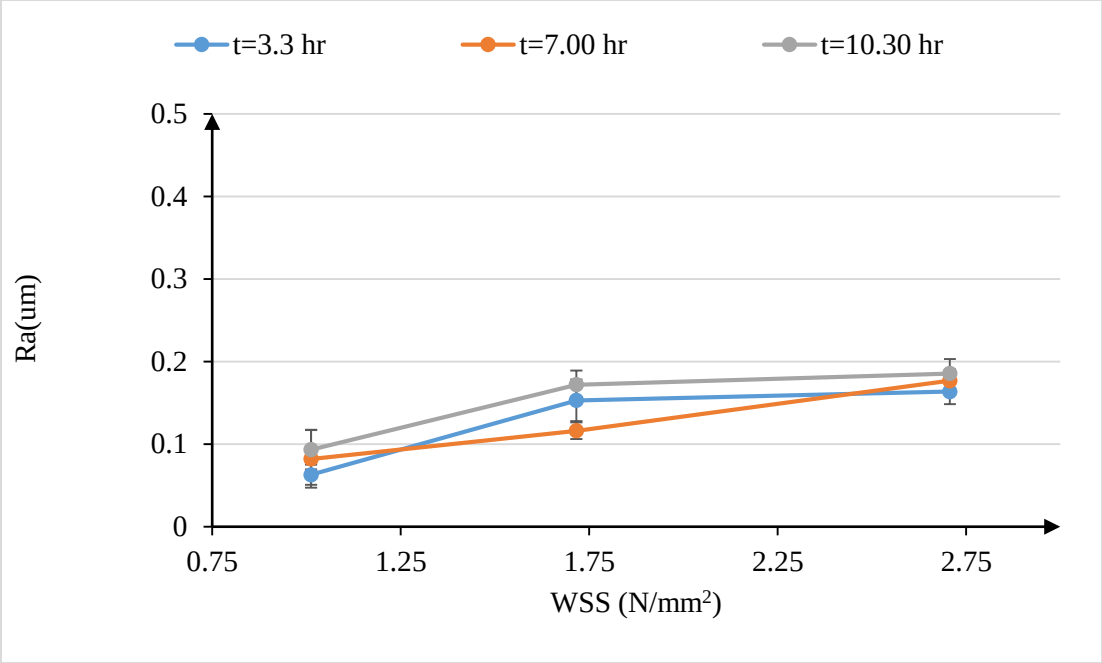

Figure 4-18 Roughness values as function of WSS for CMP treated samples with 10% silica slurry+3%H_2O_2 with polymeric pad at different test time at pH=6

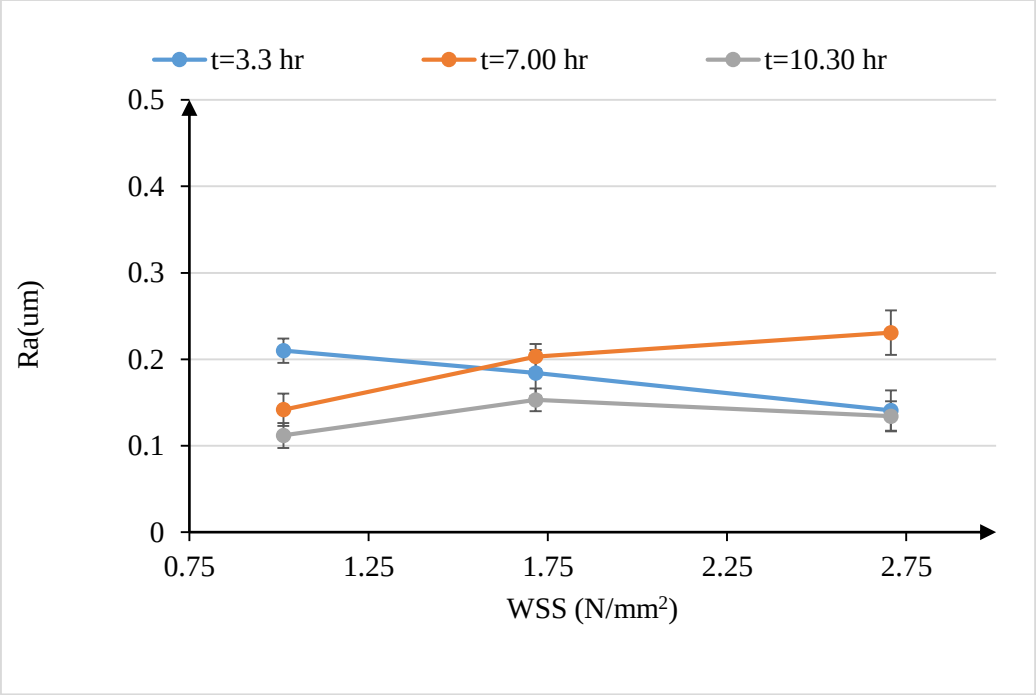

Figure 4-19 Roughness values as function of WSS for CMP treated samples with 10% silica slurry+3%H_2O_2 with polymeric pad at different test time at pH=7

4.4 Conclusions

The effect of CMP, with or without of hydrogen peroxide and silica-based slurry, on the behaviour of steel samples in DIW at different pH values has been investigated with an experimental setup. The corrosion of carbon steel has been studied under turbulent flow conditions having WSS comparable to those in the Iraqi oil fields pipelines. The first surface investigated was treated with 80um+3%H_2O_2 and the second one with 10% silica slurry+3%H_2O_2 and the higher and lower values of corrosion rate in static tests were obtained, respectively. The dynamic corrosion rates obtained utilizing the developed setup show that for the same WSS, the CR value drops with time. Furthermore, the corrosion rates increase with increasing WSS until critical value after which the corrosion rate decreases. The relationship of the average surface roughness and WSS has been found by

measuring it after dynamic corrosion tests in the developed setup for both cases as mentioned above. It has been found that the average surface roughness in case of (80um+3%H_2O_2) has higher value than the case of (10% silica slurry+3%$H_2O_{2)}$. Therefore the corrosion rate observed higher than the second case.

CHAPTER V

EFFECT OF SURFACE TREATMENT ON CORROSION PREVENTION

5.1 Introduction

Among different methods of controlling corrosion, one is the surface treatment which is an active method to resolve the problem. It includes chemical conversion coating [144-148], electroplating and electroless plating [149, 150], physical vapor deposition [151, 152] and so on. The effectiveness of the surface layer in turn depends on several characteristics (highly process dependent) such as its chemical composition, surface charge states, surface roughness, thickness, total surface area, micro porosity and critical surface tension among others. The exact method engaged to modify the surface shows a key role in determining its characteristics. For instance, the chemical composition of the surface layer may be significantly different from the bulk [153].

The CMP method of metal includes a slurry with a suspended particles that interact with the surface of the substrate because of the action of mechanical force effected between these particles and surface by the polishing pad [69, 154]. The results of the interaction can be metals' physical removal or cut off a surface film. thereafter, the creation of a protective film and electrochemical dissolution can happen after the interaction.

In this chapter, the influence of surface characteristics and CMP surface treatments on the corrosion resistance of carbon steel in harsh media are investigated. Moreover,

contact angle measurements, material removal rate and hardness measurements were conducted to understand the effect CMP treatment. The effect of CMP treatment on the corrosion resistance of steel sample in high acidic media (pH=2) has been investigated through static corrosion tests for seven days and electrochemical (Tafel polarization) corrosion analyses. In addition, silica sol gel with some additives were also prepared to study their impact on the corrosion behavior of steel samples.

5.2 Experimental

5.2.1 Static corrosion tests for MP and CMP treated samples at pH=2

The static corrosion test of the CMP treated samples were evaluated by immersion of steel samples in a high acidic medium (pH=2) for seven days using weight loss method. Two different CMP treated samples were prepared by treating the steel samples with 10% silica slurry with a polymeric pad and 10% silica slurry in the presence of 3%H_2O_2 with a polymeric pad. On the other hand, mechanical polished steel samples were prepared with different SiC abrasive papers (240, 400,600,800,1000 um grit size) to compare and understand the corrosion behavior of MP and CMP treatments. The steel samples were taken out after every 24 hours, washed with distilled water, dried with pressurized air and weighed by an electronic balance (ES 125MS) with the resolution of 0.00001 g. Corrosion rates of carbon steel were calculated by expression:

$$V_a = C \times \frac{Wo - W}{\rho A t} \qquad (5.1)$$

where, V_a is the corrosion rate or the annual speed, mm/y, C is the conversion factor, which is equal to 8.76×10^4, W_o is weight (g) of sample before test, W is weight (g) of sample after test, ρ is the density of the sample (7.85 $g.cm^{-3}$), A is working area of the specimen (cm^2) and t is the testing time (hr.).

5.2.2 Electrochemical corrosion tests for Mechanical and CMP treated samples at pH=2

The electrochemical behavior of the treated samples was studied through potentiostatic and potentiodynamic polarization measurements by using Gamry Potentiostat (model 1000 Interface). The tested samples with a visible dimension of $10x10mm^2$ were placed in a Teflon sample holder. A conventional three-electrode electrochemical cell was used where the sample was used as the working electrode, a platinum wire was utilized as the counter electrode and a saturated calomel electrode (SCE) was used as the reference electrode. 200mL DIW having pH=2 was utilized as the electrolyte. The potentiostatic scan period was set to 1800 seconds with an input potential of 0V vs. E_{ref}. Potentiodynamic scans were performed with scan range from -0.5V to 1.6V with a scanning speed of 10mV/s and a step of 1mV for each data point.

5.2.2.1 Wettability analyses

Both MP and CMP treated samples were considered for wettability for through contact angle measurements with DIW. The contact angles were measured via sessile drop using a KSV ATTENSION Theta Lite Optical Goniometer. The size of the drop was maintained at ~160 μm. Three test performed for each sample and the results were averaged.

5.2.2.2 Material Removal Rate (MRR) evaluations

The material removal rates achieved with the mechanical polishing samples and two different CMP treatments were determined by weight difference in pre and post CMP and mechanical polishing. In each case three samples were polished to measure the average material removal rate (MRR). The MRR calculation formula is shown as follows:

$$MRR = \frac{10^8 \times \Delta m}{7.98 \times \pi \times 2.54\text{^}2 \times t} \quad (5.2)$$

Where *MRR* (Å/min) is the material removal rate,

Δm (g) is the weight difference before and after the polishing process,

t (minutes) is the polishing time.

5.2.2.3 Surface roughness

Average surface roughness of the steel samples was determined with a Dektak 6M Stylus Profile. Three tests were conducted on each sample both pre and post CMP surface treatment and mechanical polishing and the average of the measurements was taken.

5.2.2.4 Hardness evaluation

The hardness test of steel samples in three different cases i.e. mechanical polishing and two cases of CMP treatments were evaluated through Vickers hardness test protocol with ARS9000 Full Automatic Micro hardness testing system (Future Teach, FM-300e, Kanagawa, Japan) with applied load of 1000 g. Three tests were conducted on each sample the mean hardness value was taken.

5.2.3 Coating steel surface for corrosion prevention

5.2.3.1 Preparation of steel samples

For static corrosion evaluation and an electrochemical investigation 1.0 cm^2 area of the steel samples was visible to the electrolyte. The surfaces of the steel specimens were polished with various grades (400, 600, 800, 1000 um) of SiC papers as a mechanical polishing and then degreased with acetone. The CMP treated samples were prepared by two treatments with 10% slurry with polymeric pad in the absence and presence of 3%H2O2. Table 5.1 shows the numbers of these treatments.

Table 5.1 Number of surface treatment of steel samples.

No.	**1**	**2**	**3**
Description	M.P	CMP(10%SiO_2+3%H_2O_2+pad)	CMP(10%SiO_2+pad)

The samples were rinsed with DIW and dried pressurized air before all the electrochemical tests. The composition (wt.%) of the steel is shown in table 5.1

Table 5.2 Chemical composition (wt%) of the steel sample

Element	C	Si	Mn	P	S	Ni	Mo	Cr	Fe
%	0.10	0.269	0.616	0.003	0.001	0.050	0.106	0.653	98.13

5.2.3.2 Preparation of coating solutions

PEO polymer (Mw= 600,000 g/mol) was purchased from Sigma Aldrich Germany. Epoxy resin (diglyceryl ether of bisphenol A (DGEBA)) with epoxide equivalent weight

185-210 g/mol was purchased from Spolchemie Company. A cycloaliphatic amine curing agent, known as Epikure F205, was supplied from Hexion (USA)., EtOH (≥99.8% GC, Sigma-Aldrich), Tetraethyl orthosilicate (≥99% GC, Sigma-Aldrich)**.** DIW was used for the preparation of all coating solutions.

5.2.3.2.1 Preparation of Polyethylene Oxide -A

A stock solution of PEO with 0.08 mM concentration was prepared by gradual addition of the polymer to 50 mL of water in an Erlenmeyer flask. The water was vigorously mixed by stirring and heated to 30-40 °C. The coatings are deposited on samples by dip-coating with a withdrawal speed corresponding to 200 mm min−1. Finally, the samples are dried for 10 min at 100 ◦C in a drying oven.

5.2.3.2.2 Preparation of Silica Sol Gel -B

1 mole of Tetraethyl orthosilicate (TEOS) and 2 moles of ethanol (EtOH) were added into a florence flask and continuously stirred for 10 min while adding, 0.1 M catalyst (H_2SO_4) in water to the solution until a water to TEOS molar ratio of 2 was reached. The solutions were then mixed at room temperature for 2 hours and further aged for 24 hours before use.

5.2.3.2.3 Preparation of silica sol gel – PEO hybrid coating –C

Silica-based WGs are generally created by utilizing alkoxysilanes, such as tetramethoxysilane (TMOS) and tetraethoxysilane (TEOS); The acid nature of the catalyst allows to get a substrate with low absorbent volume, high density and a good homogeneity. 0.05mM of polyethylene oxide (PEO) was added into a Florence flask and continuously

stirred at room temperature for 10 min and continuously with the same procedure in the previous section.

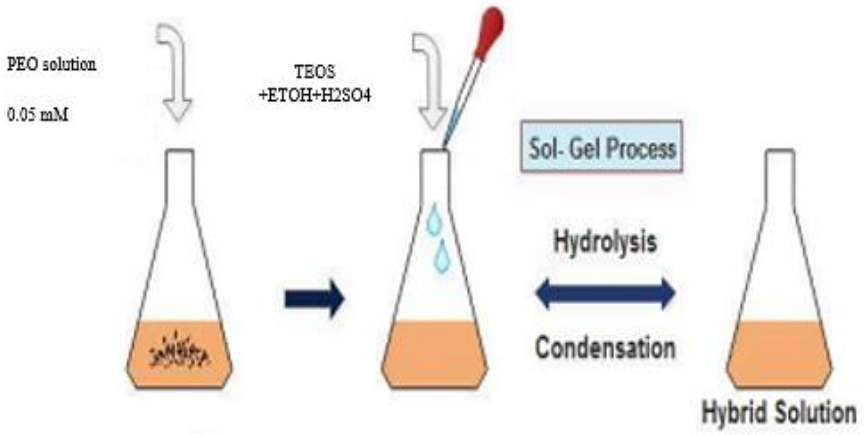

Figure 5-1 Silica sol gel – PEO polymer blending preparation.

5.2.3.2.4 Preparation of epoxy resin coating - D

Epoxy resin coating was synthesized by mixing DGEBA and EDTA curing agent at room temperature. Curing process was left to proceed at room temperature for 24h.

5.2.3.2.5 Preparation of epoxy-PEO -E

At first step, PEO gel with 0.8 mM concentration was mixed with DGEBA by continuous stirring to have homogeneous mixture. After that, amine hardener F205 was added to mixture and agitated. Dip coating method was applied to coat steel samples. after coating, samples were left at room temperature for 24hr to complete curing.

5.2.3.2.6 Preparation of Epoxy- silica -F

To prepare the silica/epoxy coating, a pre-determined amount of the silica was added to the epoxy resin and mixed for 40 min by using a magnetic stirrer. The resultant mixture was sonicated for 35 min. The ultra-sonication progression was excuted at a frequency of 20 kHz with an inlet ultrasound power of 1 W/m L (UIP 1000 ultrasonic

processor, Hielscher Ultrasound Technology). Subsequently, a stoichiometric amount of the hardener was then added and mixed. In order to reduce of air bubbles, the mixture was kept in vacuum chamber for 10 minutes. The samples were coated with the prepared mixture.

5.2.3.2.7 Preparation of epoxy-PEO and silica -G

DGEBA and hybrid mixture of PEO-silica sol gel were mixed at room temperature for a one hour, and then EDTA as a curing agent was added to the mixture with continuous stirring until the gelling time of the mixture. The samples were coated with the prepared mixture and cured after 24h at room temperature.

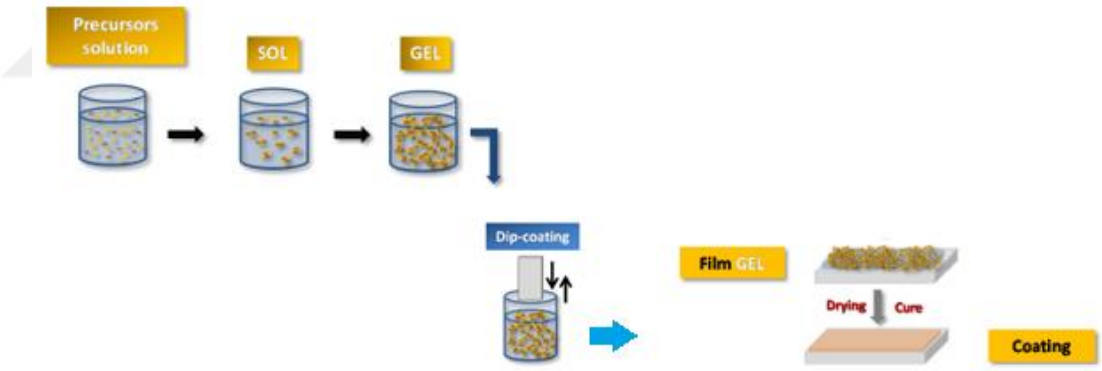

Figure 5-2 General OIH coating process [155].

5.3 Corrosion tests

5.3.1 Static corrosion tests for surface treated and sol gel coated samples

Prior to the coating tests, the specimens were polished with mechanical polishing and CMP and then coated with various types of coating. As mentioned before with the

same procedure a static corrosion tests were conducted by dipping the coated steel samples for 7 days in a DIW with pH=2.

5.3.2 Electrochemical corrosion measurements

Electrochemical corrosion tests (potentiostatic and potentiodynamic measurements) executed by utilizing Electrochemical analyzer model Gamry 1000. In the experimental setup the coated steel sample was used as a working electrode, a saturated calomel electrode as a reference electrode and the platinum wire as a reference electrode. The measurements were carried out for 30 min at room temperature. The electrochemical polarization measurements were carried out by changing the electrode potential from -0.5 V to +1.6 V with respect to OCP at a scan rate of 0.1 mV/s

5.4 Results and discussion

5.4.1 Immersion tests at pH=2

The influence of immersion time on corrosion rate can be seen in Figure 5.3. For the first two days higher corrosion rates have been observed and it decreases as the time increases. The mechanically polished samples corrode at higher rates as compared to CMP treated samples. The lower corrosion rates of CMP treated samples can be referred to the formation of protective oxide film due to the presence of oxidizer in the slurry. However, CMP treated samples in the nonexistence of oxidizer show lower corrosion rates as compared to MP treated samples yet higher when compared to CMP treated samples with the existence oxidizer.

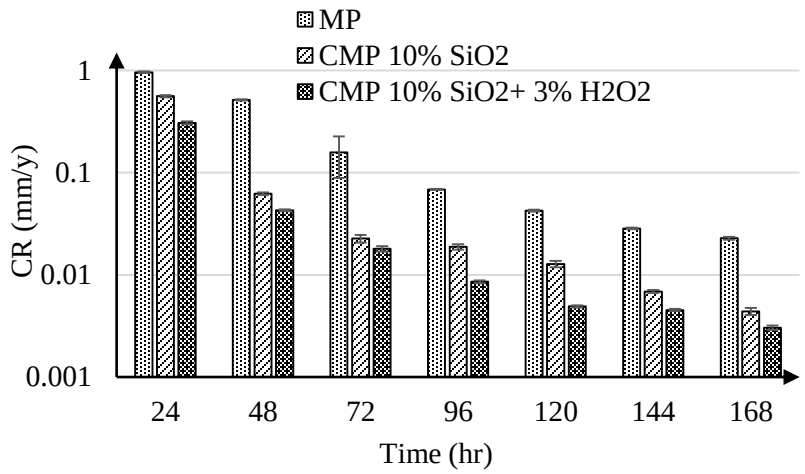

Figure 5-3 The relation between the corrosion rate and immersion time

5.4.2 Electrochemical measurements at pH=2

5.4.2.1 Potentiodynamic polarization analysis

Potentiodynamic polarization curves were performed for 45 minutes in an acidic solution (pH=2) used as electrolyte. The corresponding corrosion current densities "I_{corr}" using the Tafel extrapolation are depicted in Figure 5.4 and the data collected in Table 5.3. The software utilizes the corrosion rate calculation (equation 3.6).

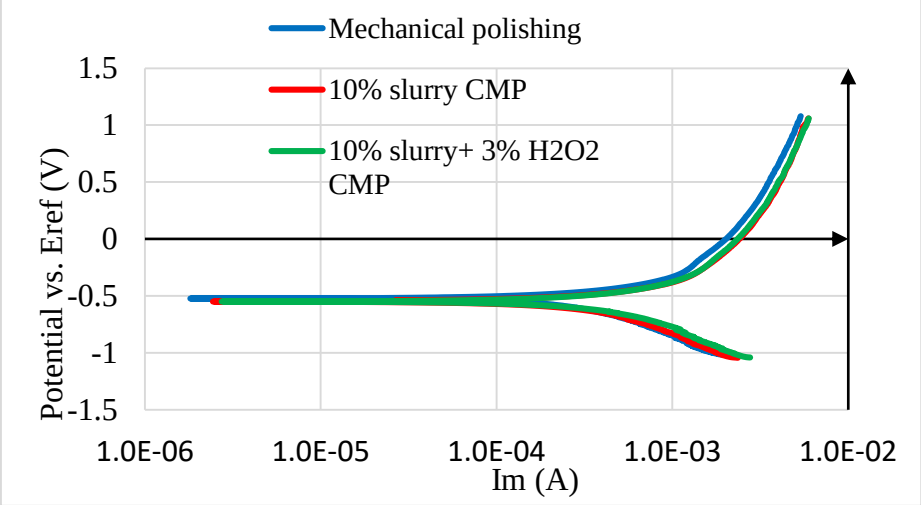

Figure 5-4 Potentiodynamic polarization curves of Steel samples at different treatment

Table 5.3 Tafel plot data of steel sample obtained based on potentiodynamic data analyses

Treatment	CR(mpy)	I_{corr} (mA/cm^2)	E_{corr} (mV)
Mechanical polishing	28.04	60.50	-525.0
CMP 10% Slurry	17.870	38.240	-549.0
CMP(10% Slurry+3% H2O2)	9.356	20.460	-550.0

CMP treated samples have lower corrosion current density and as a result are more corrosion resistant. Table 5.2 shows that the attendance of H_2O_2 in the slurry effects in lesser corrosion for CMP treated samples as compared to CMP treated samples without H_2O_2 in the slurry and due to higher current density the MP treated samples have the highest corrosion rates.

5.4.2.2 Potentiostatic analysis

The evolution of the potentiostatic scan with time and with different surface treatment in acidic medium (pH=2) is demonstrated in Figure 5.5. All curves exhibit a rapid decrease of the potential followed by a steadying period which can be recognized to the development of a film growing over the substrate surface [156].

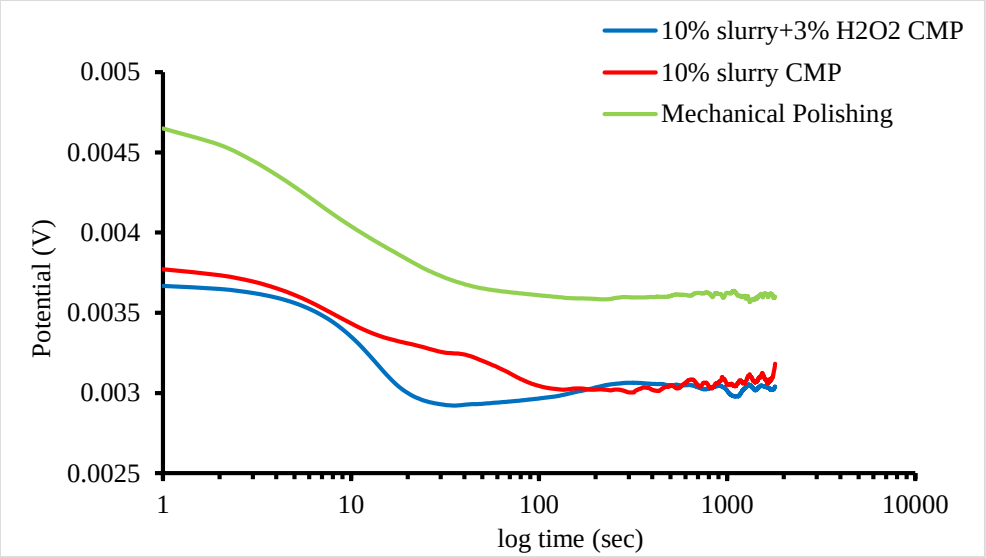

5-5 Potentiostatic (Im vs time) of steel samples at different surface treatments

5.4.3 Surface characterization

5.4.3.1 Effect of immersion time on surface roughness

Figure 5.6 illustrates the surface roughness as a function of different treatment techniques. It is observed the surface roughness in case of mechanical polishing is highest among the three cases since it has been polished with sand paper (800µm SiC). In case of samples treated with CMP having 3%wt H2O2 as oxidizer smoothest surface has been obtained. This smooth surface is due to the Nano particles in slurry and formation of protective oxide layer on the metal surface which can also protect the surface against corrosion.

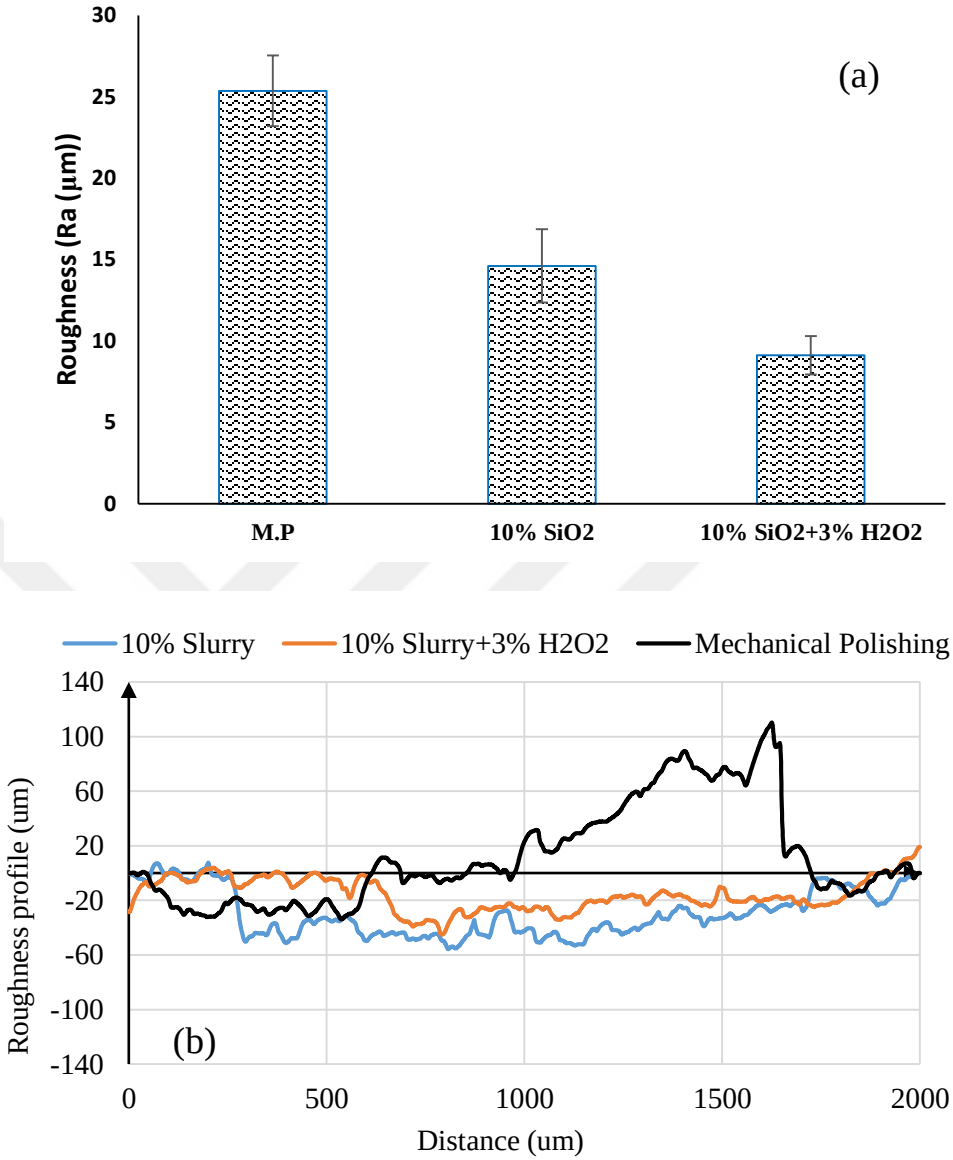

5-6 Average roughness (a) values (b) roughness profiles

5.4.3.2 Wettability analyses

Figure 5.7 demonstrates the wettability behavior of steel samples, after three different surface treatment, with DIW droplets. The contact angle value decreases when the surface become smoother. Thus in case of CMP with 10% slurry in the presence of 3% H_2O_2 treated samples are found to possess smoother surface and samples show higher wettability as compared to the other cases.

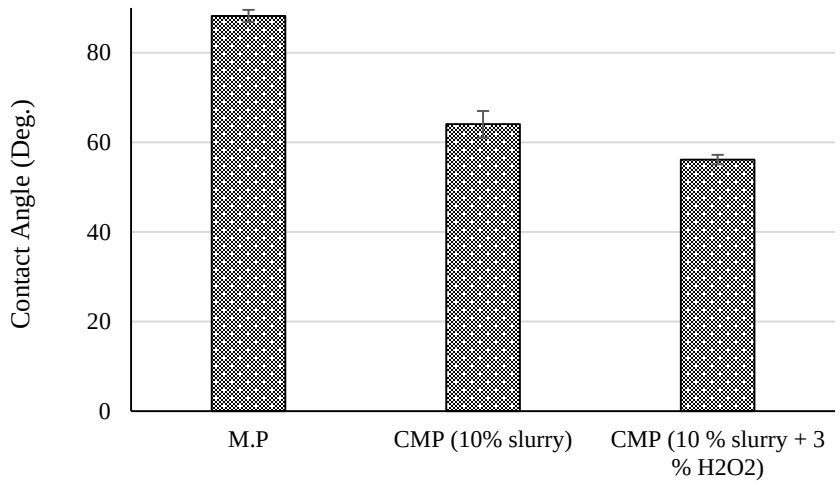

Figure 5-7 Surface wettability of steel samples at different surface treatments

5.4.3.3 Removal rate evaluation

Figure 5.8 demonstrates the removal rate of steel sample during three different surface treatments. It can be seen that MRR is higher in MP treatment because of the mechanical abrasion by abrasive paper which leads to rougher surface as shown in Figure 5.5a and b. The addition of H_2O_2 in slurry results in increase in MRR since the removal of oxide layer from the surface is relatively easier as compared to pure material, due the mechanical action of slurry particles (silica). However, despite higher MRR with oxidizer in slurry, smoother surface is obtained after CMP in the presence of oxidizer. In case of CMP only with silica lowest MRR has been observed however surface is found to have higher roughness as compared to surface treated via CMP with oxidizer in slurry as shown in Figure 5.6a.

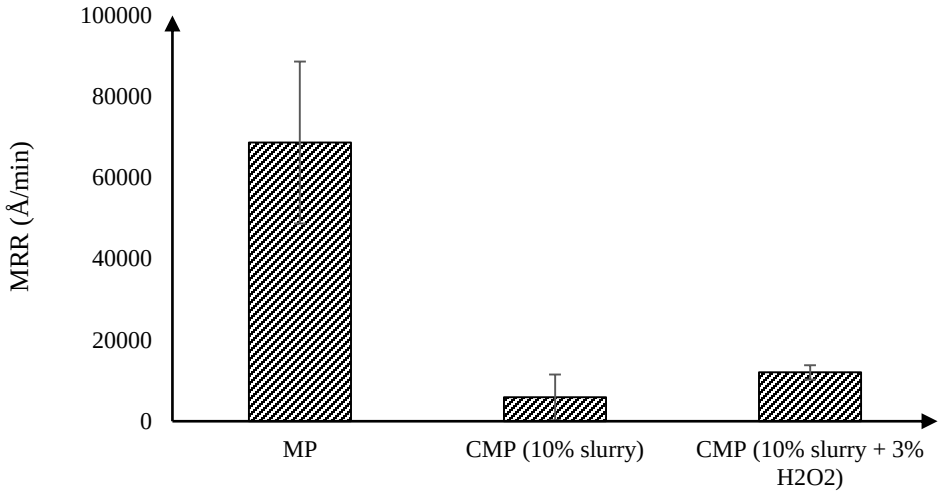

5-8 Removal rate of the steel samples at different surface treatments

5.4.3.4 Hardness measurements

Figure 5.9 illustrates the hardness measurement results of the steel samples under study. It can be seen that the CMP improve the hardness value compared to MP. This increase in hardness can be attributed to smoother surface obtained after CMP. Samples treated with CMP having oxidizer in slurry have a highest hardness values which can be referred to growth of smooth oxide film on the steel surface.

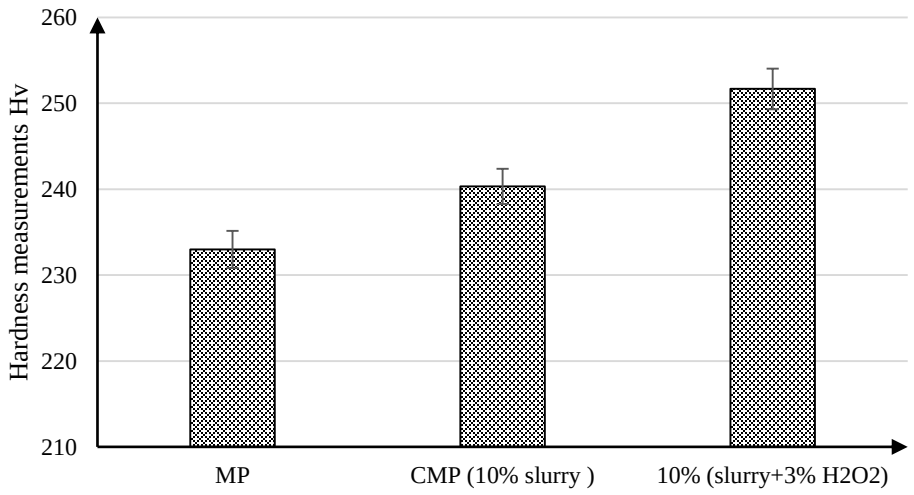

5-9 Hardness measurements of steel samples at different surface treatments

5.4.3.5 SEM measurements after 7 days of immersion

The adhesion of the silica Nano particles and hydrogen peroxide to the post-polished steel surfaces in an acidic environment was observed using SEM. The SEM image of the mechanical polishing steel substrate showed that there were no particles on the surface, as shown in Fig. 5.10 a. After CMP with silica based slurries (10 wt.%), a number of silica particles were present on the steel surface as shown in figure 5.10 b. Fig. 5.10 c shows the SEM images of the steel samples treated with silica based slurries in the presence of H_2O_2. It can be seen that a lot of aggregated silica particles are present on the steel surface.

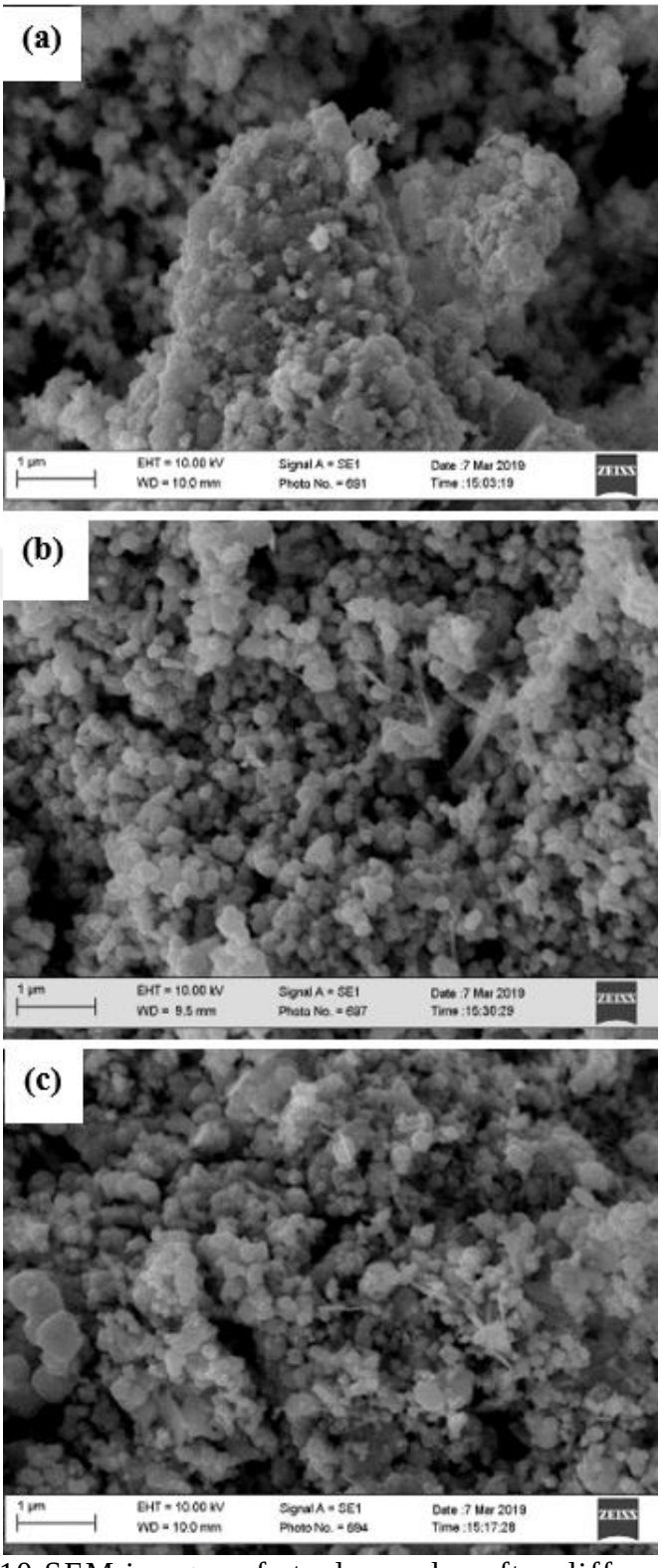

Figure5.10 SEM images of steel samples after different surface treatments immersed in an acidic environment. (a) M.P (b) CMP(10% SiO_2 (c) CMP(10%SiO_2+3%H_2O_2

5.4.4 Immersion tests for coated samples

The relation between the immersion time and the corrosion rate of the coated steel samples mechanically polished immersed at pH=2 are illustrated in figure 5.11. In the initial immersion stage, the values of the hybrid anticorrosion coating containing (PEO+Silica+Epoxy) and the other two coatings showed a decrease with permeation of an aggressive medium. For the first two days' higher corrosion rates have been observed and it decreases as the time increases. The samples of hybrid coating have lower corrosion and are more durable comparing with the other coated samples. The lower corrosion rates and higher stability of hybrid coating can be attributed to the formation of protective oxide film and due to the good adherence to the steel surface.

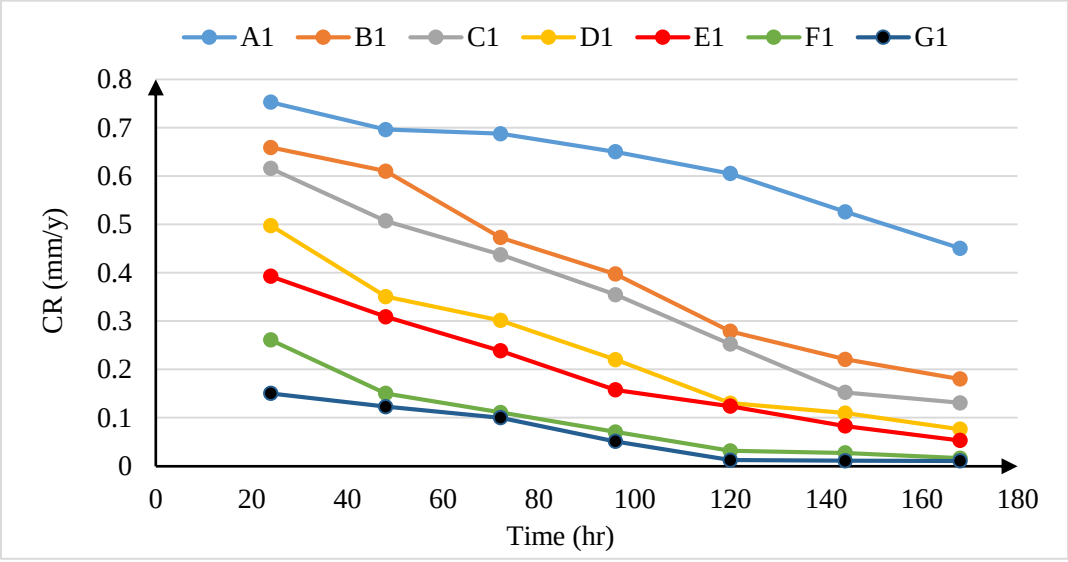

5-10 The relation between the corrosion rate and immersion time for different types of coating mechanically polished 1.

The group of hybrid coating has the lowest values of corrosion rate this means the adhesion between these types of coating are good compared to the other types of coatings. The high adhesion of epoxy to steel surface can be referred to oxidized surface of steel after CMP in the attendance of the oxidizer in the silica slurry, and offers more resistance to corrosion as shown in figure 5.12

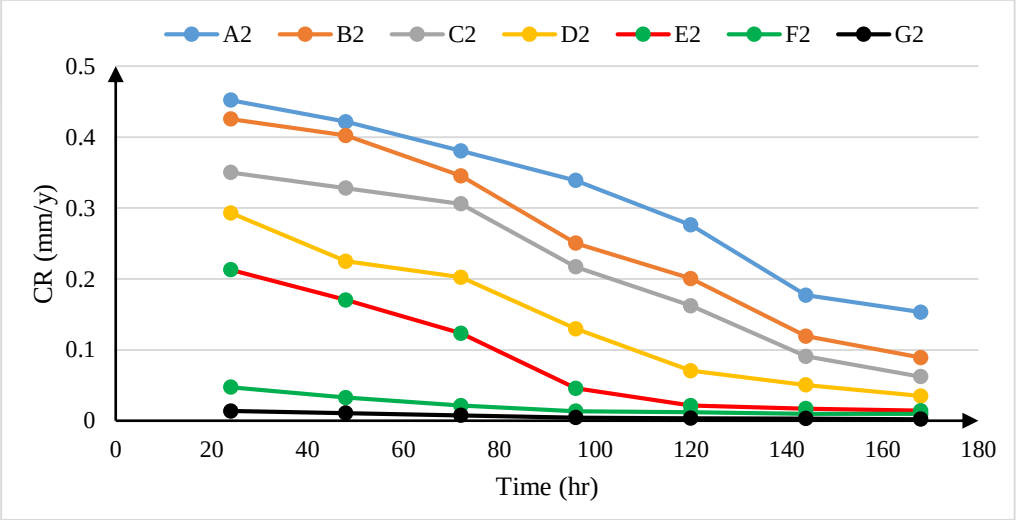

Figure 5-11 the relation between the corrosion rate and immersion time for different types of coating CMP treated 2.

Figure 5.13 demostrates the corrosion rate as a function of immersion time at pH=2 for steel sample CMP treated with silica slurry. It can be seen that the hybrid coating has high corrosion resistance among the other groups. There is a good adhesion between this type of coating and the steel surface. This behavior near to that of the steel sample CMP treated with the presence of oxidizer but with more corrosion rate.

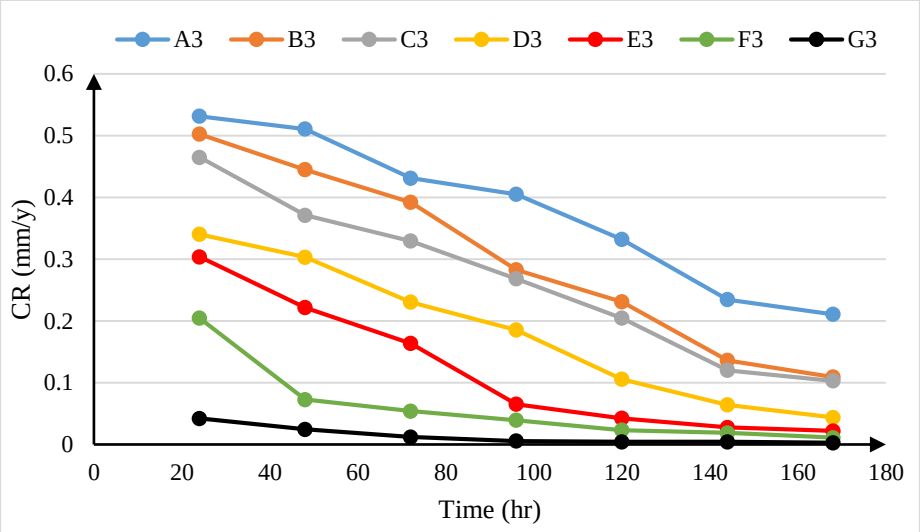

5-12 The relation between the corrosion rate and immersion time for different types of coating CMP treated 3.

5.4.5 Electrochemical measurements of coated samples

5.4.5.1 Potentiostatic measurements of coated samples

The evolution of the potentiostatic scan with time of samples, prepared with different coating types, in acidic medium (pH=2) are presented in Figure 5.14, 5.15 and 5.16. All curves display a stability in potential, some of them in a high value while the other in a low value which can be referred to the oxide film formation at different rates covering substrate surface. Figure 5.14 shows that the MP samples with the group of hybrid coating has a lower potential along the time test while the polyethylene and silica group shows higher potential with respect to time which means the oxide layer formation takes longer and sample corrodes faster. This behavior can be complemented by the potentiodynamic tests as well.

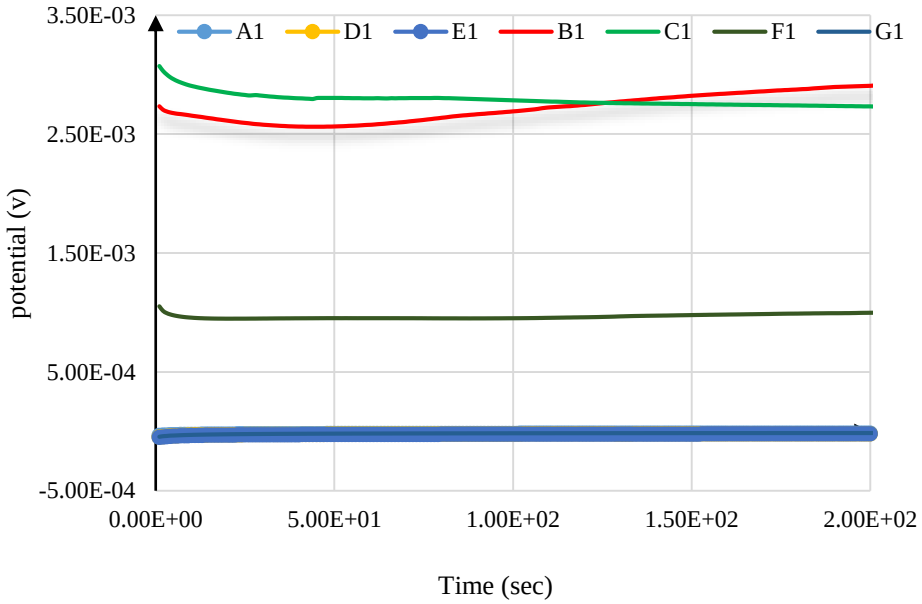

Figure 5-13 Potentiostatic (current vs time) curves of steel at pH=2 mechanically polished 1 in different types of coating.

Figure 5.15 demonstrate the potentiostatic scan of different types of coatings on steel samples CMP treated in the presence of oxidizer in silica based slurry. It can be seen that the group of hybrid coating (G) has a lower potential than the other groups which explain the effect of CMP treatment on the adhesion of coatings to steel surface. This behaviour is similar to the behaviour of steel samples CMP treated with the absence of silica slurry as shown in figure 5.16.

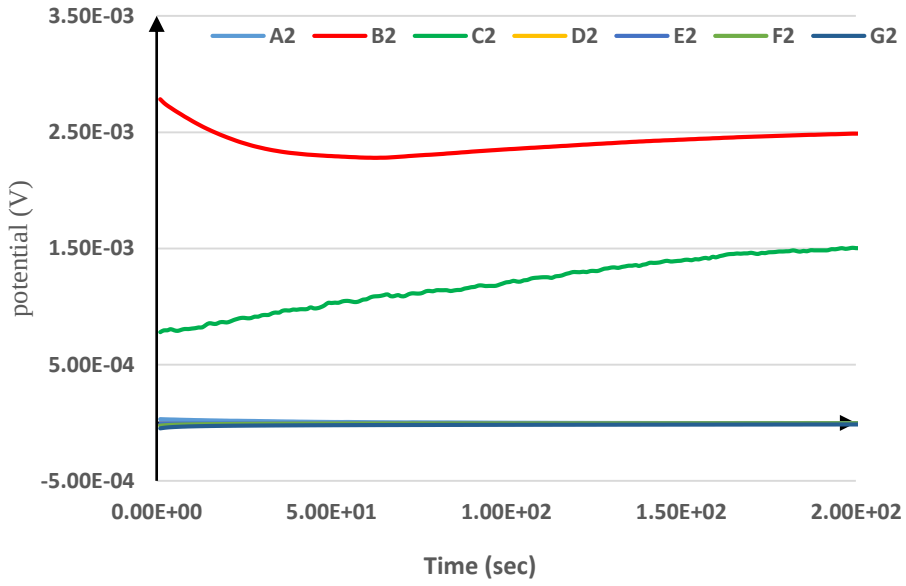

5-14 Potentiostatic (current vs time) curves of steel at pH=2 CMP treated 2 in different types of coating.

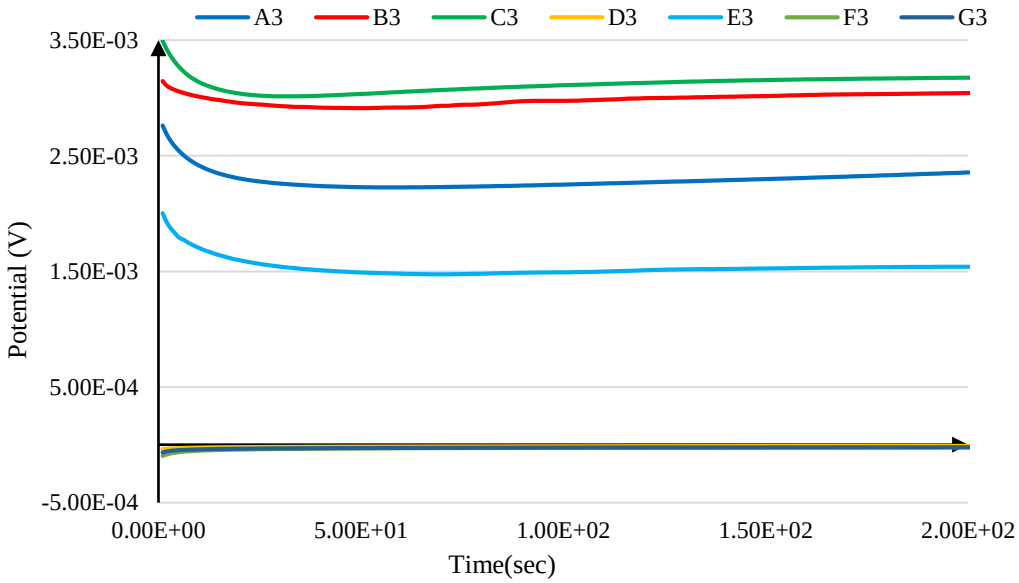

5-15 Potentiostatic (current vs time) curves of steel at pH=2 CMP treated 3 in different types of coating.

5.4.5.2 Potentiodynamic polarization measurements of coated samples

Potentiodynamic polarization analyses were perofrmed for 45 minutes in an acidic solution i.e. pH=2 used as electrolyte. The potentiodynamic polarization of steel samples mechanically polished with different coating types is presented in figure 5.17. The corresponding (E_{corr}), (I_{corr})and (CR) listed in table 5.3 were determined by the extrapolation method on Tafel plot. It has been observed that the corrosion current density increases from $2.411e^{1}$ with hybrid coating (G1) to $8.08e^{2}$ with polyethylene coating (A1). The corrosion potential decreases,can be explained by the increasing in the anodic current density and as a result the corrosion rate increases.

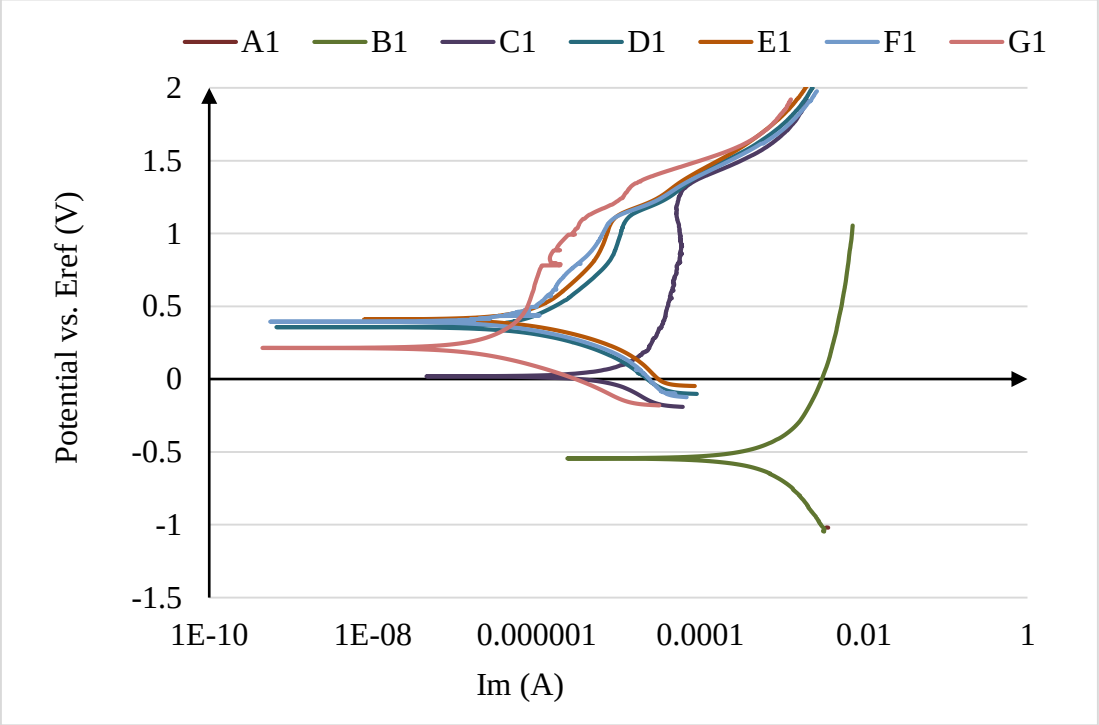

5-16 Potentiodynamic polarization curves of steel mechanically polished 1 at pH=2 in different types of coating.

.

Table 5.4 Tafel plot data of steel sample treated 1 with different coating types

Coating Type	CR(mpy)	I_{corr} (mA/cm^2)	E_{corr} (mv)
A1	3.78e2	8.08e2	-508.0
B1	2.892e2	6.182e2	-550.0
C1	2.497e2	5.337e2	-529.0
D1	6.6e1	1.413e2	-525.0
E1	4.924e1	1.053e2	-497.0
F1	1.441e1	3.078e1	-331.0
G1	1.232e1	2.411e1	-606.0

The potentiodynamic polarization of steel samples chemically mechanically polished with the presence of 3% H_2O_2 in the silica slurry with different coating types are exposed in figure 5.18. The corresponding (E_{corr}), (I_{corr})and (CR) listed in table 5.4 were determined by the extrapolation method on the Tafel plot. The corrosion current density increases from $1.513e^1$ hybrid coating (G2) to $4.06e^2$ polyethylene oxide coating (A2). It is believed that combining organic and inorganic hybrid coating form a protective layer with a good adhesion with CMP treatment in the presence of an oxidizer, flexibility and good corrosion prevention properties.

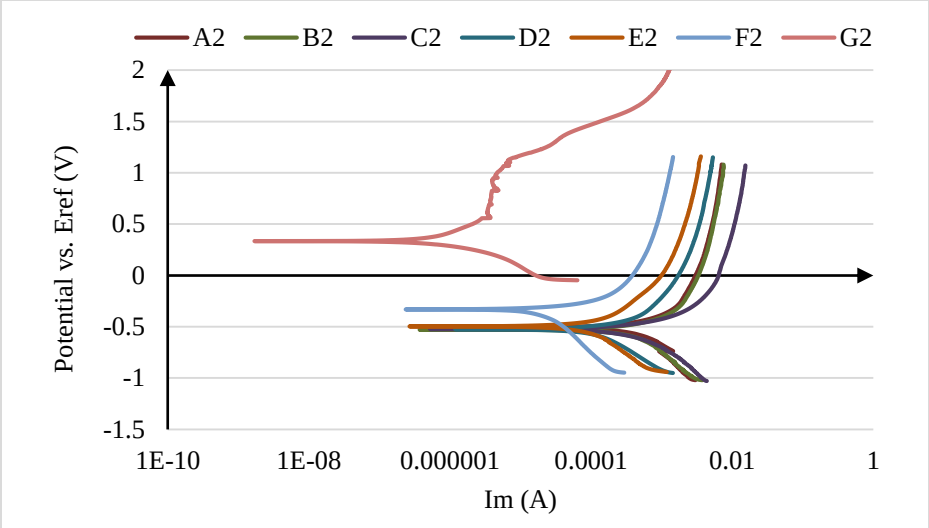

5-17 Potentiodynamic polarization curves if steel CMP treated 2 at pH=2 in different types of coating.

Table 5.5 Tafel plot data of steel sample treated 2 in different coating types

Coating Type	CR(mpy)	I_{corr} (mA/cm^2)	E_{corr} (mV)
A2	1.9e2	4.06e2	-523.0
B2	1.016e2	2.172e2	-503.0
C2	5.640e1	1.214e2	19.40
D2	2.47e1	5.983e1	357.0
E2	2.224e1	4.754e1	410.0
F2	9.6	2.065e1	395.0
G2	5.47	1.5130e-9	400.0

The potentiodynamic polarization of steel samples chemically mechanically polished with the silica slurry without an oxidizer with different coating types are illustrate in figure 5.19. The corresponding E_{corr}, I_{corr} and CR are listed in table 5.5. were evaluated by the extrapolation method on the Tafel plot. It has been observed that the corrosion current density increases from $1.696e^1$ (mA/cm^2) (G3) hybrid coating to $5.832e^2$ (mA/cm^2)

polyethylene oxide (A3). The presence of silica slurry in the CMP treatment enhance the adhesion comparing with mechanical polishing. The corrosion potential decreases, can be explained by the increasing in the anodic current density and as a result increasing the corrosion rate but less than the corrosion rate in the previous case.

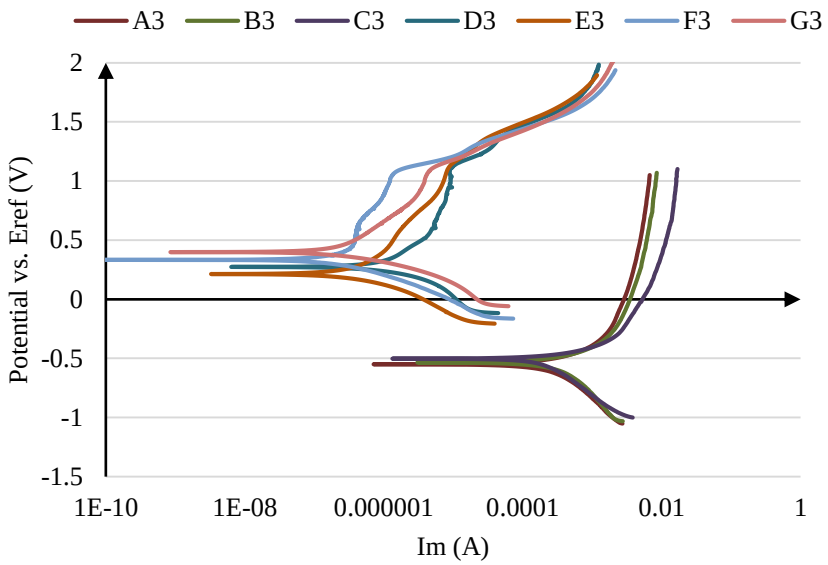

Figure 5-18 Potentiodynamic polarization curves of steel CMP treated 3 at pH=2 in different types of coating.

Table 5.6 Tafel plot data of steel sample treated 3 with different coating types

Coating Type	CR(mpy)	I_{corr} (mA/cm^2)	E_{corr} (mv)
A3	2.728e2	5.832e2	-535.0
B3	1.92e2	4.06e2	-544.0
C3	7.8e1	1.667e2	-530.0
D3	3.4e1	4.403e1	273.0
E3	2.04e1	4.444e1	213.0
F3	1.28	2.814e1	300.0
G3	9.2	1.969e1	214.0

Based on the electrochemical corrosion results, it can be detected that the steel samples CMP treated with the presence of hydrogen peroxide in the silica slurry via triple hybrid coating has highest corrosion resistance comparing with the other types of coating and surface treatment as shown in figure 5.19.

The adhesion property of the hybrid coating on the steel surface make a barrier against corrosion. While the other coatings have less adhesion on steel surface and these coating layer has been broken when the steel surface exposed to an acidic medium.

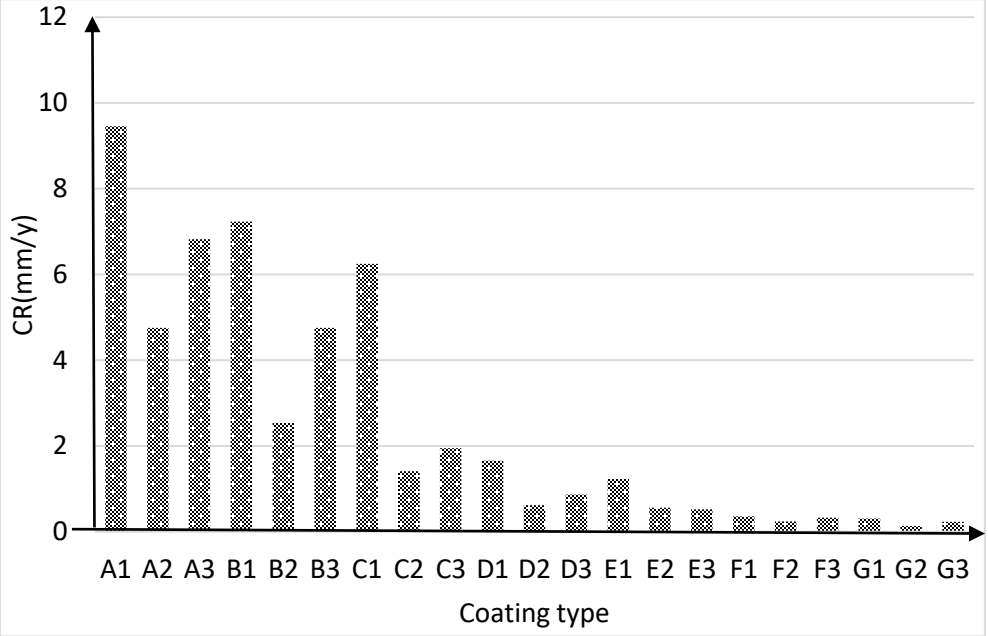

Figure 5-19 comparison of electrochemical corrosion with different types of coating and surface treatment.

5.4.6 Roughness measurements of coated samples

Figure 5.20 illustrates the surface roughness of mechanically polished samples with different types of coatings after 7 days of immersion test. The surface roughness in case of mechanically polished sample with silica sol gel has the highest roughness value as compared with the others, which is the baseline.

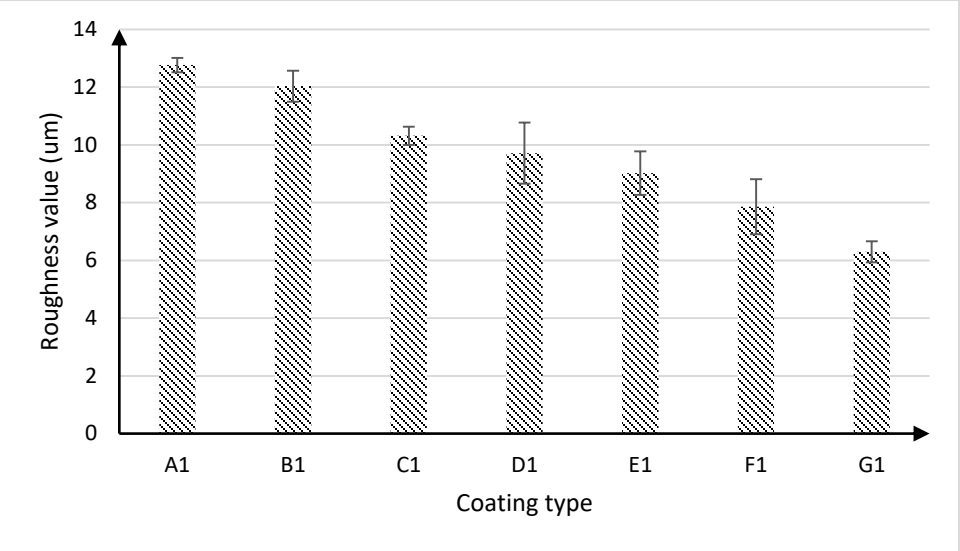

5-20 Average surface roughness as a function of different coating types of steel sample mechanically polished 1.

Figure 5.21 illustrates the surface roughness of CMP 2 treated samples with different types of coatings after 7 days of immersion test. It has been observed that the surface roughness in case of polyethylene oxide coating (A2) has the highest roughness value while the hybrid coating (G2) has the lowest value. This can be recognized to the adherence between the hybrid coating and the steel surface.

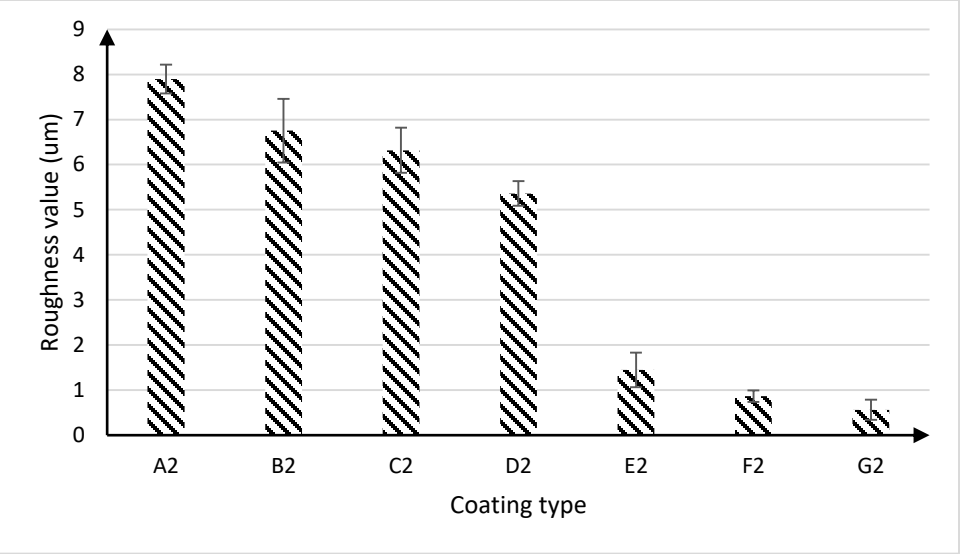

5-21 Average surface roughness as a function of different coating types of steel sample CMP treated 2.

Figure 5.22 illustrates the surface roughness of CMP 3 treated samples with different types of coatings after 7 days of immersion test. The surface roughness in case A3 which is polyethylene oxide has the highest roughness value compared to the others, while the case G3 which is polyethylene oxide+ epoxy + silica has the lowest roughness values. The presence of silica slurry with the epoxy coating enhance the adherence between the steel surface and this type of coating which protects the surface corrosion. On the other hand, the polyethylene oxide coating has almost no adherence with steel surface specially in an acidic media and the coating layer has been broken in this media which makes the surface rougher than that of hybrid group coating.

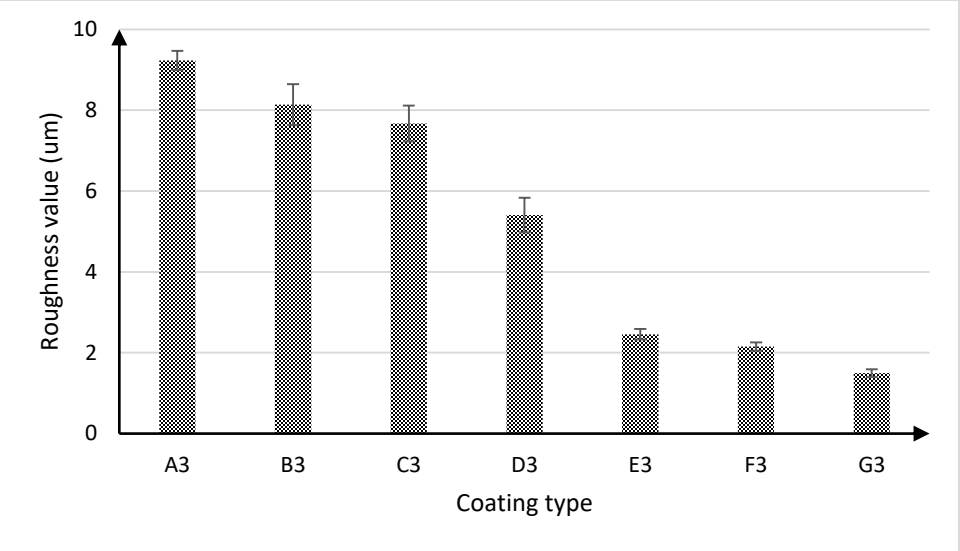

Figure 5-22 Average surface roughness as a function of different coating types of steel sample CMP treated 3.

5.5 Conclusions

The protection of steel surface in corrosive environments is one of the most promoting application of different types of coating. Different types of coating were used to investigate their effect on the corrosion behaviour of steel samples with three different surface treatments. The static corrosion tests done using weight loss method shown that the combination of CMP treatment in the existence of hydrogen peroxide in the silica slurry enhance the corrosion resistance compared to the other two cases. Furthermore, the immersion tests show that the hybrid coating (PEO+silica sol gel+epoxy) has the higher corrosion resistance among the coatings used. This behaviour can be referred to the coatings enhanced adhesion to the steel surface produced with CMP. These static corrosion results were confirmed via electrochemical analyses using potentiostatic Gamry instrument and a good agreement has been found. Average surface roughness of the coated samples

were measured after seven days of immersion and found that the hybrid coating in a case of CMP treatment with hydrogen peroxide has a smoother surface among the other coatings.

CHAPTER VI

CONCLUSION AND SUGGESTIONS FOR FUTURE WORK

6.1 Conclusions

- The current study concludes the corrosion rates in immersion tests measured after every 24 hours for seven days show an almost linear decrease with time after 48 hours.
- The dynamic corrosion rates obtained utilizing the developed setup show that for the same WSS the corrosion rate decreases with time.
- The corrosion rates increase with increasing WSS until a critical value. However, beyond critical WSS an increase in the corrosion rate was observed, which can be attributed to more pronounced effect of the acidic environment on steel corrosion.
- All the other cases of dynamic corrosion show an inverse relation between corrosion and time. This relationship has also been observed in static corrosion presented above and also proven in other studies.
- The effect of chemical mechanical polishing, in the presence of hydrogen peroxide and silica-based slurry, on the corrosion behavior of carbon steel in DIW at different pH values has been presented through an experimental setup.

- The corrosion behavior of this steel in a harsh environment after mechanical and chemical mechanical polishing treatment is reported. It can be inferred from the

findings that a combination of oxidizer (H_2O_2) and silica nanoparticles (SiO_2) in the CMP slurry enhances the material removal rate.

- The presence of oxidizers in the polishing slurry results in oxide layer formation on the surface which is easy to abrade compared to steel. However, after the CMP process, the oxide serves as a protective layer against corrosion.
- CMP with silica nanoparticles in the slurry results in smoother surfaces than that produced by pure mechanical polishing.
- The combined effect of the silica nanoparticles and oxidizers in the slurry removes the protruded parts from the surface and fills the valleys resulting in a durable and corrosion resistant surface.
- The hybrid coatings showed an improvement of the anticorrosive properties of the steel which is important to protect the metal surface.
- In addition, the study concludes that the chemical mechanical polishing with silica slurry in the presence of an oxidizer as pre-treatment method with the hybrid coating enhance the corrosion resistance better than the other pre-treatment and other coating types.

6.2 Suggestions for future work

The present study included some of the results that could be extended to include many surface-related issues that need to be taken into account to improve the performance of the laboratory-designed system for future exploration. The preparation developed in the laboratory depends on many variables that determine the desired results, including temperature, which is an important variable and their effect on the corrosion behavior of

steel, in addition to the pressure and how to control it in this system. One suggestion is to use a laboratory system with a higher design capacity than that used in our current study would give better results. The study was limited to examining the steel in different pH values. This, of course, does not give a complete idea of the conditions surrounding the steel completely, so as a very important suggestion that the steel should examined in different saline concentration, sea water is one of the most suitable for testing.

This study addressed the CMP process as one of the alternative methods for treating carbon steel surface against corrosion, study the CMP variables and investigate their effects on the treated samples and their relation and how to prevent or minimize the corrosion of steel is an important suggestion.

Addition of optimizers to the silica slurry to obtain more smooth surfaces and study their effects on the corrosion behavior of these kinds of steels or another types which is used in petroleum industries

Using other types of slurry or using a mixture of more than one compound and dealing with all the variables of chemical polishing and the use of treated metals in the developed laboratory system to examine the corrosion in various conditions.

Another suggestion is the addition of the inhibitors to the solution in the developed set up and study the effect of these inhibitors on CMP treated samples and the improvement in resistance to corrosion in acidic or saline conditions. A combination of CMP treated samples with different variables and different types of coatings and study the corrosion behavior of different metals in the developed set up with presence of H_2S and CO_2 is an

important suggestion which is mimic the real state of corrosion problems in petroleum industries.

LIST OF REFERENCES

[1] J.R. Davis, Surface engineering for corrosion and wear resistance, ASM international2001.
[2] B.A. Shaw, R.G. Kelly, What is corrosion?, Interface-Electrochemical Society 15(1) (2006) 24-27.
[3] J. Kruger, Electrochemistry of corrosion, Electrochemistry Encyclopedia (2001).
[4] C.I. Ossai, B. Boswell, I.J. Davies, Pipeline failures in corrosive environments – A conceptual analysis of trends and effects, Engineering Failure Analysis 53 (2015) 36-58.
[5] M. Singer, B. Brown, A. Camacho, S. Nešić, Combined effect of carbon dioxide, hydrogen sulfide, and acetic acid on bottom-of-the-line corrosion, Corrosion 67(1) (2011) 015004-1-015004-16.
[6] K. Ralston, N. Birbilis, Effect of grain size on corrosion: a review, Corrosion 66(7) (2010) 075005-075005-13.
[7] Y. Song, A. Palencsár, G. Svenningsen, J. Kvarekvål, T. Hemmingsen, Effect of O2 and temperature on sour corrosion, Corrosion 68(7) (2012) 662-671.
[8] V. Fajardo, C. Canto, B. Brown, S. Nesic, Effect of organic acids in CO2 corrosion, CORROSION 2007 (2007).
[9] C.I. Ossai, Advances in asset management techniques: An overview of corrosion mechanisms and mitigation strategies for oil and gas pipelines, ISRN Corrosion 2012 (2012).
[10] D.N. Veritas, Risk based inspection of offshore topsides static mechanical equipment, Oslo: DetNorske Veritas, 2002.
[11] C.E. Jaske, J.A. Beavers, N.G. Thompson, Improving plant reliability through corrosion monitoring, Fourth International Conference on Process Plant Reliability. Houston Texas. Organized by Gulf Publishing Company and Hydrocarbon Processing, 1995.
[12] N. Gloria, M. Areiza, I. Miranda, J. Rebello, Development of a magnetic sensor for detection and sizing of internal pipeline corrosion defects, NDT & e International 42(8) (2009) 669-677.
[13] H.A. Kishawy, H.A. Gabbar, Review of pipeline integrity management practices, International Journal of Pressure Vessels and Piping 87(7) (2010) 373-380.
[14] B. Babiarczuk, A. Szczurek, A. Donesz-Sikorska, I. Rutkowska, J. Krzak, The influence of an acid catalyst on the morphology, wettabillity, adhesion and chemical structure properties of TiO2 and ZrO2 sol–gel thin films, Surface and Coatings Technology 285 (2016) 134-145.
[15] P. Refait, M. Jeannin, R. Sabot, H. Antony, S.J.C.S. Pineau, Corrosion and cathodic protection of carbon steel in the tidal zone: Products, mechanisms and kinetics, 90 (2015) 375-382.
[16] J. Izquierdo, B. Fernández-Pérez, L. Martín-Ruíz, V. Mena, R. Rodríguez-Raposo, J. Santana, R.J.E.A. Souto, Evaluation of the corrosion protection of steel by anodic processing in metasilicate solution using the scanning vibrating electrode technique, 178 (2015) 1-10.
[17] M. Jokar, T.S. Farahani, B.J.J.o.t.T.I.o.C.E. Ramezanzadeh, Electrochemical and surface characterizations of morus alba pendula leaves extract (MAPLE) as a green corrosion inhibitor for steel in 1 M HCl, 63 (2016) 436-452.
[18] F. Corvo, T. Pérez, Y. Martin, J. Reyes, L. Dzib, J. González-Sánchez, A. Castañeda, Time of wetness in tropical climate: Considerations on the estimation of TOW according to ISO 9223 standard, Corrosion Science 50(1) (2008) 206-219.
[19] H. Katayama, K. Noda, M. Yamamoto, T. Kodama, Difference in corrosion behavior between pure iron and carbon steel after short-time exposure test, Corrosion and Corrosion Control in

Saltwater Environments: Proceedings of the International Symposium, The Electrochemical Society, 2000, p. 60.
[20] H. Katayama, K. Noda, H. Masuda, M. Nagasawa, M. Itagaki, K. Watanabe, Corrosion simulation of carbon steels in atmospheric environment, Corrosion science 47(10) (2005) 2599-2606.
[21] S. Ieamsupapong, B. Brown, M. Singer, S. Nesic, Effect of solution pH on corrosion product layer formation in a controlled water chemistry system, CORROSION/2017, paper 9160 (2017).
[22] I.H. Rhee, H. Jung, D. Cho, Evaluation of pH control agents influencing on corrosion of carbon steel in secondary water chemistry condition of pressurized water reactor, Nuclear engineering and technology 46(3) (2014) 431-438.
[23] M. Quraishi, D. Jamal, Dianils: new and effective corrosion inhibitors for oil-well steel (N-80) and mild steel in boiling hydrochloric acid, Corrosion 56(2) (2000) 156-160.
[24] A.L. de Queiroz Baddini, S.P. Cardoso, E. Hollauer, J.A.d.C.P. Gomes, Statistical analysis of a corrosion inhibitor family on three steel surfaces (duplex, super-13 and carbon) in hydrochloric acid solutions, Electrochimica Acta 53(2) (2007) 434-446.
[25] Z. Panossian, N.L. de Almeida, R.M.F. de Sousa, G. de Souza Pimenta, L.B.S. Marques, Corrosion of carbon steel pipes and tanks by concentrated sulfuric acid: a review, Corrosion Science 58 (2012) 1-11.
[26] S. Armini, C. Whelan, M. Moinpour, K. Maex, Composite polymer core–silica shell abrasives effect of polishing time and slurry solid content on oxide CMP, Electrochemical and Solid-State Letters 10(9) (2007) H243-H247.
[27] D. Brondel, R. Edwards, A. Hayman, D. Hill, S. Mehta, T. Semerad, Corrosion in the oil industry, Oilfield review 6(2) (1994) 4-18.
[28] S. Vishwanatham, N. Haldar, Furfuryl alcohol as corrosion inhibitor for N80 steel in hydrochloric acid, Corrosion Science 50(11) (2008) 2999-3004.
[29] M. Brust, M. Walker, D. Bethell, D.J. Schiffrin, R. Whyman, Synthesis of thiol-derivatised gold nanoparticles in a two-phase liquid–liquid system, Journal of the Chemical Society, Chemical Communications (7) (1994) 801-802.
[30] T.C. Dakal, A. Kumar, R.S. Majumdar, V. Yadav, Mechanistic basis of antimicrobial actions of silver nanoparticles, Frontiers in microbiology 7 (2016) 1831.
[31] K.J.U.s.c.h. Efird, Flow-induced corrosion, (2000) 233-248.
[32] S. Nešic, G.T. Solvi, J.J.C. Enerhaug, Comparison of the rotating cylinder and pipe flow tests for flow-sensitive carbon dioxide corrosion, 51(10) (1995) 773-787.
[33] T.-Y. Chen, The Development of Controlled Hydrodynamic Techniques for Corrosion Testing, Ohio State University, 1983.
[34] A. Mohammed Nor, The Effect of Turbulent Flow on Corrosion of Mild Steel in High Partial CO 2 Environments, Ohio University, 2013.
[35] M.G. Fontana, Corrosion engineering, Tata McGraw-Hill Education2005.
[36] P. Scheers, The effects fo flow velocity and pH on the corrosion rate of mild steel in a synthetic minewater, Journal of the Southern African Institute of Mining and Metallurgy 92(10) (1992) 275-281.
[37] N. Fredj, T. Burleigh, K. Heidersbach, B. Crowder, Corrosion Of Carbon Steel In Waters Of Varying Purity And Velocity, CORROSION 2012, NACE International, 2012.
[38] M. Ferry, W. Wan Nik, M. Noor, C. Wan, The Influence of Seawater Velocity to the Corrosion Rate and Paint Degradation at Mild Steel Plate Immersed in Sea Water, Applied Mechanics and Materials, Trans Tech Publ, 2014, pp. 218-221.
[39] E. Rabald, Corrosion guide, Elsevier2012.

[40] H. Tawancy, L.M. Al-Hadhrami, F. Al-Yousef, Analysis of corroded elbow section of carbon steel piping system of an oil–gas separator vessel, Case Studies in Engineering Failure Analysis 1(1) (2013) 6-14.
[41] M. Hernandez-Rodriguez, D. Martinez-Delgado, R. Gonzalez, A.P. Unzueta, R. Mercado-Solís, J. Rodriguez, Corrosive wear failure analysis in a natural gas pipeline, Wear 263(1-6) (2007) 567-571.
[42] A.C. Palmer, R.A. King, Subsea pipeline engineering, PennWell Books2004.
[43] G. Wranglén, An introduction to corrosion and protection of metals, Chapman and Hall London1985.
[44] S. Zhang, D. Zhao, Aerospace materials handbook, CrC Press2016.
[45] J. Hoo, Effect of Steel Manufacturing Processes on the Quality of Bearing Steels, Symposium on Effect of Steel Manufacturing Processes on the Quality of Bearing Steels, 1986.
[46] R.S. Mulik, P.M. Pandey, Magnetic abrasive finishing of hardened AISI 52100 steel, The International Journal of Advanced Manufacturing Technology 55(5-8) (2011) 501-515.
[47] Y. Guo, A. Warren, Microscale mechanical behavior of the subsurface by finishing processes, Journal of manufacturing science and engineering 127(2) (2005) 333-338.
[48] M. Sedlaček, B. Podgornik, J. Vižintin, Influence of surface preparation on roughness parameters, friction and wear, Wear 266(3-4) (2009) 482-487.
[49] M. Kao, F. Hsu, D. Peng, Synthesis and characterization of SiO2 nanoparticles and their efficacy in chemical mechanical polishing steel substrate, Advances in Materials Science and Engineering 2014 (2014).
[50] X. Chi, X.H. Suo, Study on float polishing of metal nanometer surface, Advanced Materials Research, Trans Tech Publ, 2011, pp. 1757-1760.
[51] Y.J.Z.F.D. Yifan, K.R.Y.H.L. Binghai, Development Research of Science and Technologies in Ultra-precision Machining Field [J], Journal of Mechanical Engineering 15 (2010) 025.
[52] R.S. Mulik, P.M. Pandey, Ultrasonic assisted magnetic abrasive finishing of hardened AISI 52100 steel using unbonded SiC abrasives, International Journal of Refractory Metals and Hard Materials 29(1) (2011) 68-77.
[53] D.-X. Peng, Chemical mechanical polishing of steel substrate using aluminum nanoparticles abrasive slurry, Industrial Lubrication and Tribology 66(1) (2014) 124-130.
[54] D.-J. Yun, S.-H. Lim, T.-W. Lee, S.-W. Rhee, Fabrication of the flexible pentacene thin-film transistors on 304 and 430 stainless steel (SS) substrate, Organic Electronics 10(5) (2009) 970-977.
[55] X. Hu, Z. Song, W. Liu, F. Qin, Z. Zhang, H. Wang, Chemical mechanical polishing of stainless steel foil as flexible substrate, Applied surface science 258(15) (2012) 5798-5802.
[56] R.J. Walsh, A.H. Herzog, Process for polishing semiconductor materials, Google Patents, 1965.
[57] W.C. Chen, S.C. Lin, B.T. Dai, M.S. Tsai, Chemical Mechanical Polishing of Low-Dielectric-Constant Polymers: Hydrogen Silsesquioxane and Methyl Silsesquioxane, Journal of the Electrochemical Society 146(8) (1999) 3004-3008.
[58] T. Hara, T. Tomisawa, T. Kurosu, T.K. Doy, Chemical mechanical polishing of polyarylether low dielectric constant layers by manganese oxide slurry, Journal of The Electrochemical Society 146(6) (1999) 2333-2336.
[59] J. Luo, D.A. Dornfeld, Material removal regions in chemical mechanical planarization for submicron integrated circuit fabrication: coupling effects of slurry chemicals, abrasive size distribution, and wafer-pad contact area, IEEE Transactions on Semiconductor Manufacturing 16(1) (2003) 45-56.
[60] M. Sivanandini, S. Dhami Sukhdeep, B. Pabla, Chemical mechanical polishing by colloidal silica slurry, International Journal of Engineering Research and Applications (IJERA) ISSN 6 (2013) 2248-9622.

[61] P.B. Zantye, A. Kumar, A. Sikder, Chemical mechanical planarization for microelectronics applications, Materials Science and Engineering: R: Reports 45(3-6) (2004) 89-220.
[62] P.H. Chen, B.W. Huang, H.-C. Shih, A chemical kinetics model to explain the abrasive size effect on chemical mechanical polishing, Thin solid films 476(1) (2005) 130-136.
[63] J. Schlueter, J. Henry, T.X. Shi, Managing Corrosion during the Chemical Mechanical Polishing (CMP) of Metal Films, Meeting Abstracts, The Electrochemical Society, 2012, pp. 2489-2489.
[64] Y. Kamigata, Y. Kurata, K. Masuda, J. Amanokura, M. Yoshida, M. Hanazono, Why abrasive free Cu slurry is promising?, MRS Online Proceedings Library Archive 671 (2001).
[65] A.K. Muthukumaran, Chemical systems for electrochemical mechanical planarization of copper and tantalum films, (2008).
[66] M.R. Oliver, Chemical-mechanical planarization of semiconductor materials, Springer Science & Business Media2013.
[67] R.V. Ihnfeldt, J.B. Talbot, Effects of CMP Slurry Chemistry on Agglomeration of Alumina and Copper Surface Hardness, ECS Transactions 3(41) (2007) 21-30.
[68] R. Carpio, J. Farkas, R. Jairath, Initial study on copper CMP slurry chemistries, Thin solid films 266(2) (1995) 238-244.
[69] J.M. Steigerwald, S.P. Murarka, R.J. Gutmann, Chemical mechanical planarization of microelectronic materials, John Wiley & Sons2008.
[70] S.V. Babu, K.C. Cadien, H. Yano, Chemical-Mechanical Polishing 2001-Advances and Future Challenges, Cambridge University Press2001.
[71] D.-X. Peng, Optimization of chemical mechanical polishing parameters on surface roughness of steel substrate with aluminum nanoparticles via Taguchi approach, Industrial Lubrication and Tribology 66(6) (2014) 685-690.
[72] Y. Zhao, L. Chang, A micro-contact and wear model for chemical–mechanical polishing of silicon wafers, Wear 252(3-4) (2002) 220-226.
[73] N. Saka, T. Eusner, J.-H. Chun, Nano-scale scratching in chemical–mechanical polishing, CIRP Annals-Manufacturing Technology 57(1) (2008) 341-344.
[74] G.B. Basim, I.U. Vakarelski, B.M. Moudgil, Role of interaction forces in controlling the stability and polishing performance of CMP slurries, Journal of colloid and interface science 263(2) (2003) 506-515.
[75] A. Artemov, Chemicomechanical polishing of material, Nanotechnologies in Russia 6(7-8) (2011) 419.
[76] G. Philipp, H.K. Schmidt, New materials for contact lenses prepared from Si-and Ti-alkoxides by the sol-gel process, (1984).
[77] C. VINCENT, Process for producing low-bulk density silica, US Patent App. 3/556,725, 1969.
[78] C.J. Brinker, G.W. Scherer, Sol-gel science: the physics and chemistry of sol-gel processing, Academic press2013.
[79] S. Ono, H. Tsuge, Y. Nishi, S.-i. Hirano, Improvement of corrosion resistance of metals by an environmentally friendly silica coating method, Journal of sol-gel science and technology 29(3) (2004) 147-153.
[80] K.H. Haas, Hybrid Inorganic–Organic Polymers Based on Organically Modified Si-Alkoxides, Advanced Engineering Materials 2(9) (2000) 571-582.
[81] J.N. Hay, H.M. Raval, Preparation of inorganic oxides via a non-hydrolytic sol-gel route, Journal of Sol-Gel Science and Technology 13(1-3) (1998) 109-112.
[82] M. Andrianainarivelo, R.J. Corriu, D. Leclercq, P.H. Mutin, A. Vioux, Nonhydrolytic Sol-Gel process: Aluminium and zirconium titanate gels, Journal of Sol-Gel Science and Technology 8(1-3) (1997) 89-93.

[83] M. Vallet-Regí, I. Izquierdo-Barba, F. Gil, Localized corrosion of 316L stainless steel with SiO2-CaO films obtained by means of sol–gel treatment, Journal of Biomedical Materials Research Part A: An Official Journal of The Society for Biomaterials, The Japanese Society for Biomaterials, and The Australian Society for Biomaterials and the Korean Society for Biomaterials 67(2) (2003) 674-678.
[84] M. Atik, F.P. Luna, S.H. Messaddeq, M.A. Aegerter, Ormocer (ZrO 2-PMMA) films for stainless steel corrosion protection, Journal of Sol-Gel Science and Technology 8(1-3) (1997) 517-522.
[85] M. Zheludkevich, I.M. Salvado, M. Ferreira, Sol–gel coatings for corrosion protection of metals, Journal of Materials Chemistry 15(48) (2005) 5099-5111.
[86] D. Vasconcelos, J. Carvalho, M. Mantel, W. Vasconcelos, Corrosion resistance of stainless steel coated with sol–gel silica, Journal of Non-Crystalline Solids 273(1-3) (2000) 135-139.
[87] C. Brinker, G. Scherer, The Physics and Chemistry of Sol-Gel Processing. 1990, There is no corresponding record for this reference 787-835.
[88] U. Damrau, H. Marsmann, The hydrolysis of oligomer intermediates in the sol-gel process, Journal of non-crystalline solids 168(1-2) (1994) 42-48.
[89] R. Lenza, W. Vasconcelos, Synthesis and properties of microporous sol–gel silica membranes, Journal of Non-Crystalline Solids 273(1-3) (2000) 164-169.
[90] R.F. Lenza, W.L. Vasconcelos, Preparation of silica by sol-gel method using formamide, Materials Research 4(3) (2001) 189-194.
[91] D. Wang, G.P. Bierwagen, Sol–gel coatings on metals for corrosion protection, Progress in organic coatings 64(4) (2009) 327-338.
[92] G.P. Bierwagen, L. He, J. Li, L. Ellingson, D. Tallman, Studies of a new accelerated evaluation method for coating corrosion resistance—thermal cycling testing, Progress in organic coatings 39(1) (2000) 67-78.
[93] C. Brinker, A. Hurd, P. Schunk, G. Frye, C. Ashley, Review of sol-gel thin film formation, Journal of Non-Crystalline Solids 147 (1992) 424-436.
[94] J.D. Wright, N.A. Sommerdijk, Sol-gel materials: chemistry and applications, CRC press2014.
[95] K. Joncoux-Chabrol, J.-P. Bonino, M. Gressier, M.-J. Menu, N. Pébère, Improvement of barrier properties of a hybrid sol–gel coating by incorporation of synthetic talc-like phyllosilicates for corrosion protection of a carbon steel, Surface and Coatings Technology 206(11-12) (2012) 2884-2891.
[96] P. Galliano, J.J. De Damborenea, M.J. Pascual, A. Duran, Sol-gel coatings on 316L steel for clinical applications, Journal of sol-gel science and technology 13(1-3) (1998) 723-727.
[97] E. Kiele, J. Senvaitiene, A. Grigucevičienė, R. Ramanauskas, R. Raudonis, A. Kareiva, Sol-gel derived coatings for the conservation of steel, Processing and Application of Ceramics 9(2) (2015) 81-89.
[98] A. Tiwari, L. Hihara, J. Rawlins, Intelligent coatings for corrosion control, Butterworth-Heinemann2014.
[99] R. Figueira, C.J. Silva, E. Pereira, Organic–inorganic hybrid sol–gel coatings for metal corrosion protection: a review of recent progress, Journal of Coatings Technology and Research 12(1) (2015) 1-35.
[100] M. Menning, C. Schelle, A. Durán, J. Damborena, M. Guglielmi, G. Brusatin, Investigation of glass-like sol-gel coatings for corrosion protection of stainless steel against liquid and gaseous attack, Journal of sol-gel science and technology 13(1-3) (1998) 717-722.
[101] M. Guglielmi, Sol-gel coatings on metals, Journal of sol-gel science and technology 8(1-3) (1997) 443-449.
[102] T.J. Garino, The cracking of sol-gel films during drying, MRS Online Proceedings Library Archive 180 (1990).

[103] O. Sanctis, N. Pellegri, L. Gomez, A. Marajofsky, C. Parodi, A. Duran, J. of Non-Cryst, Solids, 1990.
[104] J. De Damborenea, N. Pellegri, O. De Sanctis, A. Durán, Electrochemical behaviour of SiO2 sol-gel coatings on stainless steel, Journal of Sol-Gel Science and Technology 4(3) (1995) 239-244.
[105] J. Gallardo, P. Galliano, A. Duran, Thermal evolution of hybrid sol-gel silica coatings: A structural analysis, Journal of Sol-Gel Science and Technology 19(1-3) (2000) 393-397.
[106] P. De Lima Neto, M. Atik, L.A. Avaca, M.A. Aegerter, Sol-gel coatings for chemical protection of stainless steel, Journal of Sol-Gel Science and Technology 2(1-3) (1994) 529-534.
[107] N. Voevodin, C. Jeffcoate, L. Simon, M. Khobaib, M. Donley, Characterization of pitting corrosion in bare and sol–gel coated aluminum 2024-T3 alloy, Surface and Coatings Technology 140(1) (2001) 29-34.
[108] G.P. Thim, M.A. Oliveira, E.D. Oliveira, F.C. Melo, Sol–gel silica film preparation from aqueous solutions for corrosion protection, Journal of non-crystalline solids 273(1-3) (2000) 124-128.
[109] M. Zheludkevich, R. Serra, M. Montemor, K. Yasakau, I.M. Salvado, M. Ferreira, Nanostructured sol–gel coatings doped with cerium nitrate as pre-treatments for AA2024-T3: corrosion protection performance, Electrochimica Acta 51(2) (2005) 208-217.
[110] A. Khramov, N. Voevodin, V. Balbyshev, R. Mantz, Sol–gel-derived corrosion-protective coatings with controllable release of incorporated organic corrosion inhibitors, Thin Solid Films 483(1-2) (2005) 191-196.
[111] A.S. Hamdy, D. Butt, Novel anti-corrosion nano-sized vanadia-based thin films prepared by sol–gel method for aluminum alloys, Journal of materials processing technology 181(1-3) (2007) 76-80.
[112] F. Riffard, H. Buscail, E. Caudron, R. Cueff, C. Issartel, S. Perrier, Effect of yttrium addition by sol–gel coating and ion implantation on the high temperature oxidation behaviour of the 304 steel, Applied Surface Science 199(1-4) (2002) 107-122.
[113] J. Masalski, J. Gluszek, J. Zabrzeski, K. Nitsch, P. Gluszek, Improvement in corrosion resistance of the 316l stainless steel by means of Al2O3 coatings deposited by the sol-gel method, Thin Solid Films 349(1-2) (1999) 186-190.
[114] J. Shankar, A. Upadhyaya, R. Balasubramaniam, Corrosion behavior of sintered oxide dispersion strengthened stainless steels, Journal of materials science 39(5) (2004) 1815-1817.
[115] J.-M. Hu, X.-L. Liu, J.-Q. Zhang, C.-N. Cao, Corrosion protection of Nd–Fe–B magnets by silanization, Progress in organic coatings 55(4) (2006) 388-392.
[116] J. da Silva Peltz, L. Beltrami, S. Kunst, C. Brandolt, C. de Fraga Malfatti, Effect of the Shot Peening Process on the Corrosion and Oxidation Resistance of AISI430 Stainless Steel, Mater. Res 18 (2015) 538-45.
[117] L. Rivera-Grau, M. Casales, I. Regla, D. Ortega-Toledo, J. Ascencio-Gutierrez, J. Porcayo-Calderon, L. Martinez-Gomez, Effect of organic corrosion inhibitors on the corrosion performance of 1018 carbon steel in 3% NaCl solution, International Journal of Electrochemical Science 8(2) (2013) 2491-2503.
[118] R. Yıldız, A. Döner, T. Doğan, İ. Dehri, Experimental studies of 2-pyridinecarbonitrile as corrosion inhibitor for mild steel in hydrochloric acid solution, Corrosion Science 82 (2014) 125-132.
[119] I. Aiad, S.M. Shaban, A.H. Elged, O.H. Aljoboury, Cationic surfactant based on alignate as green corrosion inhibitors for the mild steel in 1.0 M HCl, Egyptian journal of petroleum 27(4) (2018) 877-885.

[120] A.A. Abd-Elaal, S.M. Shaban, S.M. Tawfik, Three Gemini cationic surfactants based on polyethylene glycol as effective corrosion inhibitor for mild steel in acidic environment, Journal of the Association of Arab Universities for Basic and Applied Sciences 24(1) (2017) 54-65.
[121] X. He, Y. Chen, H. Zhao, H. Sun, X. Lu, H. Liang, Y 2 O 3 nanosheets as slurry abrasives for chemical-mechanical planarization of copper, Friction 1(4) (2013) 327-332.
[122] J. Rossum, Fundamentals of metallic corrosion in fresh water, Roscoe Moss Company (2000).
[123] V. Chandrasekaran, K. Kannan, M. Natesan, Inhibiting properties of some amines on corrosion behaviour of mild steel in phosphoric acid solution at various temperatures, Asian Journal of Chemistry 17(3) (2005) 1921.
[124] R. Yagan, Electrochemical evaluations of TiO2 nano films for advanced engineering applications, (2018).
[125] H. Xue, Y. Cheng, Electrochemical corrosion behavior of X80 pipeline steel in a near-neutral pH solution, Materials and corrosion 61(9) (2010) 756-761.
[126] S. Raicheva, B. Aleksiev, E. Sokolova, The effect of the chemical structure of some nitrogen- and sulphur-containing organic compounds on their corrosion inhibiting action, Corrosion Science 34(2) (1993) 343-350.
[127] S. Bargir, S. Dunn, B. Jefferson, J. Macadam, S. Parsons, The use of contact angle measurements to estimate the adhesion propensity of calcium carbonate to solid substrates in water, Applied Surface Science 255(9) (2009) 4873-4879.
[128] C.J. Van Oss, M.K. Chaudhury, R.J. Good, Interfacial Lifshitz-van der Waals and polar interactions in macroscopic systems, Chemical Reviews 88(6) (1988) 927-941.
[129] C. Massaro, P. Rotolo, F. De Riccardis, E. Milella, A. Napoli, M. Wieland, M. Textor, N. Spencer, D. Brunette, Comparative investigation of the surface properties of commercial titanium dental implants. Part I: chemical composition, Journal of Materials Science: Materials in Medicine 13(6) (2002) 535-548.
[130] I. Braceras, M. De Maeztu, J. Alava, C. Gay-Escoda, In vivo low-density bone apposition on different implant surface materials, International journal of oral and maxillofacial surgery 38(3) (2009) 274-278.
[131] S. Peng, Z. Zeng, An experimental study on the internal corrosion of a subsea multiphase pipeline, Petroleum 1(1) (2015) 75-81.
[132] Q.J. Slaimana, B.O. Hasan, Study on corrosion rate of carbon steel pipe under turbulent flow conditions, The Canadian Journal of Chemical Engineering 88(6) (2010) 1114-1120.
[133] S. Kerr, K. Rosenberg, An index of cavitation erosion by means of radioisotopes, Trans. Am. Soc. Mech. Engrs. 80 (1958).
[134] R. Knapp, J. Daily, F. Hammitt, 1970, Cavitation, McGraw-Hill, New York.
[135] R.H. Hausler, C. Consulta, G. Schmitt, Hydrodynamic and flow effects on corrosion inhibition, CORROSION 2004, NACE International, 2004.
[136] K.D. Efird, Jet impingement testing for flow accelerated corrosion, CORROSION 2000, NACE International, 2000.
[137] C.-J. Chia, F. Giralt, O. Trass, Mass transfer in axisymmetric turbulent impinging jets, Industrial & Engineering Chemistry Fundamentals 16(1) (1977) 28-35.
[138] V.C. Patel, M.R. Head, Reversion of turbulent to laminar flow, Journal of Fluid Mechanics 34(2) (1968) 371-392.
[139] U. Lotz, J. Postlethwaite, Erosion-corrosion in disturbed two phase liquid/particle flow, Corrosion science 30(1) (1990) 95-106.
[140] X. Yong, Y. Zhang, D. Li, Near the wall of the fluid mechanics, the effect of flow parameters on the corrosion, Corros. Prot. Tec 3 (2011) 245-250.

[141] D.A. Dawson, O.J.I.J.o.H. Trass, M. Transfer, Mass transfer at rough surfaces, 15(7) (1972) 1317-1336.
[142] V.G.e. Levich, Physicochemical hydrodynamics, (1962).
[143] G. Fogg, J. Morse, Development of a new solvent-free flow efficiency coating for natural gas pipelines, Rio Pipeline 2005 Conference and Exposition, IBP1233, 2005.
[144] C. Tomachuk, C.I. Elsner, A.R. Di Sarli, Electrochemical characterization of chromate free conversion coatings on electrogalvanized steel, Materials Research 17(1) (2014) 61-68.
[145] W. Acchar, L.S. Barreto, H.R. Paes Junior, C.R. Cruz, E.E. Feistauer, LaCrO3 composite coatings for AISI 444 stainless steel solid oxide fuel cell interconnects, Materials Research 15(6) (2012) 1064-1069.
[146] A.M. Saliba-Silva, M.C.L.d. Oliveira, I. Costa, Effect of molybdate on phosphating of Nd-Fe-B magnets for corrosion protection, Materials Research 8(2) (2005) 147-150.
[147] H. Bahri, I. Danaee, G. Rashed, The effect of curing time and curing temperature on the corrosion behavior of nanosilica modified potassium silicate coatings on AA2024, Surface and Coatings Technology 254 (2014) 305-312.
[148] I. Danaee, H. Zamanizadeh, M. Fallahi, B. Lotfi, The effect of surface pre-treatments on corrosion behavior of cerium-based conversion coatings on Al 7075-T6, Materials and Corrosion 65(8) (2014) 815-819.
[149] M.E.P.d. Souza, E. Ariza, M. Ballester, I.V.P. Yoshida, L.A. Rocha, C.M.d.A. Freire, Characterization of organic-inorganic hybrid coatings for corrosion protection of galvanized steel and electroplated ZnFe steel, Materials Research 9(1) (2006) 59-64.
[150] C.A.d. Cunha, N.B.d. Lima, J.R. Martinelli, A.H.d.A. Bressiani, A.G.F. Padial, L.V. Ramanathan, Microstructure and mechanical properties of thermal sprayed nanostructured Cr3C2-Ni20Cr coatings, Materials Research 11(2) (2008) 137-143.
[151] C.d.S. Brandolt, J.G.d. Souza Junior, S.R. Kunst, M.R.O. Vega, R.M. Schroeder, C.d.F. Malfatti, Niobium and niobium-iron coatings on API 5LX 70 steel applied with HVOF, Materials Research 17(4) (2014) 866-877.
[152] A.-M. Lazar, W.P. Yespica, S. Marcelin, N. Pébère, D. Samélor, C. Tendero, C. Vahlas, Corrosion protection of 304L stainless steel by chemical vapor deposited alumina coatings, Corrosion Science 81 (2014) 125-131.
[153] S. Trigwell, G. Selvaduray, Effect of surface treatment on the surface characteristics of AISI 316L stainless steel, Medical Device Materials III, Venugopalan R, Wu M (eds): ASM International, Materials Park, OH (2006) 208-213.
[154] F. Kaufman, D. Thompson, R. Broadie, M. Jaso, W. Guthrie, D. Pearson, M. Small, Chemical-mechanical polishing for fabricating patterned W metal features as chip interconnects, Journal of the Electrochemical Society 138(11) (1991) 3460-3465.
[155] C. Sanchez, K. Shea, S. Kitagawa, Hybrid materials, Chem. Soc. Rev 40 (2011) 453-1152.
[156] Y. Hamlaoui, F. Pedraza, C. Remazeilles, S. Cohendoz, C. Rébéré, L. Tifouti, J. Creus, Cathodic electrodeposition of cerium-based oxides on carbon steel from concentrated cerium nitrate solutions: Part I. Electrochemical and analytical characterisation, Materials Chemistry and Physics 113(2-3) (2009) 650-657.